

Dissertation for Doctor of Philosophy

Inverse Problems of Compressed Sensing and
Cooperative Networks over Finite Fields

Jin-Taek Seong

School of Information and Communications

Gwangju Institute of Science and Technology

2014

박 사 학 위 논 문

유한체에서 압축센싱과 협력 네트워크의 역문제

성 진 택

정 보 통 신 공 학 부

광 주 과 학 기 술 원

2014

Inverse Problems of Compressed Sensing and Cooperative Networks over Finite Fields

Advisor: Heung-No Lee

by

Jin-Taek Seong

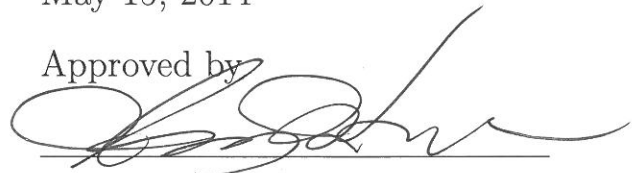
School of Information and Communications
Gwangju Institute of Science and Technology

A thesis submitted to the faculty of the Gwangju Institute of Science
and Technology in partial fulfillment of the requirements for the degree of
Doctor of Philosophy in the School of Information and Communications

Gwangju, Republic of Korea

May 15, 2014

Approved by



Professor Heung-No Lee

Thesis Advisor

Inverse Problems of Compressed Sensing and
Cooperative Networks over Finite Fields

Jin-Taek Seong

Accepted in partial fulfillment of the requirements for the
degree of Doctor of Philosophy

May 15, 2014

Thesis Advisor



Prof. Heung-No Lee

Committee Member



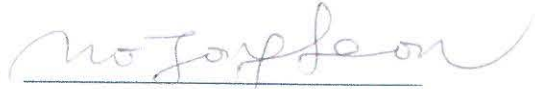
Prof. Kiseon Kim, GIST

Committee Member



Prof. Jinho Choi, GIST

Committee Member



Prof. Jong-Seon No, SNU

Committee Member



Prof. Mikael Skoglund, KTH

To my parents for their devoted support,
my wife for her endurance and love,
and my lovely daughter, Chae-Yeon.

국 문 요 약

본 학위논문은 크게 두 부분으로 구성되어 있으며, 유한체에서 압축센싱(Compressed Sensing)과 협력 네트워크(Cooperative Networks)의 역문제를 다루고 있다. 논문의 첫 부분은 압축센싱의 성능 한계치에 대한 연구로써 희소 신호를 복원하기 위한 조건들을 살펴보고 복원 알고리즘을 제안하고 있다. 두 번째 부분은 네트워크 코딩을 이용한 무선 협력 네트워크에서 새로운 평가방법을 제안하고 있고, 이를 이용한 시스템 성능을 분석하고 있다. 본 논문의 두 부분들은 각각 다른 문제를 다루고 있지만, 역문제의 측면에서 되짚어 보면 서로 밀접한 연관성을 갖고 있다.

본 학위논문의 첫 부분은 유한체에서 압축센싱 문제를 고려하고 있으며, 희소 신호를 복원하기 위한 필요충분조건들을 다루고 있다. 그 신호 복원 조건들은 압축센싱의 주요 성능 지표들로 표현이 된다. 예를 들어, N 차원 희소 신호를 복원하기 위해 얼마만큼의 측정 샘플 수가 필요한지 그 비율로써 나타내고 있다. 본 연구에서는 센싱행렬이 조밀하게 0이 아닌 값들로 구성되어 있다면 희소 신호 복원을 위한 충분조건은 필요조건과 일치함을 밝히고 있다. 이것은 신호의 길이와 유한체의 필드 크기가 무한대로 증가했을 때 얻은 결과로써 실수체계에서 얻은 결과와 일치함을 보여 주고 있다. 또 다른 결과로써 찾고자 하는 신호가 희소하지 않을 경우 대부분 0의 값들로 구성된 센싱행렬만으로도 필요충분조건을 일치성을 말하고 있다. 더불어서 희소 신호를 효과적으로 복원하기 위해 부호이론에서 제안된 메시지 전달 알고리즘 기반의 복원 기법을 소개한다. 제안된 알고리즘을 이용하여 신호 복원 성능의 우수성을 보여 주고 있으며, 이산 형태의 신호들을 실질적이면서 유용하게 복원할 수 있는 기법을 제안하고 있다.

다음으로, 네트워크 코딩을 이용한 무선 협력 네트워크의 성능평가를 위한 분석 프레임워크를 처음으로 제안한다. 무선 네트워크 특성상 송수신 간의 연결상태는 지속적으로 변하므로 랜덤 변수를 이용하여 그 연결성을 표현하고 이를 활용하여 성능을 평가한다. 이와 같은 방법은 구조적이고 시스템적인 접근법으로써 무선채널의 연결상태를 표현하

고 있기 때문에 무선 협력 네트워크의 성능을 손쉽게 평가할 수 있다. 본 연구에서는 랜덤 행렬의 nullity와 복원 실패 확률(decoding failure probability)과 같은 평가지표들을 이용하여 무선 협력 네트워크의 성능 상계치를 얻는다. 이와 더불어 간단한 형태의 무선 협력 네트워크에서 네트워크 코딩의 이점들을 살펴본다. 또한 2차원 평면에 놓인 소스 노드에 대한 최적의 송신전력 분배 문제를 다루고 있다. 그 결과로써 네트워크 코딩의 필드 크기와 무선 채널의 변화에 따라 그 소스 노드에 할당된 최적의 송신전력 값이 변하게 됨을 보여 준다.

©2014

성진택

Ph.D/IC Jin-Taek Seong. Inverse Problems of Compressed Sensing and Cooperative
20102043 Networks over Finite Fields. School of Information and Communications.
2014. 143p. Advisor: Prof. Heung-No Lee.

Abstract

This dissertation consists of two parts, both of which consider linear inverse problems of compressed sensing and cooperative networks for the recovery of unknown signals over finite fields. The first part of this dissertation addresses the performance evaluation of compressed sensing. The second part studies an analytical framework for the recovery of source information in cooperative communications combined with network coding. The two parts of this dissertation are clearly different, but they are also related with regard to the study of inverse problems.

In the first part of this dissertation, we address the problem of reconstructing sparse signals over finite fields. We derive necessary and sufficient conditions for the recovery of sparse signals in terms of key parameters in compressed sensing. The results are valuable because the sufficient condition coincides with the necessary condition if the sensing matrix is sufficiently dense when both the length of the signal and the field size grow to infinity. Another interesting conclusion is that unless the signal is very sparse, the sensing matrix does not have to be dense for the upper bound to coincide with the lower bound. For the efficient recovery of sparse signals, we propose probabilistic decoding based on the message passing algorithm used in coding theory. We show that the proposed recovery algorithm is practical and useful when applied to a set of discrete signals.

In the second part, we first propose an analytical framework for the performance evaluation of cooperative wireless coding schemes to cope with any family of network scenarios. For a dynamic network topology, we consider random elements of the transmission matrix that rely on the connectivity of a pair of transceivers. Using a systematic

approach, we derive an upper bound on the reconstruction performance in terms of the decoding failure probability and the nullity of a random matrix. Moreover, we also consider a simple class of cooperative wireless networks that offers the benefits of network coding. In addition, we consider an optimal power allocation of source nodes moving in a two-dimensional space. We show that the optimum ratio of power allocation varies according to the wireless channel environments and the field size of network codes.

©2014

Jin-Taek Seong

ALL RIGHTS RESERVED

Acknowledgements

There are many people who have contributed in different ways to this dissertation. Without all of them, it is impossible to write this dissertation and complete my research work behind it.

First and foremost, I would like to express my sincerest gratitude to my advisor, Prof. Heung-No Lee, who has steadfastly supported me during the Ph.D course in both teaching and academic terms. I am indebted to my dissertation committee, Prof. Kiseon Kim, Prof. Jinho Choi, Prof. Jong-Seon No from the Seoul National University, and Prof. Mikael Skoglund from the KTH Royal Institute of Technology, for their help and advice throughout this review. I would also like to express my sincere appreciation and affection to all colleagues in the INFONET Lab and Sensor System Lab of the Gwangju Institute of Science Technology (GIST) for their friendship and support over the past years. I have shared with them enlightening discussions, gratifying experiments, and we have had many great times together. In addition, I would like to thank my friends for unforgettable memories throughout the time being with them.

Most importantly, I wish to express my deepest gratitude to my parents. Your support, love, and faith alone kept me going in the hard times. A portion of this degree should be conferred to you. Finally, I wish to thank my wife, Kye-Ok, for her love and invaluable support. Without her patience and sacrifice, everything would have been much harder. And my daughter, Chae-Yeon, has given our family a joy of life since she was born. I love my family forever.

Contents

| | |
|--|-----------|
| Abstract (Korean) | i |
| Abstract (English) | iii |
| Acknowledgements | vi |
| Contents | vii |
| List of Tables | x |
| List of Figures | xi |
| List of Symbols | xv |
| 1 Introduction | 1 |
| 1.1 Motivation | 3 |
| 1.2 Research Background | 4 |
| 1.2.1 Compressed Sensing | 5 |
| 1.2.2 Network Coding | 8 |
| 1.3 Contributions and Outline of this Dissertation | 12 |
| 2 Lower and Upper bounds on Recovery of Sparse Signals over Finite Fields | 20 |
| 2.1 Introduction | 20 |
| 2.2 Description of Compressed Sensing Frameworks | 21 |
| 2.3 Upper and Lower Bounds for Recovery Performance | 22 |
| 2.3.1 Probability of Error for L_0 norm Minimization | 22 |
| 2.3.2 Upper Bound | 24 |
| 2.3.3 Lower Bound | 28 |
| 2.4 Numerical Results and Discussion | 30 |
| 2.5 Conclusions | 33 |
| 3 Recovery Algorithm for Compressed Sensing Frameworks over Finite Fields | 34 |
| 3.1 Introduction | 34 |
| 3.2 Compressed Sensing over Finite Fields | 35 |
| 3.2.1 System Description | 35 |

| | | |
|----------|---|-----------|
| 3.2.2 | Connection to Syndrome Decoding | 36 |
| 3.3 | Recovery Algorithm of Sparse Signals | 37 |
| 3.3.1 | Message Passing Algorithm | 37 |
| 3.3.2 | Probabilistic Decoding Algorithm for Recovery of Sparse Signals | 39 |
| 3.4 | Simulation and Discussion | 40 |
| 3.4.1 | Simulation Results | 40 |
| 3.5 | Conclusion | 44 |
| 4 | New Performance Evaluation Framework of Cooperative Wireless Networking Schemes with Random Network Coding | 45 |
| 4.1 | Introduction | 45 |
| 4.2 | Other Recent Works and Relation to Our Work | 50 |
| 4.3 | Cooperative Network | 53 |
| 4.4 | Modeling of Transmission Matrices | 56 |
| 4.4.1 | Transmission Matrix | 56 |
| 4.4.2 | Modeling of Random Elements | 61 |
| 4.5 | Upper Bound on Reconstruction of Messages | 64 |
| 4.5.1 | Homogeneous and Heterogeneous Connectivity | 67 |
| 4.5.2 | General Connectivity | 72 |
| 4.5.3 | Asymptotic Nullity | 78 |
| 4.6 | Numerical and Simulation Results | 80 |
| 4.7 | Conclusions | 88 |
| 5 | Outage Probability for Cooperative Network Coding Schemes | 90 |
| 5.1 | Introduction | 90 |
| 5.2 | System Description | 91 |
| 5.2.1 | Cooperative Schemes | 91 |
| 5.2.2 | Channel Model | 94 |
| 5.2.3 | Outage Probability | 96 |
| 5.3 | Outage Probability for Cooperative Coding Schemes | 97 |
| 5.3.1 | Outage Events in Cooperative Networks | 98 |
| 5.3.2 | Derivation on Outage Probability | 99 |
| 5.3.3 | Performance Evaluation for Various Channel Environments . . . | 104 |

| | | |
|----------|---|------------|
| 5.4 | Power Efficiency Schemes | 105 |
| 5.4.1 | Coverage Expansion | 107 |
| 5.4.2 | Optimal Power Allocation | 111 |
| 5.5 | Conclusions | 119 |
| 6 | Conclusions and Future Research | 121 |
| 6.1 | Summary and Conclusions | 121 |
| 6.2 | Directions for Future Research | 123 |
| 6.2.1 | Construction of Sensing Matrix over Finite Fields | 123 |
| 6.2.2 | Sparse Representation over Finite Fields | 124 |
| | Bibliography | 126 |

List of Tables

| | | |
|-----|---|-----|
| 2.1 | The number of difference vectors $N_{h,k_1,k_2,t}$ | 26 |
| 4.1 | Summary of Recent Techniques for Cooperative Communications. | 50 |
| 4.2 | Determination of the Transmission Matrix for all Cases of Failures for $q = 2$, where “O” indicates no outage, “×” indicates an outage, and “-” indicates Don’t care | 60 |
| 4.3 | Determination of the Conditional Joint Probability for the Two Elements β_{11} and β_{12} “O” indicates no outage and “×” indicates an outage | 77 |
| 5.1 | Transmitting messages for two nodes according to the four cases. | 100 |

List of Figures

| | | |
|-----|--|----|
| 1.1 | An simplified model of input–output processing. | 2 |
| 1.2 | Linear inverse problems in compressed sensing and cooperative networks. | 3 |
| 1.3 | An Butterfly Network. Sources A and B send their information: (a) to the receiver E using the conventional routing, (b) to the receiver F using the conventional routing, (c) to E and F using NC. | 9 |
| 1.4 | Nodes A and C exchange a pair of messages using relay B: (a) without NC in 4 transmissions, (b) with NC in 3 transmissions. | 10 |
| 1.5 | Mixing information streams offer natural protection against wiretapping, (a) without NC, (b) with NC. | 11 |
| 1.6 | Contributions of this dissertation for compressed sensing and cooperative networks. | 15 |
| 2.1 | One example for \mathbf{x} and $\bar{\mathbf{x}}$ | 25 |
| 2.2 | Lower bounds for $N = 1000$ (note that if N is sufficiently large and $\gamma = 1 - q^{-1}$, the upper and lower bounds coincide with each other). Solid black line indicates the lower bound [56] in the real number, $M \geq K$ | 31 |
| 2.3 | Upper and lower bounds with different sparse factors for $N = 1000$ and $q = 4$. In the region above the upper bound, the probability of error is less than 10^{-2} , while in the region below the lower bound, the probability of error is greater than 10^{-2} | 32 |
| 3.1 | A CS framework over a finite field. | 35 |

| | | |
|-----|---|----|
| 3.2 | Graphical representation of the sensing matrix \mathbf{A} with the measured signal \mathbf{y} and the sparse signal \mathbf{x} | 38 |
| 3.3 | Failure probability for recovery of sparse signals with fixed $N = 1200$, $M = 600$, and $\epsilon = 0.1$ varying K | 42 |
| 3.4 | Failure probability for recovery of sparse signals with fixed $N = 1200$, $M = 600$, and $K = 120$ varying ϵ | 43 |
| 4.1 | An (N, M) cooperative network with N sources and M relays. | 54 |
| 4.2 | The $(2,1)$ cooperative wireless network with $N = 2$ and $M = 1$. The solid lines indicate the broadcasting phase, and the dashed line indicates the relay phase. | 58 |
| 4.3 | The nullity of random matrix \mathbf{A} for a homogeneous $(10, M)$ cooperative wireless network with $N = 10$ and $M = 3, 10$, and 20 . Solid lines indicate the upper bounds on $\mathbb{E}[\text{nullity}(\mathbf{A})]$ using Proposition 4.6, and markers indicate numerically simulated results of $\mathbb{E}[\text{nullity}(\mathbf{A})]$, respectively: (a) $q = 2$ and (b) $q = 4$ | 81 |
| 4.4 | Upper bounds on $\mathbb{E}[\text{nullity}(\mathbf{A})]$ using Proposition 4.3 and 4.7 in a heterogeneous $(20, 20)$ cooperative wireless network with two outage probabilities δ_1 and δ_2 for (a) $q = 2$, and (b) $q = 4$ | 82 |
| 4.5 | (a) Location of 16 sources and 6 relays in 2D space for an $(16, 6)$ cooperative wireless network. (b) Results of upper bounds on $\mathbb{E}[\text{nullity}(\mathbf{A})]$ with differing NC field sizes $q = 2, 4$, and 8 , (c) varying the number of relays at $q = 4$ | 84 |

| | | |
|-----|---|-----|
| 4.6 | (a) Comparison of upper bounds on $\mathbb{E}[\text{nullity}(\mathbf{A})]$ for the uniform and MDS distributions. (b) Comparison of the decoding failure probabilities with the numerical simulation and the upper bound using Proposition 4.8 for $q = 2$ and 4. | 85 |
| 4.7 | (a) Location of 100 sources and 10 relays in 2D space for an (100, 10) cooperative wireless network, (b) Comparison of $\mathbb{E}[\text{nullity}(\mathbf{A})]$ with numerically simulated result and the asymptotic upper bound Corollary 4.9 with $q = 2$ and the uniform distribution. (c) Comparison of decoding failure probability with the numerical simulation and the upper bound using Corollary 4.9. | 86 |
| 5.1 | Two transmissions for cooperative schemes: (a) broadcasting, (b) relaying. Solid lines indicate the transmission of N1, and dashed lines for N2. | 91 |
| 5.2 | Four cooperative scenarios for relay phase transmission based on the decoding results in the broadcasting phase. | 99 |
| 5.3 | Exact outage probability with BNC and NBNC-4 for N1: $P_1 = P_2$, (a) $\sigma_{1,d}^2 = 1, \sigma_{2,d}^2 = 125, \sigma_{1,2}^2 = 2$, (b) $\sigma_{1,d}^2 = 1, \sigma_{2,d}^2 = \sigma_{1,2}^2 = 8$, (c) $\sigma_{1,d}^2 = 1, \sigma_{2,d}^2 = 2, \sigma_{1,2}^2 = 125$ | 106 |
| 5.4 | Contour plot of the locations of the source node (N1) whose outage probability is less than or equal to 10^{-4} , with the fixed BS and N2 locations as shown in the plot: the blue and red lines indicate for BNC and NBNC-4 schemes, respectively. | 109 |

| | | |
|-----|---|-----|
| 5.5 | Coverage area of the source node (N1) for the outage probability of 10 ⁻⁴ with the fixed BS and N2 in a 2D space: the blue and red lines indicate for BNC and NBNC-4 schemes. | 110 |
| 5.6 | Outage probability as a function of total transmit power: (a) $P_1 = P_2$, (a) $\sigma_{1,d}^2 = \sigma_{2,d}^2 = \sigma_{1,2}^2 = 1$, (b) $\sigma_{1,d}^2 = 1, \sigma_{2,d}^2 = \sigma_{1,2}^2 = 8$, (c) $\sigma_{1,d}^2 = 1, \sigma_{2,d}^2 = 0.125, \sigma_{1,2}^2 = 0.037$ | 115 |
| 5.7 | Outage probability as a function of the power allocation ratio ρ at $P_t/N_0 = 20$ dB. | 116 |
| 5.8 | Optimum ratio of power allocation for the position of the relay node (N2) from 0 to 1 at $P_t/N_0 = 20$ dB. | 117 |

List of Symbols

| | |
|------------------------------|--|
| \mathbb{R} | Real number |
| \mathbb{F}_q | Finite field of Size q |
| $\Pr \{\cdot\}$ | Probability |
| $\mathbb{E}[\cdot]$ | Expectation |
| \mathbf{A} | Matrix \mathbf{A} |
| \mathbf{x} | Vector \mathbf{x} |
| \mathcal{L} | Set \mathcal{L} |
| $\text{rank}(\mathbf{A})$ | Rank of the matrix \mathbf{A} |
| $\text{nullity}(\mathbf{A})$ | Nullity of the matrix \mathbf{A} |
| $\ \mathbf{x}\ _0$ | The number of nonzero entries of the vector \mathbf{x} |
| $\prod(\cdot)$ | Product |
| $\setminus \{\dots\}$ | Exclusion of the elements $\{\dots\}$ |
| $\binom{\cdot}{\cdot}$ | Binomial coefficient |
| $H_b(\cdot)$ | Binary entropy |
| $I(\cdot)$ | Mutual information |
| $C(\cdot)$ | Channel capacity |
| N_0 | Power spectral density of noise |

Chapter 1

Introduction

The aim of collecting data is to obtain meaningful information about a physical system or phenomenon of interest. However, in many situations the quantities that we wish to determine are different from the ones which we are able to measure, or have measured. If the measured data is quite related to the quantities we want in some ways, then the data at least contains some information about those quantities. Starting with the data that we have measured, the problem of trying to reconstruct the quantities that we really want is called an inverse problem [1]. In general, the inverse problem is a general framework that is used to convert observed measurements into information about a physical object or system that we are interested in.

Suppose that we have a mathematical model of a physical process. We assume that this model gives a description of the system behind the process and its operating conditions and explains the principal quantities of the model: *input*, *system function*, *output* as shown in Figure 1.1. The analysis of the given process via the mathematical model may then be separated into three different types of problems.

- (A) **Forward problem.** Given the input and the system function, find out the output of the model.

- (B) **Inverse problem.** Given the system function and the output, find out which

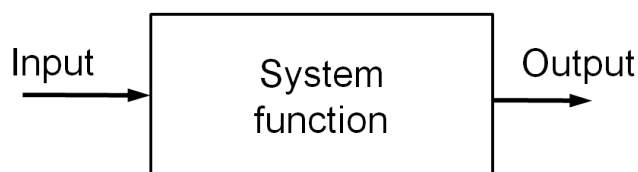


Figure 1.1: An simplified model of input–output processing.

input has led to this output

(C) **Identification problem.** Given the input and the output, determine the system function which is in agreement with the relation between input and output.

We call a problem of type (A) a forward problem since it is oriented towards a cause-effect sequence. In this sense, problems of type (B) and (C) are called inverse problems because they are problems of finding out unknown causes of known consequences. Due to uncertainty of the unique solution, most researches have been mainly focused on the inverse problems.

Here are some typical inverse problems: computed tomography [2], [3], deconvolution [4], navigation [5], image analysis [6], geophysics [7], [8], model fitting [9], gridding or regridding [10], radio-astronomical imaging [11], numerical analysis [12]. From this very short and incomplete list, it is apparent that inverse problem theory is an important topic and its applications can be found in many different fields. Examples of domains where it is possible and required to apply inverse problems and model fitting mathematical methods for image reconstruction are astronomy, medical imaging microscopy.

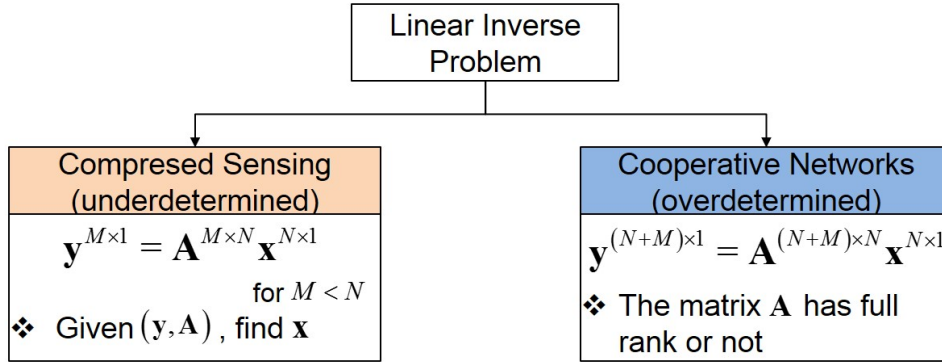


Figure 1.2: Linear inverse problems in compressed sensing and cooperative networks.

1.1 Motivation

In this dissertation, we consider linear inverse problems in the areas of Compressed Sensing (CS) and cooperative wireless networks using Network Coding (NC). This dissertation deals with recovery of unknown signals over a finite field or Galois field (GF), which is a field that contains a finite number of elements, instead of real and complex-valued numbers. The reason to be considered can be found as follows. Let us consider measurements of real-valued signals in practical situations. The signals are acquired from continuous values, and measurements are performed with linear combinations of data in a real field as well. In practice, measurements are often digitized, and operations at sensors or equipment are optimized to preserve a limit resource. For this reason, different to the previous works, data manipulation in the proposed method of this dissertation is performed in a finite field of arbitrary size, which restricts us from straightforward development of performance evaluation frameworks for inverse problems.

The CS problem is regarded as one of the linear inverse problems. In other words, given a sensing matrix and an measured signal, a feasible signal is found. In CS, this is an underdetermined problem, which means that the dimension of the input signal is greater than that of the output signal. A core idea to solve the CS problem comes from that the sparsity of the input signal is exploited. On the other hand, the problem of cooperative networks we consider in this dissertation deals with an overdetermined system. The solutions for cooperative wireless coding schemes are obtained from inversions of the system functions. Figure 1.2 shows mathematical expressions for CS and cooperative networks problems we consider in this dissertation.

We narrow down our interest of research to the areas of CS and cooperative wireless networks over finite fields. More specifically, the following questions are answered in this dissertation: i) how can we efficiently estimate an unknown signal given a system function and an output signal, ii) recovery bounds required for successful reconstruction of the input signals are investigated in terms of key parameters of the interested system, e.g., the dimensions of input and output signals, the characteristics of a system function, and the size of finite fields.

1.2 Research Background

The following overview for CS and NC is briefly described. More details of both theories are referred to: [13]-[16] for CS, and [17]-[21] for NC.

1.2.1 Compressed Sensing

Recently, CS theory has emerged as a new paradigm for signal acquisition in which compression and sampling of signals can be done simultaneously, introduced in the signal processing and information theory, such as Candes and Tao [13] and Donoho [14]. One of the main issues in the CS problems has been to quantify how many measurements are needed for perfect recovery of unknown signals. The most surprising and interesting conclusion is that perfect recovery is possible with the number of measurements much smaller than the ambient dimension of the unknown signal as long as the signal is sufficiently sparse in a certain domain.

We say a signal $\mathbf{x} \in \mathbb{R}^N$ is K sparse in a basis Ψ if the following holds,

$$\mathbf{x} = \Psi \mathbf{s}, \tag{1.1}$$

for some $\mathbf{s} \in \mathbb{R}^N$ with no more than K nonzero elements. This notion of sparsity is commonly applied as a means to compress signals. Rather than measuring all elements of \mathbf{x} , we can store the few nonzero elements in \mathbf{s} . One of examples is a transform coding for the compression of natural images. While the naive representation of an picture is a description of each pixel, we minimize storage space by utilizing transformed elements in its frequency or wavelet domain, and discarding meaningless elements. This use of the sparsity of signals requires all the elements of \mathbf{x} to be measured before transformation, but, it motivates the question of whether we can use the sparsity of \mathbf{x} to not only compress it, but also measure it more efficiently. Why measure a signal only to discard much of what is measured? CS theory has shown that we can indeed preserve a completion of a signal \mathbf{x} using far fewer than measurements.

CS performs this with a general idea of measurement. In CS, a measurement is obtained from a linear combination of a row of a matrix and a signal \mathbf{x} as an inner product. Let Φ be the sensing (or measurement) matrix. A vector of measurements $\mathbf{y} \in \mathbb{R}^M$ can be written by

$$\mathbf{y} = \Phi \mathbf{x} = \Phi \Psi \mathbf{s} = \Theta \mathbf{s}. \quad (1.2)$$

If we use $M < N$, Θ is a flat matrix, and the unique recovery of \mathbf{s} from \mathbf{y} and Θ is unfeasible. The interesting result of CS is that, with a good choice of the sensing matrix Φ and the fact that \mathbf{x} is sparse in a certain domain, we can recover the signal \mathbf{x} [13]–[15].

In CS, two major issues are considered: i) construction of a stable sensing matrix such that the salient information in any K sparse or compressible signal is not damaged by the dimensional reduction from the vector \mathbf{x} , ii) a recovery algorithm to reconstruct the sparse vector \mathbf{x} from only M measurements.

Due to the fact, $M < N$, the problem of (1.2) is ill-conditioned. If, however, the signal \mathbf{x} is K sparse and the K locations of the nonzero coefficients are known, then the problem can be solved provided $M \geq K$. A necessary and sufficient condition for this simplified problem under the known locations of the nonzero coefficients in \mathbf{x} is that, for any vector ν sharing the same K nonzero entries as \mathbf{s} and for some $\epsilon > 0$,

$$(1 - \epsilon) \|\nu\|_2^2 \leq \|\Theta \nu\|_2^2 \leq (1 + \epsilon) \|\nu\|_2^2 \quad (1.3)$$

In other words, the matrix Θ must project the energy of these particular K sparse vectors without loss. A sufficient condition for a stable solution for both K sparse and

compressible signals is that Θ satisfies (1.3) for an arbitrary $3K$ sparse vector ν . This condition is referred to as the restricted isometry property (RIP) [16]. For example, the Gaussian sensing matrix Φ has good properties [14] and [16]: i) incoherence with the basis Ψ and ii) being universal in the sense that the matrix Θ will be identically and independent distributed (i.i.d.) Gaussian and thus have the RIP with high probability regardless of the choice of orthonormal basis Ψ .

For recovery of the signal \mathbf{s} , the optimization problem is set as

$$\hat{\mathbf{s}} = \arg \min_{\bar{\mathbf{s}}} \|\bar{\mathbf{s}}\|_p, \quad \text{subject to} \quad \mathbf{y} = \Theta \bar{\mathbf{s}} \quad (1.4)$$

The conventional approach to inverse problems of this optimization is to find the vector in the nullspace with the smallest L_2 norm ($p = 2$). The closed-form solution for the L_2 norm is obtained as $\hat{\mathbf{s}} = \Theta^T (\Theta \Theta^T)^{-1} \mathbf{y}$. However, this conventional solution gives us a non-sparse solution, and may not be appropriate. For the L_0 norm ($p = 0$), the solution to this problem recover a K sparse signals exactly with high probability using only $M = K + 1$ i.i.d. Gaussian measurements. However, solving (1.4) is known to be NP hard. Based on the L_1 norm ($p = 1$), the optimization problem can exactly recover K sparse signals and closely approximate compressible signals with high probability using only $M \geq cK \log(N/K)$ with i.i.d. Gaussian measurements [14] and [16]. This is a convex optimization problem that conveniently reduces to a linear program known as basis pursuit [14] and [16] whose computational complexity is about $\mathcal{O}(N^3)$.

1.2.2 Network Coding

The concept of NC was first proposed by Ahlswede *et al.* in [17]. With the advent of NC, the simple but interesting result was made that in network systems, we can allow intermediate nodes to not only forward but also process the incoming independent messages. Combining independent messages at a node enables us to maximize the information flow in the networks. Since then, NC has been a recent alternative to routing that offers the potential to surpass performance limits (i.e., throughput, delay, and optimization of wireless resources) throughout various network environments.

NC provides some benefits in the areas of communication networks, i.e., throughput, wireless resources and security. Showing the following examples for the benefits of NC, we illustrate the basic notions of NC.

■ Maximizing Throughput [17]-[19]

Let us consider the butterfly network shown in Figure 1.3, assuming that per time slot one bit can be sent through corresponding channel. There are two sources A and B, and two receivers E and F. Let x_1 and x_2 denote one bit of each source.

We send x_1 from A along the path (A \rightarrow E), and x_2 from B along the path (B \rightarrow C \rightarrow D \rightarrow E) to the receiver E as shown in Figure 1.3(a). Similarly, F also receives two bits x_1 and x_2 from both sources. We route x_1 from A along the path (A \rightarrow C \rightarrow D \rightarrow F), and x_2 from B along the path (B \rightarrow F) to the receiver F as shown in Figure 1.3(b).

Now suppose that both receivers wish to simultaneously receive the information from both sources. In other words, we consider multicasting schemes. We assume that

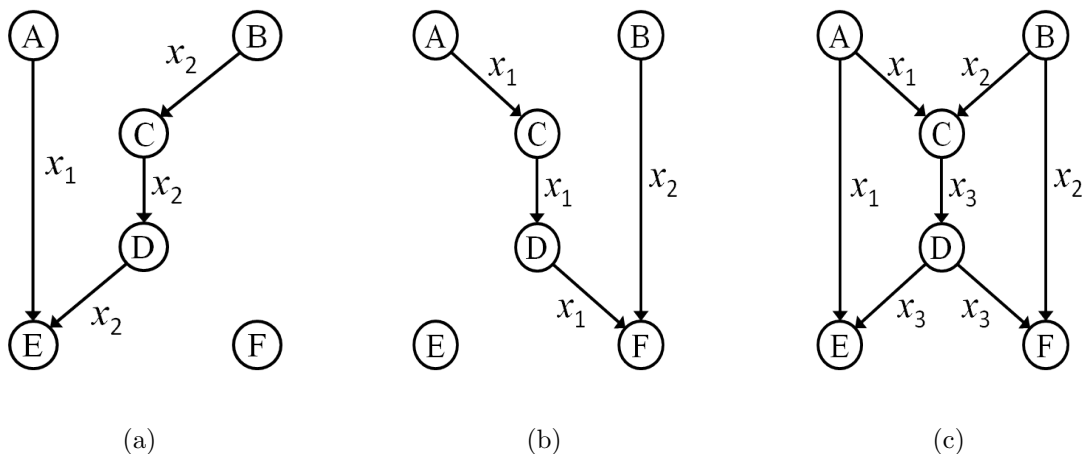


Figure 1.3: An Butterfly Network. Sources A and B send their information: (a) to the receiver E using the conventional routing, (b) to the receiver F using the conventional routing, (c) to E and F using NC.

only one bit per time slot is sent, while we wish to simultaneously send x_1 to the receiver F, and x_2 to the receiver E.

In this multicasting network, we would have to make a decision at the node C: either use it to send x_1 , or use it to send x_2 in a conventional approach. Therefore, if we send x_1 , then the receiver E will only receive x_1 , while the receiver F will receive both x_1 and x_2 .

The simple but important observation made in the seminal work by Ahlswede *et al.* is that we allow intermediate nodes in the network to process their incoming information, and not just forward them. In particular, the node C takes both bits x_1 and x_2 , and XOR them to generate a new bit as $x_3 = x_1 + x_2$, which it can be then sent via the path (C \rightarrow D). The receiver E receives x_1 and x_3 , and can retrieve x_1 and x_2 . Similarly, the receiver F receives both bits x_2 and x_3 , and can also retrieve x_1 and x_2 .

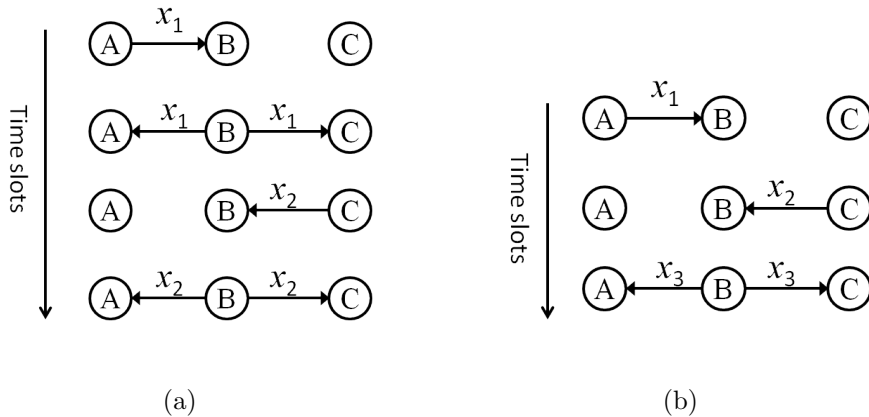


Figure 1.4: Nodes A and C exchange a pair of messages using relay B: (a) without NC in 4 transmissions, (b) with NC in 3 transmissions.

by solving the linear system.

The previous example shows that if we allow intermediate node in the network to combine information and decode the information at the receivers, we can increase the throughput when multicasting.

■ Resource Efficiency ([17], [19], and [20])

Let us consider a wireless ad-hoc network, where nodes A and C wish to exchange their information x_1 and x_2 using the node B as a relay. We assume that time is slotted, and that a node use only half-duplex communications. Figure 1.4(a) shows the conventional approach: nodes A and C send their information to the relay B, who in turn forwards each message to the corresponding destination.

NC takes advantage of the wireless nature for broadcasting to provide benefits in terms of resource utilization as shown in Figure 1.4(b). In particular, the node B receives both information x_1 and x_2 , and take XOR them to generate a new message as

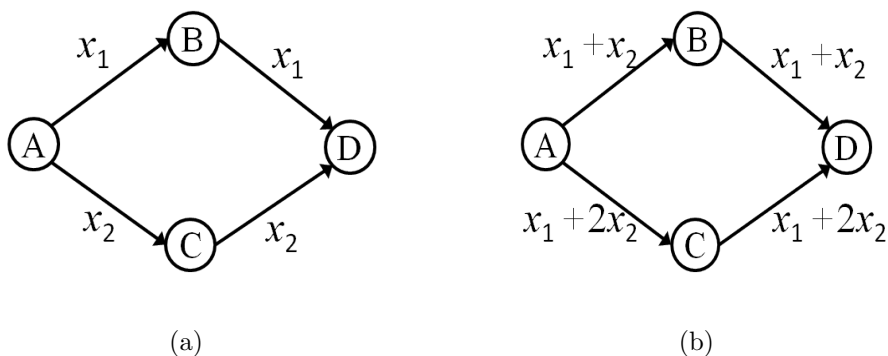


Figure 1.5: Mixing information streams offer natural protection against wiretapping, (a) without NC, (b) with NC.

$x_3 = x_1 + x_2$, which it then broadcasts to both receivers using a common transmission. The node A has x_1 and can thus decode x_2 . Also the node C has x_2 and can thus decode x_1 .

This idea offers benefits in terms of energy efficiency (the node B transmits once instead of twice), delay (the exchange of data is completed after three time slots instead of four), wireless bandwidth (the wireless channel is occupied for a smaller amount of time).

The benefits in the previous example originate from the fact that broadcasting transmissions are made maximally useful to all their receivers.

■ Security [21]

Sending linear combinations of packets instead of uncoded data provides an improved way to avoid wiretapping attacks. Thus, networks that only require protection against such simple attacks can get it for free without additional security mechanisms.

Let us consider the node A that sends information to the node D through two paths

($A \rightarrow B \rightarrow D$) and ($A \rightarrow C \rightarrow D$) shown in Figure 1.5. Assume that an adversary can wiretap a single path, and does not have access to the complementary path. If the independent uncoded symbols x_1 and x_2 are sent, the adversary can intercept one of them. If instead linear combinations (over some finite field) of the symbols are sent through the different routes, the adversary cannot decode any part of the data. Although the adversary retrieves $x_1 + x_2$ or $x_1 + 2x_2$, the symbols x_1 and x_2 cannot be decoded successfully.

NC allows intermediate nodes to perform encoding operations on packets traversing the network [17]. Interestingly, linear mixing of packets is sufficient for achieving multicast capacity in wireline networks [18], [19]. This optimality result has encouraged harvesting the benefits of linear NC to areas as diverse as distributed storage [22], [23], peer-assisted file delivery [24], streaming media [25], [26], [27], network tomography [28], [29], security [30], [31], data collection in sensor networks [32], and ad hoc networks [33]. The potential of NC in wireless applications is also well appreciated by now [34], [35], and some of the early prototypes include [36], [37]. The emerging conclusion is that NC is not just a simple routing, but a new paradigm for information collection, storage, and dissemination.

1.3 Contributions and Outline of this Dissertation

The first part of this dissertation considers the inverse problems of CS schemes for recovery of sparse signals in Chapter 2 and 3, which were published in [38]–[40].

[38] **Jin-Taek Seong** and Heung-No Lee, “Necessary and Sufficient Conditions for

Recovery of Sparse Signals over Finite Fields,” *IEEE Communications Letters*, vol. 17, no. 10, pp. 1976–1979, Oct. 2013.

- [39] **Jin-Taek Seong** and Heung-No Lee, “Method for reconstructing sparse signal in finite field, apparatus for reconstructing sparse signal in finite field, and recording medium for recording reconstruction method,” *US patent*, Pending, PCT/KR2013/004875.
- [40] **Jin-Taek Seong** and Heung-No Lee, “Concatenation of LDPC codes with Golden Space-Time Block Codes over the Block Fading MIMO Channels: System Design and Performance Analysis,” *45th Annual Conference on Information Science and Systems (CISS)*, MD, USA, Mar. 2011.

The second part of this dissertation considers the inverse problems of cooperative wireless networks for recovery of source information in Chapter 4 and 5, for more details, see [41]–[45].

- [41] **Jin-Taek Seong** and Heung-No Lee, “Predicting the Performance of Cooperative Wireless Networking Schemes with Random Network Coding,” *Early Access, IEEE Transactions on Communications*
- [42] **Jin-Taek Seong** and Heung-No Lee, “4-ary Network Coding for Two Nodes in Cooperative Wireless Networks: Exact Outage Probability and Coverage Expansion,” *EURASIP Journal on Wireless Communications and Networking*, 2012:366, Dec. 2012.

- [43] **Jin-Taek Seong** and Heung-No Lee, “Evaluation Framework for Reconstruction of Messages in Cooperative Coding Schemes of Multiple-Sources and Multiple-Relays,” *IEEE International Conference on Computing, Networking and Communications (ICNC)*, Honolulu, USA, Feb. 2014.
- [44] **Jin-Taek Seong** and Heung-No Lee, “Exact Outage Probability of Two Nodes for Cooperative Networking using GF(4),” *IEEE International Workshop Signal Processing Advances in Wireless Communications (SPAWC)*, Darmstadt, Germany, Jun. 2013.
- [45] **Jin-Taek Seong** and Heung-No Lee, “Exact Outage Probability and Power Allocation of Two Nodes in Cooperative Networks,” *IEEE International Wireless Communications and Networking Conference (WCNC)*, Shanghai, China, Apr. 2013.

Let us consider the problem of the data collection of spatially correlated measurements in a wireless sensor network. All sensors quantize their measured values, and map them to q level symbols. In decoding processing, each decoded symbol is reversed to a quantized value with one-to-one corresponding. A sink receives coded packets which are linear combinations of source packets over finite fields in a cooperative scheme. In this case, NC is used for data delivery at intermediate nodes. Due to the physical nature of the sensed phenomenon, and to the spatial distribution of the nodes in the network, correlation between the measurements at different nodes occurs. It means that measured values at nodes are represented as sparse signals in a certain domain, which

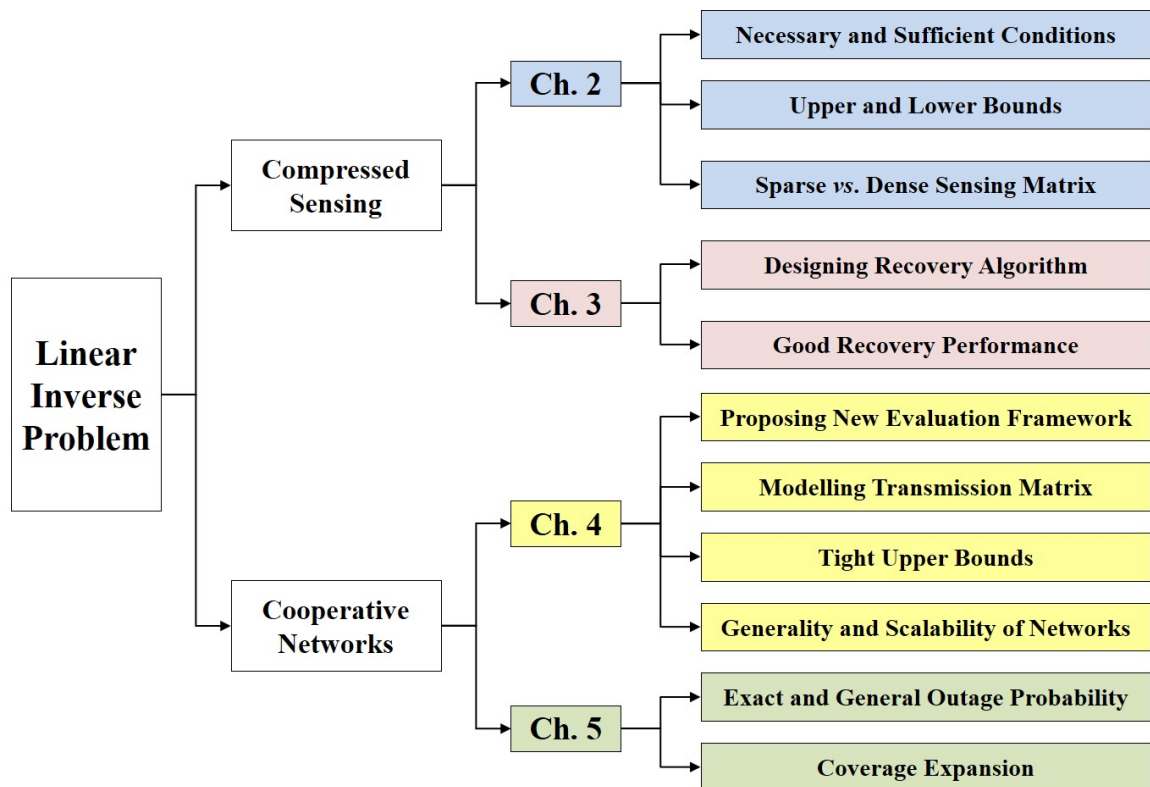


Figure 1.6: Contributions of this dissertation for compressed sensing and cooperative networks.

has been well known in CS theory. Thus, this problem of cooperative communications combined with NC is connected to the problem of CS over finite fields. Several papers discuss reconstruction of correlated signals in wireless sensor networks, e.g., [46], [47], and [48]. The following describes the contributions of each chapter in detail.

In general, the problems of CS have been considered mainly over the field of real and complex numbers. One of the key points in CS problems is to minimize the number of measurements while unknown signals are perfectly recovered. In this chapter, we aim to again investigate the core question of CS problems, but for the CS systems over finite fields where the sparse signals, the sensing matrix, and the measurements are made of the elements from a finite field. We use the ideal L_0 norm (which is equal to the Hamming weight in coding theory) minimization with a goal of providing benchmark to performance of any practical recovery routines. We address in Chapter 2 the problem of reconstruction of sparse signals over finite fields. We derive sufficient and necessary conditions for recovery of sparse signals in terms of the ambient dimension of the signal space, the sparsity of the signal, the number of measurements, and the field size. We show that the sufficient condition coincides with the necessary condition if the sensing matrix is sufficiently dense while both the length of the signal and the field size grow to infinity. One of the interesting conclusions includes that unless the signal is very sparse, the sensing matrix does not have to be dense to have the upper bound coincide with the lower bound. Recently, [49] as an extension of our work [38] showed necessary and sufficient conditions for exact recovery of sparse signals, assuming a Bayesian setting and MAP decoding. The authors considered three classes of prior

distributions on the signal vector: i) elements are statistically independent, and the signal vector is ii) a Markov process and iii) an ergodic process. The result of our work is the same of the work [49], considering that there exists no communications noise and no measurement noise. In addition, Draper and Malekpour [50] showed the error exponents for recovery of sparse signals using uniform sensing matrices over finite fields. Tan *et al.* [51] extended the work of [50] to the problem of rank minimization, and showed that the minimum rank decoder achieves the information theoretic lower bound as long as the fraction of nonzero entries of the sensing matrices scales as $\Omega(\frac{\log N}{N})$ where N denotes the size of signals.

Furthermore, in Chapter 3, we propose a recovery algorithm of sparse signals for a CS framework. The main idea of this algorithm originates from the message passing algorithm in coding theory. A probability passing in the recovery algorithm is derived which utilizes the *a priori* information of signal sparsity. The Gallager's low density parity check codes (LDPC) are used as sensing matrices. We show that proposed algorithm is practical and useful when the size of signals increases. In addition, Rajawat *et al.* [48] proposed a network-compressive transmission protocol, and modeled statistical dependencies of source information by using factor graphs. The authors developed a sum-product algorithm to estimate a set of measured values.

Next, we study in Chapter 4 a performance evaluation framework for a cooperative wireless network in which there are multiple sources and multiple relays. The inherent nature of wireless channels includes that unreliable links occur between users; this in turn leads to variant network connections in the spatial and temporal domains. In

other words, when a user cannot successfully decode incoming messages received from other users, the corresponding link failure results in the modification of the network code matrix. Since an intermediate node is not able to combine the failed messages to generate coded messages, the predefined coefficients of a network code matrix cannot be used for linear combinations in NC schemes. For performance evaluation of these dynamic network topologies, in [68] and [69], Xiao and Skoglund proposed a DNC scheme varying the network code matrices according to the conditions of the wireless links. Furthermore, Rebelatto *et al.* [70] extended and generalized the framework of the DNC to the GDNC to increase the rate and diversity order. In addition, Nguyen *et al.* [74] have derived upper and lower bounds on recovery performance for GDNC schemes. For random linear NC schemes, Trullols-Cruces *et al.* [73] have shown the exact decoding probability having network codes of full rank. In this chapter, we propose an analytical framework to evaluate the recovery performance of source messages at the base station. To this end, we consider a random transmission matrix by which each element of the transmission matrix as a random variable whose distribution is function of the outage probability. We derive an upper bound for the reconstruction performance, i.e., decoding failure probability and nullity. The proposed framework provides an evaluation tool which allows us to investigate the impact of a large number of sources and relays as well as the field size of network codes on the system performance.

Analyses of outage probability in cooperative networks are presented in [65]–[68], [70], [72], [116]. Chen *et al.* [66] showed that binary NC, based on the arithmetic of a Galois Field of size 2, provides improved diversity gains and bandwidth efficiencies in

wireless networks in which each user employs a simple decode-and-forward scheme that assumes a perfect inter-user channel. It was recently shown in [68] that BNC is not optimal for achieving full diversity in a system of multiple users and multiple relays. It has also been shown that full diversity order can be achieved using non-binary NC with $\text{GF}(q)$ for $q > 2$ [68], [70], [72]. In Chapter 5, we consider a cooperative wireless network with two nodes and one base station, and investigate the effect of using nonbinary NC on the enhancement in power efficiency. First, we derive the exact and general outage probability in our NC scheme. We show that full diversity order can be obtained using a nonbinary network code with $\text{GF}(4)$ in the considered network. We use this result to study the extent to which the coverage area of a wireless source node can be expanded by NC without increasing transmit power. Our results indicate that the benefit in terms of coverage expansion is substantial. The results included in this study show the influence of optimal power allocation on power efficiency. The optimum ratio of power allocation varies according to the wireless channel environments and the field size of network codes.

Finally, concluding remarks and summary of this dissertation is given in Chapter 6. Figure 1.6 briefly summarizes the overall contributions of this dissertation.

Chapter 2

Lower and Upper bounds on Recovery of Sparse Signals over Finite Fields

2.1 Introduction

In general, the problems of CS have been considered mainly over the field of real and complex numbers. One of the key points in CS problems is to minimize the number of measurements while unknown signals are perfectly recovered. There are some applications that this CS problem over finite fields can be useful, including, i) the problems of collecting data samples from a group of correlated sources [46], [47], ii) group testing [52], iii) the problem of sensor failure detection [53], and iv) minimization of file servers in order to complete download in file sharing networks [54].

For instance, in [46], Bassi *et al.* addressed the problem of the collecting spatially correlated measurements in a wireless sensor network. All sensors quantize their measured values, and map them to q -level symbols. A sink receives coded packets which are linear combinations of source packets over Galois fields. In addition, in network tomography, Firooz *et al.* [55] introduced an innovative approach based on linear NC. The authors provided sufficient conditions on NC coefficients and trade-offs between the length of training slots and the size of a finite field to uniquely detect one failure link. This network tomography allows us to consider one of CS problems in finite fields

as long as failure links of the network are sparse.

In this chapter, we aim to investigate the core question of CS problems, but for the CS systems over finite fields where the sparse signals, the sensing matrix, and the measurements are made of the elements from a finite field. We use the ideal L_0 norm (which is equal to the Hamming weight in coding theory) minimization with a goal of providing benchmark to performance of any practical recovery routines. We first derive an upper bound on the probability of error. By using Fano's inequality [57], we derive a lower bound. We show that the upper bound and the lower bound converge with each other if the sensing matrix is sufficiently dense

2.2 Description of Compressed Sensing Frameworks

We describe the CS framework over a finite field of size q , \mathbb{F}_q : Let $\mathbf{x} \in \mathbb{F}_q^N$ be a sparse signal of length N with sparsity k_1 which indicates the number of nonzero entries in \mathbf{x} , $k_1 \in \{1, 2, \dots, K\}$, where K , $2K \leq N$, denotes the maximum number of nonzero entries in \mathbf{x} . Let \mathcal{L} denote the set of sparse signals, $\mathcal{L} := \bigcup_{k_1=1}^K \mathcal{L}_{k_1}$ where \mathcal{L}_{k_1} denotes the set of signals \mathbf{x} of length N with sparsity k_1 . The size of the set \mathcal{L} is given by $|\mathcal{L}| = \sum_{k_1=1}^K \binom{N}{k_1} (q-1)^{k_1}$ where $|\cdot|$ denotes the cardinality of the set. A sparse signal \mathbf{x} is randomly and uniformly selected from the set \mathcal{L} . Let $\mathbf{A} \in \mathbb{F}_q^{M \times N}$ be an $M \times N$ sensing matrix with $N > M$. The measured signal \mathbf{y} is given by

$$\mathbf{y} = \mathbf{A}\mathbf{x}. \tag{2.1}$$

We assume that the elements of the sensing matrix \mathbf{A} are independent and identi-

cally distributed (i.i.d.), so that

$$\Pr\{A_{ij} = \alpha\} = \begin{cases} 1 - \gamma, & \text{if } \alpha = 0 \\ \gamma/(q - 1), & \text{if } \alpha \neq 0 \end{cases} \quad (2.2)$$

where γ denotes the sparse factor which is the probability that an element of the sensing matrix has nonzero values, and A_{ij} denotes the element of the i th row and the j th column of the sensing matrix, for $i \in \{1, 2, \dots, M\}$ and $j \in \{1, 2, \dots, N\}$, and α denotes a dummy variable, i.e., $\alpha \in \mathbb{F}_q$.

2.3 Upper and Lower Bounds for Recovery Performance

2.3.1 Probability of Error for L_0 norm Minimization

In this section, we aim to derive an upper and a lower bound for recovery of sparse signals in a CS framework for given parameters, i.e., N , K , M , and γ . We assume that the decoder in our scheme finds the sparsest feasible solution $\hat{\mathbf{x}}$ using the L_0 norm minimization as follows,

$$(\mathbf{P}_0) \quad \hat{\mathbf{x}} = \min \|\bar{\mathbf{x}}\|_0 \quad \text{subject to} \quad \mathbf{A}\bar{\mathbf{x}} = \mathbf{y}, \quad (2.3)$$

where $\bar{\mathbf{x}} \in \mathcal{L}$ is a feasible solution. Let k_2 be the sparsity of $\bar{\mathbf{x}}$ as $k_2 := \|\bar{\mathbf{x}}\|_0$.

For a given \mathbf{x} , the decision $\hat{\mathbf{x}}$ is a function of the random matrix \mathbf{A} . Let us define two sets of matrices, $\mathcal{E}_0(\mathbf{x}) := \{\mathbf{A} : \mathbf{x} \neq \hat{\mathbf{x}}\}$ and $\mathcal{E}(\mathbf{x}, \bar{\mathbf{x}}) := \{\mathbf{A} : \mathbf{A}\mathbf{x} = \mathbf{A}\bar{\mathbf{x}}\}$. Given these definitions, an error is then said to occur when a realized sensing matrix belongs to the set $\mathcal{E}_0(\mathbf{x})$, i.e., $\mathbf{A} \in \mathcal{E}_0(\mathbf{x})$. Note the following inclusion: $\mathcal{E}_0(\mathbf{x}) \subseteq \bigcup_{\bar{\mathbf{x}} \in \mathcal{L}, \bar{\mathbf{x}} \neq \mathbf{x}} \mathcal{E}(\mathbf{x}, \bar{\mathbf{x}})$. Let $\Pr\{\mathbf{x} \neq \hat{\mathbf{x}}\}$ be the probability of error averaged over all \mathbf{x} . We consider $\Pr\{\mathbf{x} \neq \hat{\mathbf{x}}\} =$

$\sum_{\mathbf{x} \in \mathcal{L}} \Pr\{\mathbf{A} \in \mathcal{E}_0(\mathbf{x})|\mathbf{x}\} \Pr\{\mathbf{x}\}$. Then, the probability of error is upper bounded by the inclusion as follows:

$$\begin{aligned}
\Pr\{\mathbf{x} \neq \hat{\mathbf{x}}\} &\leq \frac{1}{|\mathcal{L}|} \sum_{\mathbf{x} \in \mathcal{L}} \Pr\left\{\mathbf{A} \in \bigcup_{\bar{\mathbf{x}} \in \mathcal{L}, \mathbf{x} \neq \bar{\mathbf{x}}} \mathcal{E}(\mathbf{x}, \bar{\mathbf{x}}) \mid \mathbf{x}\right\} \\
&\stackrel{(a)}{\leq} \frac{1}{|\mathcal{L}|} \sum_{\mathbf{x} \in \mathcal{L}} \sum_{\substack{\bar{\mathbf{x}} \in \mathcal{L} \\ \mathbf{x} \neq \bar{\mathbf{x}}}} \Pr\left\{\mathbf{A} \in \mathcal{E}(\mathbf{x}, \bar{\mathbf{x}}) \mid \mathbf{x}\right\} \\
&\stackrel{(b)}{=} \frac{1}{|\mathcal{L}|} \sum_{\mathbf{x} \in \mathcal{L}} \sum_{h=1}^{2K} \sum_{\bar{\mathbf{x}} \in \bar{\mathcal{L}}_h(\mathbf{x})} \Pr\left\{\mathbf{A}\mathbf{x} = \mathbf{A}\bar{\mathbf{x}} \mid \mathbf{x}\right\} \\
&\stackrel{(c)}{=} \frac{1}{|\mathcal{L}|} \sum_{\mathbf{x} \in \mathcal{L}} \sum_{h=1}^{2K} \left|\bar{\mathcal{L}}_h(\mathbf{x})\right| \Pr\left\{\mathbf{A}\mathbf{d}_h = 0\right\} \tag{2.4} \\
&= \frac{1}{|\mathcal{L}|} \sum_{h=1}^{2K} \sum_{k_1=1}^K \sum_{\mathbf{x} \in \mathcal{L}_{k_1}} \left|\bar{\mathcal{L}}_h(\mathbf{x})\right| \Pr\left\{\mathbf{A}\mathbf{d}_h = 0\right\} \\
&= \frac{1}{|\mathcal{L}|} \sum_{h=1}^{2K} \Pr\left\{\mathbf{A}\mathbf{d}_h = 0\right\} \sum_{k_1=1}^K \binom{N}{k_1} (q-1)^{k_1} \left|\bar{\mathcal{L}}_h(\mathbf{x})\right| \\
&\stackrel{(d)}{=} \frac{1}{|\mathcal{L}|} \sum_{h=1}^{2K} N_h \Pr\left\{\mathbf{A}\mathbf{d}_h = 0\right\},
\end{aligned}$$

where inequality (a) is due to the union bound, and (b) is due to partition of the set $\{\bar{\mathbf{x}} \in \mathcal{L}\}$ with respect to the Hamming weight h , i.e., $\bar{\mathcal{L}}_h(\mathbf{x}) := \{\bar{\mathbf{x}} \in \mathcal{L} : \|\mathbf{x} - \bar{\mathbf{x}}\|_0 = h\}$, for $h = 1, 2, \dots, 2K$. For equality (c), we will show shortly that for each $\bar{\mathbf{x}} \in \bar{\mathcal{L}}_h(\mathbf{x})$, the probability is identically the same with each other, i.e., $\Pr\{\mathbf{A}\mathbf{x} = \mathbf{A}\bar{\mathbf{x}}|\mathbf{x}\} = \Pr\{\mathbf{A}\mathbf{d}_h = 0\}$, where $\mathbf{d}_h := \mathbf{x} - \bar{\mathbf{x}}$ denotes a difference vector with the Hamming weight h . Before moving on, please note that $\Pr\{\mathbf{A}\mathbf{d}_h = 0\} = \prod_{i=1}^M \Pr\{A_i \mathbf{d}_h = 0\}$ where A_i denotes the i th row of \mathbf{A} since the elements of \mathbf{A} are i.i.d.

For example, let us take $h = 1$. Then, it is easy to show $\Pr\{A_{i1}\beta_1 = 0\} = \Pr\{A_{i1} = 0\}$ for any $\beta_1 \in \mathbb{F}_q \setminus \{0\}$ since it follows the property of multiplication over finite fields. Thus, $\Pr\{\mathbf{A}\mathbf{x} = \mathbf{A}\bar{\mathbf{x}}|\mathbf{x}\} = \Pr\{\mathbf{A}\mathbf{d}_1 = 0\}$ for each $\bar{\mathbf{x}} \in \bar{\mathcal{L}}_1(\mathbf{x})$ re-

regardless of position of the nonzero entry in \mathbf{d}_1 . For $h = 2$ and two nonzero elements $\beta_1, \beta_2 \in \mathbb{F}_q \setminus \{0\}$, the following holds: $\Pr\{A_{i1}\beta_1 + A_{i2}\beta_2 = 0\} = \sum_{\alpha \in \mathbb{F}_q} \Pr\{A_{i1}\beta_1 = \alpha, A_{i2}\beta_2 = -\alpha\} = \sum_{\alpha \in \mathbb{F}_q} \Pr\{A_{i1} = \alpha\beta_1^{-1}\} \Pr\{A_{i2} = -\alpha\beta_2^{-1}\}$. It is trivial to show $A_{i1} = A_{i2} = 0$ for $\alpha = 0$. A little tricky is the case for any $\alpha \in \mathbb{F}_q \setminus \{0\}$. But note that both $\alpha\beta_1^{-1}$ and $-\alpha\beta_2^{-1}$ are nonzero, thus from the probability distribution (2.2), $\sum_{\alpha \in \mathbb{F}_q \setminus \{0\}} \Pr\{A_{i1} = \alpha\beta_1^{-1}\} \Pr\{A_{i2} = -\alpha\beta_2^{-1}\} = \sum_{\alpha \in \mathbb{F}_q \setminus \{0\}} \Pr\{A_{i1} = \alpha\} \Pr\{A_{i2} = -\alpha\}$. Thus, $\Pr\{A_{i1}\beta_1 + A_{i2}\beta_2 = 0\} = \Pr\{A_{i1} + A_{i2} = 0\}$. For $3 \leq h \leq 2K$, we can show $\Pr\{\sum_{j=1}^h A_{ij}\beta_j = 0\} = \Pr\{\sum_{j=1}^h A_{ij} = 0\}$ using a recursion, i.e., $\Pr\{\sum_{j=1}^h A_{ij}\beta_j = 0\} = \sum_{\alpha \in \mathbb{F}_q} \Pr\{\sum_{j=1}^{h-1} A_{ij}\beta_j = \alpha\} \Pr\{A_{ih}\beta_h = -\alpha\}$.

The last equality (d) of (2.4) is due to the collection of difference vectors with the same Hamming weight, where N_h denotes the total number of difference vectors with $\|\mathbf{x} - \bar{\mathbf{x}}\|_0 = h$, i.e., $N_h = \sum_{k_1=1}^K \binom{N}{k_1} (q-1)^{k_1} |\bar{\mathcal{L}}_h(\mathbf{x})|$, which will be exactly figured out in Chapter 2.3.2.

2.3.2 Upper Bound

In this subsection, we aim to complete the derivation on the upper bound given in (2.4). Let P_h be denoted as $P_h := \Pr\{A_i \mathbf{d}_h = 0\} = \Pr\{\sum_{j=1}^h A_{ij} = 0\}$. Given the distribution (2.2) and noting $P_0 = 1$, P_h can be rewritten in a recursive form,

$$\begin{aligned}
P_h &= \Pr\left\{\sum_{j=1}^{h-1} A_{ij} = 0\right\} \Pr\{A_{ih} = 0\} \\
&\quad + \sum_{\alpha \in \mathbb{F}_q \setminus \{0\}} \Pr\left\{\sum_{j=1}^{h-1} A_{ij} = \alpha\right\} \Pr\{A_{ih} = -\alpha\} \\
&= P_{h-1} (1 - \gamma) + (1 - P_{h-1}) \frac{\gamma}{q-1}.
\end{aligned} \tag{2.5}$$

$$\begin{array}{c}
\mathbf{x} = \left[\overbrace{x_1 \cdots x_{k_2-t}}^{k_1} \mid \overbrace{x_{k_2-t+1} \cdots x_{k_1}}^{N-k_1} \mid \overbrace{0 \cdots 0}^{N-k_1} \right] \\
\mathbf{\bar{x}} = \left[\overbrace{\bar{x}_1 \cdots \bar{x}_{k_2-t}}^{k_2-t} \mid \overbrace{0 \cdots 0}^{k_1-k_2+t} \mid \overbrace{\bar{x}_{k_1+1} \cdots \bar{x}_{k_1+t}}^t \mid \overbrace{0 \cdots 0}^{N-k_1-t} \right]
\end{array}$$

Figure 2.1: One example for \mathbf{x} and $\bar{\mathbf{x}}$.

Let $Q_h := P_h - q^{-1}$. Then, the following equality can be obtained

$$Q_h = Q_{h-1} \left(1 - \frac{\gamma}{1 - q^{-1}} \right). \quad (2.6)$$

Solving the recursion, a closed form expression for P_h is obtained

$$P_h = q^{-1} + (1 - q^{-1}) \left(1 - \frac{\gamma}{1 - q^{-1}} \right)^h. \quad (2.7)$$

Next step is to compute N_h . To this end, we use a combinatorial approach which is to enumerate all difference vectors into mutually exclusive groups with the same Hamming weight. Please see Figure 2.1 for counting N_h . Let us consider \mathbf{x} in which the first k_1 elements are nonzero and the rest of the $N - k_1$ elements are zero, i.e., $\mathbf{x} = [x_1 x_2 \cdots x_{k_1} 0 \cdots 0]$ where x_j denotes the j th element of \mathbf{x} . Let the first and second index set denote $\{1, 2, \dots, k_1\}$ and $\{k_1 + 1, k_1 + 2, \dots, N\}$ respectively. Suppose that a candidate signal $\bar{\mathbf{x}}$ has k_2 nonzero entries in total. Among them, $t \in \{0, 1, \dots, k_2\}$ nonzero elements are placed in the second index set of $\bar{\mathbf{x}}$. The rest $k_2 - t$ nonzero elements of $\bar{\mathbf{x}}$ are in the first index set as shown in Figure 2.1, where \bar{x}_j denotes the j th element of $\bar{\mathbf{x}}$.

Table 2.1: The number of difference vectors $N_{h,k_1,k_2,t}$.

| $N_{h,k_1,k_2,t}$ | $t = 0$ | $t = 1$ | $t = 2$ | $t = 3$ |
|-------------------|---------|---------|---------|---------|
| $h = 1$ | 6 | 0 | 0 | 0 |
| $h = 2$ | 12 | 63 | 0 | 0 |
| $h = 3$ | 8 | 252 | 0 | 0 |
| $h = 4$ | 0 | 252 | 567 | 0 |
| $h = 5$ | 0 | 0 | 1134 | 0 |
| $h = 6$ | 0 | 0 | 0 | 945 |

We enumerate all feasible signals $\bar{\mathbf{x}}$ with sparsity k_2 corresponding to the same Hamming weight h . It is to be noted that for a given t , the Hamming weight of the difference vector is in the following range, i.e., $k_1 - k_2 + 2t \leq h \leq k_1 + t$. Given k_1 , k_2 , and t , the number of difference vectors with the Hamming weight h for $q > 2$ can be computed by

$$N_{h,k_1,k_2,t} = \binom{N-k_1}{t} (q-1)^t \binom{k_1}{k_2-t} \binom{k_2-t}{h-2t-k_1+k_2} (q-2)^{h-2t-k_1+k_2}, \quad (2.8)$$

where the first term $\binom{N-k_1}{t} (q-1)^t$ indicates the number of sequences of the length $N-k_1$ with t nonzero entries in the second set, and the second term $\binom{k_1}{k_2-t} \binom{k_2-t}{h-2t-k_1+k_2} (q-2)^{h-2t-k_1+k_2}$ indicates the number of sequences of the length k_1 having $h-2t-k_1+k_2$ nonzero entries. For $q = 2$, the second term is $\binom{k_1}{k_2-t}$ by only considering binary sequences.

Example 2.1: Let us consider one example of counting $N_{h,k_1,k_2,t}$ where $N = 10$, $k_1 = 3$, $k_2 = 3$ and $q = 4$. There are $\binom{10}{3} (4-1)^3$ signal vectors with sparsity 3. We assume that the first 3 elements of \mathbf{x} are nonzero, i.e., $\mathbf{x} = [1110000000]$, a feasible signal $\bar{\mathbf{x}}$ has t nonzero entries in the second set, i.e., for $t = 2$, $\bar{\mathbf{x}} = [1001100000]$. In

this example, the maximum t is 3, the Hamming weight of the difference vectors ranges from 1 to 6. Table 2.1 shows the number of difference vectors, $N_{h,k_1,k_2,t}$, with respect to t and h . **End of Example**

So far, we have found $N_{h,k_1,k_2,t}$ for given k_1 , k_2 , and t . Since we aim to find N_h , we take summation with respect to k_1 , k_2 , and t ,

$$N_h = \sum_{k_1=1}^K \binom{N}{k_1} (q-1)^{k_1} \sum_{k_2=1}^{k_1} \sum_{t=0}^{k_2} N_{h,k_1,k_2,t}. \quad (2.9)$$

Substituting (2.7) and (2.9) into (2.4), we complete the derivation on the upper bound.

Theorem 2.1 (*Upper bound*). For any sensing matrix with the distribution (2.2), an upper bound on probability of error for the \mathbf{P}_0 problem is given by

$$\Pr\{\mathbf{x} \neq \hat{\mathbf{x}}\} \leq \frac{1}{|\mathcal{L}|} \sum_{h=1}^{2K} \sum_{k_1=1}^K \binom{N}{k_1} (q-1)^{k_1} \sum_{k_2=1}^{k_1} \sum_{t=0}^{k_2} N_{h,k_1,k_2,t} P_h^M. \quad (2.10)$$

This result is general. For sparse sensing matrices, one may use the distribution given in (2.2) and obtain P_h from (2.7).

For dense sensing matrices, let $\gamma = 1 - q^{-1}$ in (2.2); then, $\Pr\{A_{ij} = \alpha\} = q^{-1}$ for any $\alpha \in \mathbb{F}_q$ and the matrix becomes uniform random. In this special case, $P_h = q^{-1}$.

Note there is no dependency on h . Thus, the upper bound (2.10) can be simplified as

$$\begin{aligned} \Pr\{\mathbf{x} \neq \hat{\mathbf{x}}\} &\leq \frac{1}{|\mathcal{L}|} \sum_{h=1}^{2K} N_h q^{-M} \\ &\stackrel{(a)}{=} (|\mathcal{L}| - 1) q^{-M} \\ &< K q^{-M} \binom{N}{K} (q-1)^K \\ &\leq 2^{\log_2 K - M \log_2 q + N H_b(K/N) + K \log_2 (q-1)}, \end{aligned} \quad (2.11)$$

where $H_b(\cdot)$ denotes the binary entropy function. The equality (a) originates from the fact that $\sum_{h=1}^{2K} N_h = (|\mathcal{L}| - 1) |\mathcal{L}|$, which is the total number of sequences except for

the original vector \mathbf{x} . Consequently, from the condition that the exponent of the R.H.S. of (2.11) remains negative so that the probability of error goes to 0 as $N \rightarrow \infty$, we derive the following sufficient condition on M ,

$$M \geq \frac{\log_2 K + NH_b(K/N) + K \log_2(q-1)}{\log_2 q}. \quad (2.12)$$

Corollary 2.2 (*Sufficient condition on M*). Let $\gamma = 1 - q^{-1}$. If (2.12) is satisfied, then $\Pr\{\mathbf{x} \neq \hat{\mathbf{x}}\} \rightarrow 0$ as $N \rightarrow \infty$.

2.3.3 Lower Bound

Next, we aim to derive the lower bound on the probability of error for the \mathbf{P}_0 problem. For this, we use the Markov chain relation, a decision $\hat{\mathbf{x}}$ is made given \mathbf{A} and \mathbf{y} , i.e., $\mathbf{x} \rightarrow (\mathbf{A}, \mathbf{y}) \rightarrow \hat{\mathbf{x}}$, a standard approach in information theory. Then, by the Fano's inequality, the probability of error is lower bounded as follows,

$$\begin{aligned} \Pr\{\mathbf{x} \neq \hat{\mathbf{x}}\} &\geq \frac{H(\mathbf{x}|\mathbf{y}, \mathbf{A}) - 1}{\log_q |\mathcal{L}|} \\ &= \frac{H(\mathbf{x}) - H(\mathbf{y}|\mathbf{A}) - 1}{\log_q |\mathcal{L}|}, \end{aligned} \quad (2.13)$$

where $H(\cdot)$ denotes the entropy. According to the definition of conditional entropy, $H(\mathbf{x}|\mathbf{y}, \mathbf{A}) = H(\mathbf{x}) - I(\mathbf{x}; \mathbf{y}, \mathbf{A})$ where $I(\cdot)$ denotes the mutual information. Assuming that \mathbf{A} is independent of \mathbf{x} , we have $I(\mathbf{x}; \mathbf{y}, \mathbf{A}) = I(\mathbf{x}; \mathbf{y}|\mathbf{A})$. We use the following $I(\mathbf{x}; \mathbf{y}|\mathbf{A}) = I(\mathbf{y}; \mathbf{x}|\mathbf{A}) = H(\mathbf{y}|\mathbf{A}) - H(\mathbf{y}|\mathbf{x}, \mathbf{A})$. Since \mathbf{y} is a function of \mathbf{A} and \mathbf{x} , then $H(\mathbf{y}|\mathbf{x}, \mathbf{A}) = 0$, so that $H(\mathbf{x}|\mathbf{y}, \mathbf{A}) = H(\mathbf{x}) - H(\mathbf{y}|\mathbf{A})$. Since $H(\mathbf{y}|\mathbf{A}) \leq H(\mathbf{y}) \leq MH(y_1) \leq M \log_q q = M$ and \mathbf{x} is randomly and uniformly chosen from the

set \mathcal{L} , we obtain the lower bound,

$$\Pr\{\mathbf{x} \neq \hat{\mathbf{x}}\} \geq 1 - \frac{M+1}{\log_q |\mathcal{L}|}. \quad (2.14)$$

If the number of measurements is smaller than $\log_q |\mathcal{L}| - 1$ in the R.H.S. of (2.14), the probability of error of the CS system is strictly away from and greater than or equal to the positive number in the R.H.S. of (2.14). This means that the negated condition, $M > \log_q |\mathcal{L}| - 1$, is a necessary condition for an unboundedly arbitrary probability of error. Note the following inequities, $\log_q |\mathcal{L}| > \log_q \binom{N}{K} + \log_q (q-1)^K \geq \log_q \frac{2^{NH_b(K/N)}}{N+1} + \log_q (q-1)^K$.

Theorem 2.3 (*Necessary condition on M*). For an arbitrarily small probability of error, the following

$$M > \frac{NH_b(K/N) + K \log_2(q-1) - \log_2(N+1)}{\log_2 q}, \quad (2.15)$$

is a necessary condition.

Furthermore, in the limit case, we prove that $M > K$ is necessary and sufficient for successful recovery by solving \mathbf{P}_0 problem. To do this, from both Corollary 2.2 and Theorem 2.3, by dividing both sides of the inequalities by N , and we have $\frac{\log_q K}{N} \rightarrow 0$ in (2.12) and $\frac{\log_2(N+1)}{N} \rightarrow 0$ in (2.15) as $N \rightarrow \infty$ while the ratios M/N and K/N are fixed. In addition, when the field size goes to infinity, $q \rightarrow \infty$, then $\frac{H_b(K/N)}{\log_2 q} \rightarrow 0$ and $\frac{\log_2(q-1)}{\log_2 q} \rightarrow 1$. Thus, for both the necessary and the sufficient condition, we come to the following condition, $M > K$.

Corollary 2.4 (*Coincidence*). For fixed ratios M/N and K/N , as $N \rightarrow \infty$ and $q \rightarrow \infty$, the necessary, and the sufficient condition, for successful recovery of the K

sparse signals over finite fields \mathbb{F}_q is $M > K$.

2.4 Numerical Results and Discussion

Figure 2.2 and 2.3 shows the compression ratio ($=M/N$) versus the sparsity ratio ($=K/N$) for recovery of a K sparse signal of length $N = 1000$ at the probability of error of 10^{-2} . We consider the following size finite fields: $q = 2, 4, 16,$ and 256 . Fixing K , we find the smallest integer M satisfying the upper (2.10) and the lower bound (2.14) at 10^{-2} . One interesting feature of Figure 2.2 is that for the lower bound, the compression ratio required for recovery of unknown sparse signals dramatically decreases as the field size grows. This result means that less number of measurements is needed for a larger finite field. In addition, the upper bound for uniform random sensing matrix is nearly identical with the lower bound.

In Figure 2.2, with respect to different sparse factor γ for a fixed field size, i.e., $q = 4$, we obtain the compression ratio which satisfies the upper bound at 10^{-2} . It can be observed that a higher value of sparse factor γ is required for recovery of very sparse signals. The aim of Figure 2.2 is to show that as the sparse factor of the sensing matrix increases, the upper bound approaches the lower bound even in the region of small sparsity ratios. In other words, if the sensing matrix is sufficiently dense, the upper bound coincides with the lower bound over finite fields. It is easy to see that if the signal and the sensing matrix are both sparse, the chance of making a zero measurement gets high; then the number of measurements needs to increase so as to compensate for missed sensing opportunities.

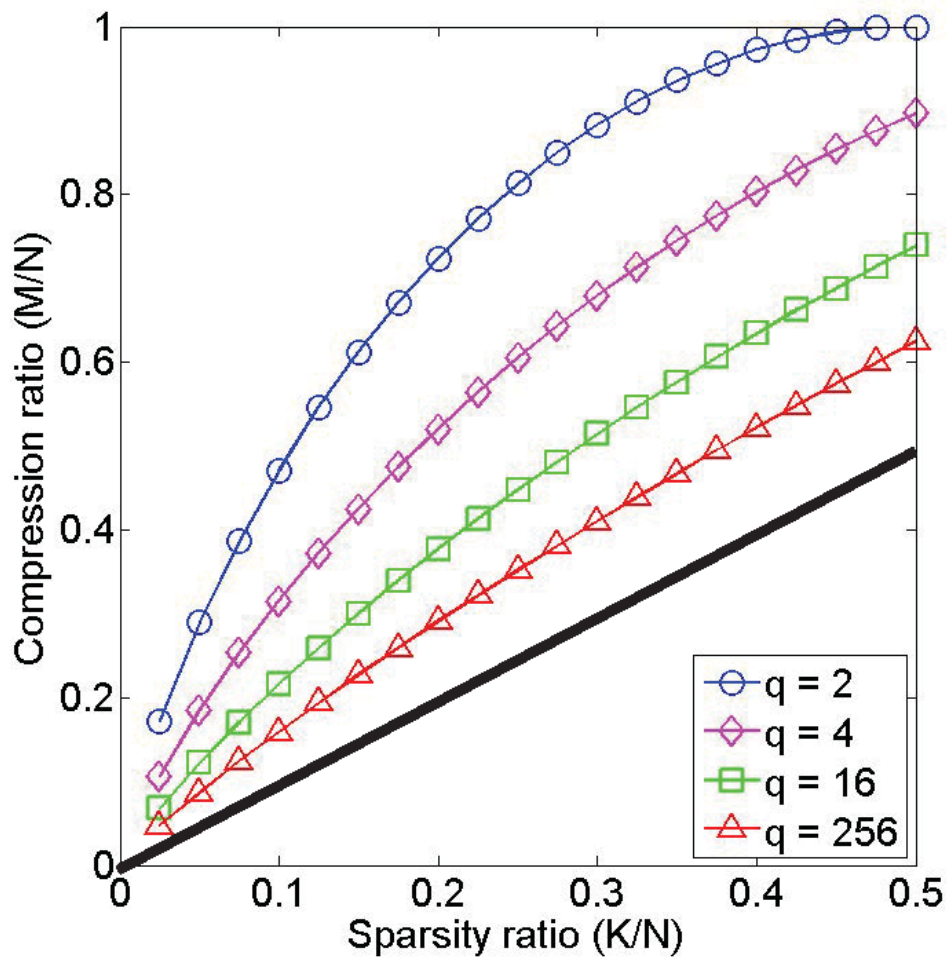


Figure 2.2: Lower bounds for $N = 1000$ (note that if N is sufficiently large and $\gamma = 1 - q^{-1}$, the upper and lower bounds coincide with each other). Solid black line indicates the lower bound [56] in the real number, $M \geq K$.

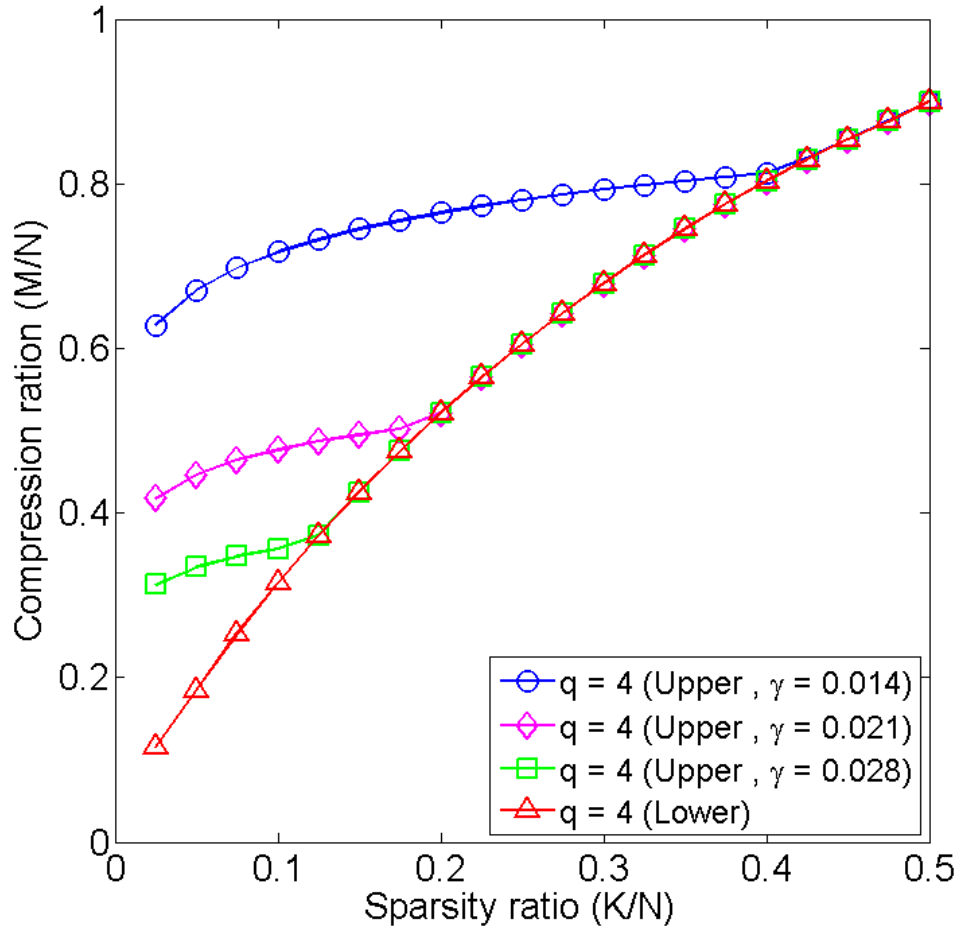


Figure 2.3: Upper and lower bounds with different sparse factors for $N = 1000$ and $q = 4$. In the region above the upper bound, the probability of error is less than 10^{-2} , while in the region below the lower bound, the probability of error is greater than 10^{-2} .

2.5 Conclusions

In this chapter, we considered a CS framework over finite fields. We derived the sufficient and necessary conditions for recovery of sparse signals. We showed that the both conditions are tight, and they coincide when the sparse factor of the sensing matrix is sufficiently large. We found that for recovery of ultra-sparse signals, the sensing matrix is required to be dense. One interesting result is that when the sensing matrix is sufficiently large and dense, and the field size is large, the number of measurements needed for perfect recovery is only $M > K$.

Chapter 3

Recovery Algorithm for Compressed Sensing Frameworks over Finite Fields

3.1 Introduction

In CS, a sparse signal can be recovered from a small number of linear projection measurements [14]. The reconstruction of a sparse signal is performed through an optimization process such as linear programming and greedy algorithms. For sparse signals with discrete values, e.g., bit streams for computer storage and pixel images, the recovery algorithms developed thus far for CS are mainly for the real valued system. They are not efficient for discrete signals as they cannot effectively exploit the digitized nature of the signal and the sensing matrix elements. This motivates us to explore an efficient recovery algorithm for a CS framework for finite fields.

In CS, one compressed sample is obtained by the inner product of a row of the so-called sensing matrix and a sparse signal. From some compressed samples, the sparse signal can be reconstructed using a CS recovery algorithm. This has a strong analogy with the syndrome decoding in the linear channel coding context. In other words, sparse error patterns are identified from the syndrome equation which is obtained by multiplying the parity-check matrix to the received signal vector. From this observation, we aim to utilize the parity-checking frames as the sensing matrix over finite fields. In

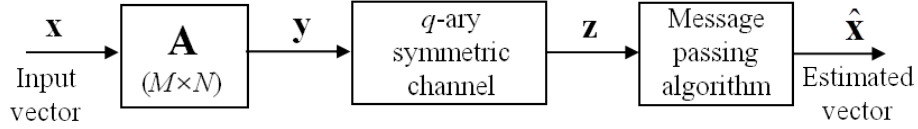


Figure 3.1: A CS framework over a finite field.

particular, we use the Gallager’s parity-check matrices and extend his probabilistic decoding (PD) method for CS context [58]. In other words, low density frames over finite fields are used for sensing matrices. Then, we can see the possibility of using this framework for CS of discrete valued signals. We design a sparse signal recovery routine which is a PD algorithm utilizing signal sparseness. We provide extensive system simulation verification of this recovery algorithm.

3.2 Compressed Sensing over Finite Fields

3.2.1 System Description

In Figure 3.1, we describe a compressed sensing framework in a finite field of size q , \mathbb{F}_q : Let $\mathbf{x} \in \mathbb{F}_q^N$ be a signal vector of length N with sparsity K which indicates the number of the nonzero entries in \mathbf{x} , $\mathbf{A} \in \mathbb{F}_q^{M \times N}$ be an $M \times N$ sensing matrix with $N > M$. The measured signal \mathbf{y} is

$$\mathbf{y} = \mathbf{A}\mathbf{x}. \quad (3.1)$$

The received signal \mathbf{z} obtained after passing the q -ary symmetric channel is

$$\mathbf{z} = \mathbf{y} + \mathbf{e}. \quad (3.2)$$

where $\mathbf{e} \in \mathbb{F}_q^M$ is the $M \times 1$ noise vector whose element follows an independently identical distribution (i.i.d.). The distribution p_i of the q -ary symmetric channel for a noise vector \mathbf{e} is defined by

$$\Pr \{z_i | y_i\} = \begin{cases} 1 - \epsilon & \text{for } y_i = z_i, \\ \epsilon / (q - 1) & \text{otherwise,} \end{cases} \quad (3.3)$$

where y_i and z_i are the i th measured and received signal for $i \in \{1, 2, \dots, M\}$, i.e., $\epsilon = 0$ is the noiseless case. In this chapter, we assume that an element of the signal \mathbf{x} follows a probability distribution p_j with i.i.d.,

$$\Pr \{x_j = \theta\} = \begin{cases} 1 - \delta & \text{if } \theta = 0, \\ \delta / (q - 1) & \text{if } \theta \neq 0, \end{cases} \quad (3.4)$$

where x_j are the j th element of \mathbf{x} for $j \in \{1, 2, \dots, N\}$, δ is the sparsity ratio ($= K/N$), and a dummy variable $\theta \in \mathbb{F}_q$.

In this chapter, we use a sparse matrix for \mathbf{A} . The generation of a sparse sensing matrix \mathbf{A} follows the Gallager approach named as a parity-check matrix randomly chosen from the ensemble of a regular (d_c, d_v) LDPC codes, where d_c and d_v are the number of nonzero entries in the column and the row of the matrix. In this chapter, all arithmetic operations for multiplication and addition are performed over a finite field. In order to recover an unknown sparse signal \mathbf{x} , we use a variant of the message passing algorithm [64].

3.2.2 Connection to Syndrome Decoding

Error correction is required for reliable communications, and performed by adding redundant parities to original information. Suppose that a codeword $\mathbf{c} \in \mathbb{F}^n$ with length

n is chosen from the codebook \mathcal{C} over finite fields \mathbb{F} . And it is transmitted through a noisy channel, and received as $\hat{\mathbf{c}}$, where $\hat{\mathbf{c}} = \mathbf{c} + \mathbf{w}$ and $\mathbf{w} \in \mathbb{F}^n$ is the additive noise. With the received codeword $\hat{\mathbf{c}}$ and the knowledge of the codebook \mathcal{C} , the decoder tries to estimate the correct codeword \mathbf{c} . For linear codes, the codebook \mathcal{C} can be described in terms of its $m \times n$ parity-check matrix $\mathbf{H} \in \mathbb{F}^{m \times n}$ as $\mathcal{C} = \{\mathbf{c} \in \mathbb{F}^n | \mathbf{H}\mathbf{c} = 0\}$.

At the receiver, a syndrome decoder performs the computation of the syndrome in the enabling way: $\mathbf{r} = \mathbf{H}\hat{\mathbf{c}} = \mathbf{H}(\mathbf{c} + \mathbf{w}) = \mathbf{H}\mathbf{w}$ since $\mathbf{H}\mathbf{c} = 0$. From the syndrome \mathbf{r} , it is desired to find the exact error pattern \mathbf{w} by using the calculated syndrome \mathbf{r} and the parity-check matrix \mathbf{H} . The error correction capability of this code \mathcal{C} mainly relies on its minimum distance, which is the minimum Hamming weight (the number of nonzero elements) of any codeword. Recently, the tight connection between CS and coding theory was reported in [59], [60], and [61].

3.3 Recovery Algorithm of Sparse Signals

3.3.1 Message Passing Algorithm

In this section, we discuss the PD algorithm. The *maximum a posterior* (MAP) detection is used which utilizes the prior knowledge that the distribution of each element defined in (3.4) is known for reconstruction. Then, the reconstruction problem of x_j is expressed by

$$\hat{x}_j := \arg \max \Pr\{x_j = \theta | \mathbf{y}, \mathbf{A}\}. \quad (3.5)$$

Figure 3.2 shows the graphical representation of the reconstruction problem, which is drawn from a sensing matrix \mathbf{A} by mapping the rows to the measured signal \mathbf{y} and

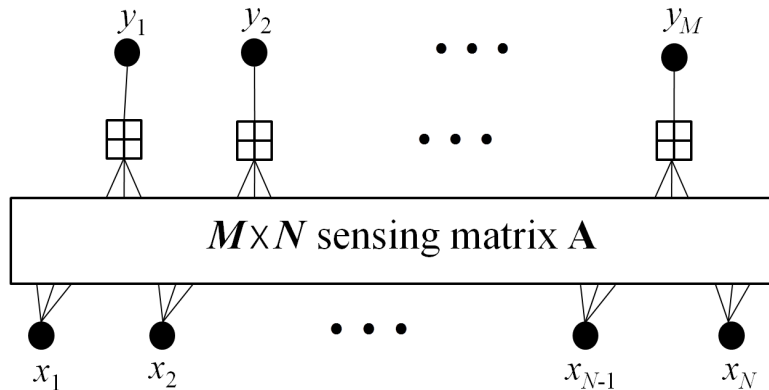


Figure 3.2: Graphical representation of the sensing matrix \mathbf{A} with the measured signal \mathbf{y} and the sparse signal \mathbf{x} .

the columns to the sparse signal \mathbf{x} with the entries forming the edges of the graph. The presence of an edge between a sensing node and a signal node represents the nonzero coefficient of the sensing matrix \mathbf{A} . In order to perform the PD algorithm in the graphical representation, we define the two extrinsic probabilities as follows: $f_{v,ij}$ is the message from the i th sensing node to the j th signal node; $f_{h,ji}$ is the message from the j th signal node to the i th sensing node.

We now discuss several related works. Sarvotham *et al.* proposed a belief propagation algorithm for recovery of real valued sparse signals in [62]. Donoho *et al.* in [63] proposed an approximate message passing algorithm for CS with dense Gaussian sensing matrices. In this algorithm, the authors introduced a variant of density evolution that provides a precise characterization of its performance.

3.3.2 Probabilistic Decoding Algorithm for Recovery of Sparse Signals

The idea behind this algorithm is based on decoding of nonbinary LDPC codes in Davey and Mackay [64]. The main difference between our algorithm and the work [64] is that we exploit the knowledge of the prior information of sparse signals for reconstruction. Then, the initial process of decoding is different as well as updating the probability messages between sensing nodes and signal nodes. We assume the following ways: an unknown signal \mathbf{x} is compressed into a measured signal \mathbf{y} , and it is transmitted through the noisy channel. With the received signal \mathbf{z} and a prior distribution of \mathbf{x} , we determine the unknown signal \mathbf{x} by using the proposed recovery algorithm.

For reconstruction, there are four main steps: i) initialization, ii) update of message $f_{v,ij}$, iii) update of message $f_{h,ji}$, and iv) tentative decoding. In the initialization, we set the values for all the nodes. The prior probability distribution p_j of the j th signal \mathbf{x} defined in (3.4) is used. Also the transition probability for each sensing node \mathbf{z} is as given in (3.3). This information is utilized to determine the message $f_{v,ij}$. This makes it possible to the major difference from Davey's work. In the next step, we update all the messages $f_{v,ij}$ as follows. The transformed version $\mathbf{F}_{v,ij}$ of the message $f_{v,ij}$ is calculated

$$\mathbf{F}_{v,ij} = \left(\prod_{\tilde{j} \in L(i) \setminus \{j\}} \mathbf{H}_q \tilde{f}_{h,\tilde{j}i} \right) \times \mathbf{H}_q p_i, \quad (3.6)$$

where $L(i) = \{j : A_{ij} \neq 0\}$ denotes the set of indices of x_j that participate in the i th row of the sensing matrix, \mathbf{H}_q is the $q \times q$ transform matrix, i.e., the Hadamard transform matrix or the Fourier transform matrix. In this case, we set the rearranged message $\tilde{f}_{h,\tilde{j}i}$ corresponding to its coefficient of the sensing matrix \mathbf{A} , which is initially

the same with the signal probability p_j . And then, using the inverse transform, the message $f_{v,ij}$ is obtained from

$$f_{v,ij} = \mathbf{H}_q^{-1} \mathbf{F}_{v,ij}. \quad (3.7)$$

The i th sensing node follows the constraint, i.e., $y_i = \sum_j A_{ij}x_j$.

In the third step, the computation of the message $f_{h,ji}$ from messages $f_{v,ij}$ is performed by

$$f_{h,ji} = \gamma p_j \prod_{\tilde{i} \in M(j) \setminus \{i\}} \tilde{f}_{v,\tilde{i}j}, \quad (3.8)$$

where $M(j) = \{i : A_{ij} \neq 0\}$ denotes the set of indices of y_i that participate in the j th column of the sensing matrix, the message $\tilde{f}_{v,\tilde{i}j}$ is obtained from rearranging the message $f_{v,\tilde{i}j}$ according to the coefficient of the sensing matrix. Then f_j denotes the posterior probability of the j th signal node x_j , which is conditioned on the information obtained via y_i and p_j . Then, the posterior probability is obtained from as follows,

$$f_j = p_j \prod_{i \in M(j)} \tilde{f}_{v,ij}. \quad (3.9)$$

The j th signal node x_j is then estimated: $\hat{x}_j = \arg \max_{\theta \in \mathbb{F}_q} \{f_j\}$. The decoder checks if $\hat{\mathbf{x}}$ satisfies the constraint condition, i.e., $\mathbf{A}\hat{\mathbf{x}} = \mathbf{y}$.

3.4 Simulation and Discussion

3.4.1 Simulation Results

In Figure 3.3 and Figure 3.4, we evaluate the performance of our CS scheme considered in finite fields. In all simulations, the maximum number of iterations is set to 50 for the PD algorithm. For simulation, we use a sparse signal of length 1200, $N = 1200$.

Algorithm 1: Proposed Probabilistic Decoding (PD) Algorithm

Input: Prior probability p_j of a sparse signal

Channel error probability p_i

Randomly generated sensing matrix \mathbf{A}

Output: Estimated \hat{x}_j

1) **Initialization:**

Set p_j and p_i

Initialize message $f_{h,ji} \leftarrow p_j$

Set maximum iterations

while $\mathbf{A}\hat{\mathbf{x}} = \mathbf{z}$ **or** *Maximum Iterations* **do**

2) **Update the message** $f_{v,ij}$:

$$\mathbf{F}_{v,ij} = \left(\prod_{\tilde{j} \in L(i) \setminus \{j\}} \mathbf{H}_q \tilde{f}_{h,\tilde{j}i} \right) \times \mathbf{H}_q p_i$$
$$f_{v,ij} = \mathbf{H}_q^{-1} \mathbf{F}_{v,ij}$$

3) **Update the message** $f_{h,ji}$:

$$f_{h,ji} = \gamma p_j \prod_{\tilde{i} \in M(j) \setminus \{i\}} \tilde{f}_{v,\tilde{i}j}$$

4) **Tentative decoding:**

$$f_j = p_j \prod_{i \in M(j)} \tilde{f}_{v,ij}$$

$$\hat{x}_j = \arg \max_{\theta \in \mathbb{F}_q} \{f_j^\theta\}$$

return *Estimated* $\hat{\mathbf{x}}$

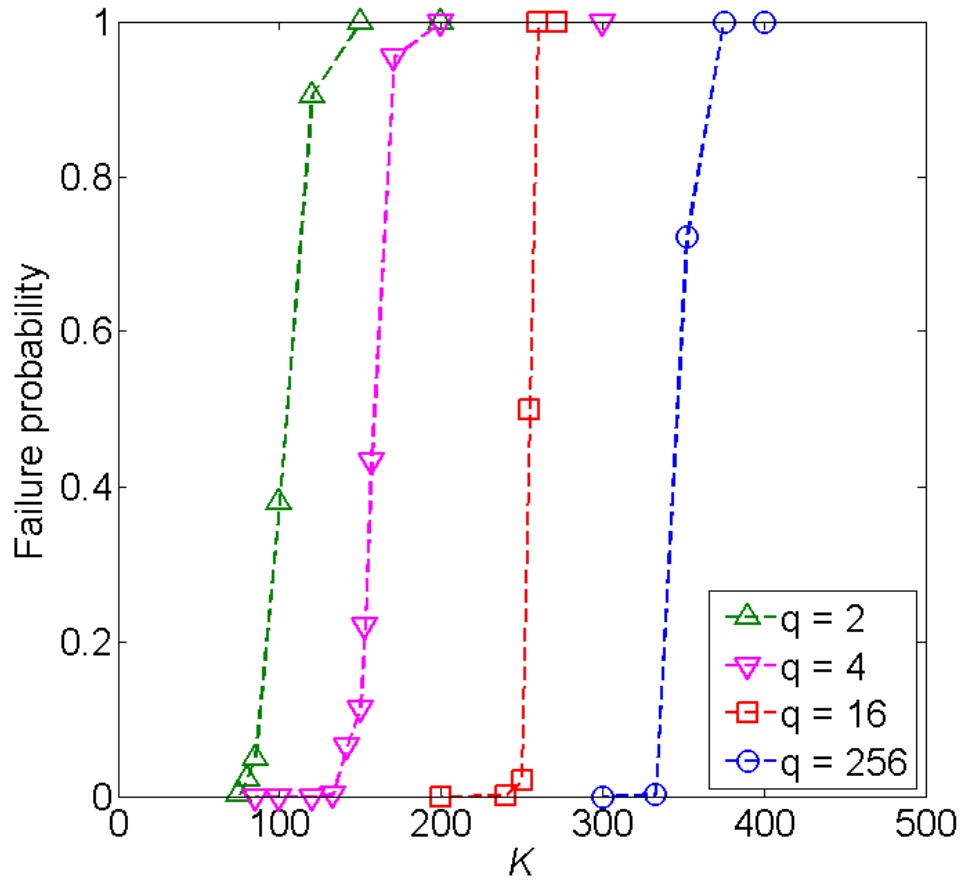


Figure 3.3: Failure probability for recovery of sparse signals with fixed $N = 1200$, $M = 600$, and $\epsilon = 0.1$ varying K

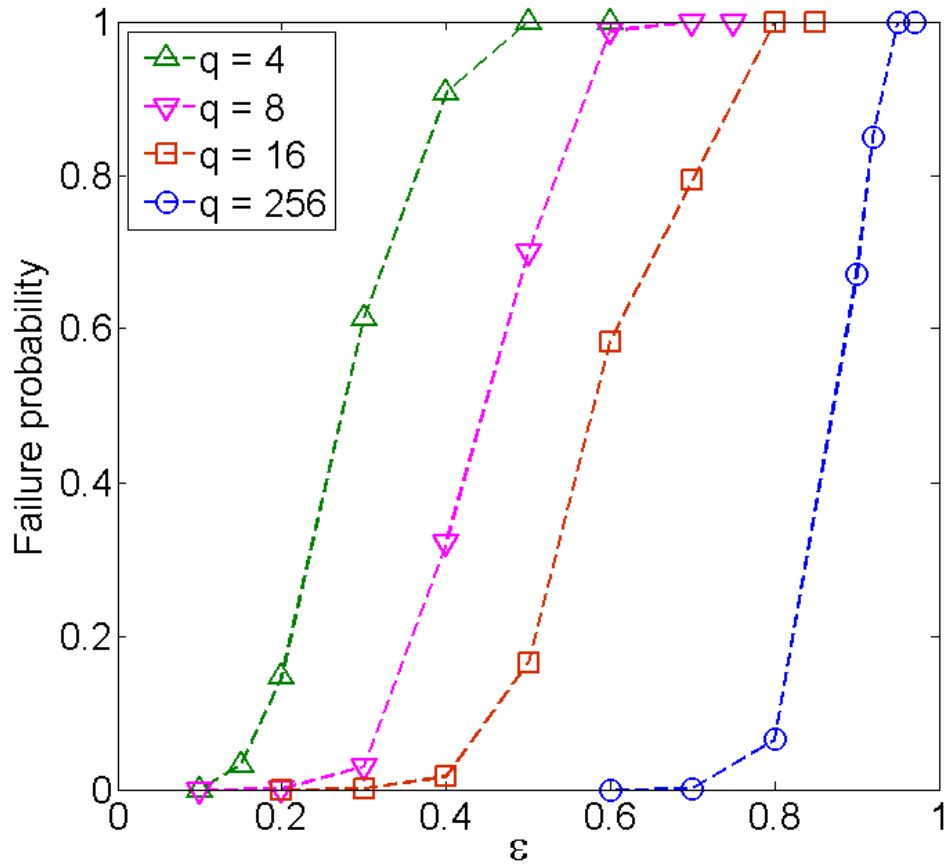


Figure 3.4: Failure probability for recovery of sparse signals with fixed $N = 1200$, $M = 600$, and $K = 120$ varying ϵ .

With the sparsity ratio $\delta(= K/N)$, the compression ratio $\rho(= M/N)$, and the error probability ϵ of the q -ary symmetric channel, we show the failure probabilities for reconstruction of CS. Figure 3.3 shows the performance of our CS scheme with a regular ($d_c = 3$, $d_v = 6$) sensing matrix \mathbf{A} , i.e., $M = 600$, over a finite field of size: $q = 2, 4, 16$, and 256 . In this case, we set the error probability $\epsilon = 0.1$ for the q -ary symmetric channel. The horizontal axis indicates sparsity K . It is obvious that as the size of finite fields increases, the larger number of the sparsity can be successfully decoded. In Figure 3.4, we show the failure probability with different error probability ϵ . We observe that a larger finite alphabet is not sensible with the channel noise.

3.5 Conclusion

In this chapter, we considered a CS framework over finite fields. In this framework, low-density frames were used as the sensing matrices. We proposed a PD based the message passing algorithm which shows very good performance closely achieving the theoretical bounds in coding theory. This allows us to utilize the low-density sensing matrices to be good reconstruction performance into a CS framework.

Chapter 4

New Performance Evaluation Framework of Cooperative Wireless Networking Schemes with Random Network Coding

4.1 Introduction

Channel fading is one of the underlying causes of performance degradation in wireless networks. One naive approach to combat channel fading is to increase the transmit power. A more advanced approach is to utilize modern diversity techniques, which can be performed without increasing the transmit power. In recent years, numerous diversity techniques have been proposed and employed in the time, frequency, and space domains. Cooperative networking is one of the current approaches that aim to utilize spatial diversity via user cooperation. Each user participates collaboratively, and shares the benefit of a virtual antenna array in transceiver messages that are available through another user's antenna [65].

Network coding [17] first proposed by Ahlswede *et al.* is shown to achieve maximum information flow in a single source multicast network. Numerous efforts have subsequently been attempted; these efforts focused on elucidating if network coding can provide additional advantages compared to other cooperative networking schemes.

For example, network coding over the binary field [66], [67] has shown to improve diversity gain and provide higher spectral efficiency in wireless networks, whereas network coding with a nonbinary field further increases those benefits [68]–[72]. In particular, numerous studies have investigated the extent to which network coding can improve the performance of media access control and routing protocols, in terms of energy efficiency [84], transmission delay [86], and throughput [85], [87], compared to traditional forward-and-relay-only based designs [81]–[83]. The performance of cooperative wireless networking schemes with network coding has been analyzed, and compared with erasure channel models [68]–[71], and error propagation models [92]–[95]. We will further address recent cooperative communication schemes in Chapter 4.2 by categorizing them with respect to their decoding techniques, spectral efficiencies, and cooperative strategies.

Xiao and Skoglund [68], [69] recently proposed a network coding scheme called Dynamic Network Codes (DNC) to handle a dynamic network topology. The inherent nature of wireless channels implies that links are unreliable and that link failures will occur randomly in the inter-user channels. DNC is designed to perform successfully over such a dynamic network channel topology, in conjunction with techniques such as enhanced diversity order. In the DNC scheme, multiple network code matrices are used; each one is designed to manage a particular occurrence of link outages. In particular, an intermediate node in a network may fail to decode some of the messages received from the other nodes. The intermediate node creates a linear combination of the messages it could successfully decode, and then forwards it to the base station. That is, a certain

occurrence of link outages results in a particular restriction to the elements of the network code matrix. Thus, each network code matrix in the DNC scheme, referred to as the *transmission matrix* in this chapter, is designed carefully to work effectively for the occurrence of a specific set of link failures. In addition, Rebelatto *et al.* in [70], [71] extended the two-phase transmission framework of the DNC to multiple phases in the Generalized Dynamic Network Codes (GDNC), to further enhance the transmission rate and the diversity order.

In this chapter, our goal is to focus on the system models of the DNC and GDNC schemes, and provide a novel analysis framework for them. As noted earlier, there are other recently studied cooperative communications schemes, each with an advantage in a different perspective such as spectral efficiency and higher decoding performance. These will be discussed further in Chapter 4.2. DNC's system model was selected, because it is the first network coding schemes designed for dynamic network topology. To the best of the authors' knowledge, DNC is the first attempt to adaptively use different network code matrix as the link failure varies, and is designed to achieve the so-called the *min-cut capacity* of randomly changing links [68]. GDNC is shown to achieve full diversity order and increases the transmission [70].

Although a series of performance analyses for DNC and GDNC are provided in [68]–[71], the authors rely on the exhaustive investigation of all individual network code matrices to determine if the resultant transmission matrix at the base station is sufficiently able to decode the source messages. This is an exceedingly time-consuming and tedious process; thus, it cannot be extended to larger and more general networks

where the link outage probabilities throughout the networks are, in general, different from each other.

In particular, the performance analyses in [68]–[71] to determine the probability of successful decoding at the base station are performed only for small and non-general networks. A successful decoding is assumed to be achieved when the network code matrix at the base station has a sufficient number of linearly independent vectors that at least equals the number of unknown source messages. The successful event begins by determining whether the rank of the network code matrix at the base station is full. Then, the success probability is obtained by adding all individual probabilities of such events over all possible link failures. To achieve this outcome, the authors, Theorem 1 in [68] and Section V in [70], followed the approach of tracking down each network code matrix individually, and determining if each was full in rank. This is an exhaustive process. When the number of nodes in a network increases, it is evident that this approach becomes intractable, because of the exponential increase in possible combinations. For example, the total number of distinct $N \times N$ random matrices with full rank is $\prod_{i=1}^N (q^N - q^{i-1})$ for the finite field of size q [73].

As a result, the analyses performed in [68]–[71] are limited to small and homogeneous networks, i.e., a network of fewer than 10 nodes, with link failure probabilities set to be equal throughout the network. These methods are not suitable for analyzing networks where nodes are randomly deployed in an area of interest, and wireless networks present heterogeneous link outage probabilities. The lack of a general and systematic performance analysis framework to deal with such networks has motivated

this study.

In this chapter, our main goal is to propose a novel evaluation framework for cooperative network coding schemes. The contributions of this work are summarized as follows.

- (*Design of random transmission matrix*) We model a random transmission matrix with uniform and maximum distance separable (MDS) distributions in (4.6), (4.7), and (4.8) of Chapter 4.4. The elements of this matrix are represented with random variables as a function of the outage probability of each wireless link. This new system model enables us to avoid the exhaustive counting of each network code metric occurrence.
- (*Tight upper bounds to probability of decoding failure*) We derive a series of tight upper bounds on the probability of failure. In particular, the dimension of the nullspace of the random transmission matrix is used to derive an upper bound, as discussed in Proposition 4.3. It is then linked to the decoding failure probability where the rank of the network code matrix is not full, which is defined in Theorem 4.4. The upper bounds have proven to be considerably tight in comparison to simulation results.
- (*Generality and scalability*) The developed analysis framework is general and scalable, offering the capability of analyzing large wireless networks with random deployments where all outage probabilities of wireless links are different. For example, see one network scenario of randomly deployed nodes. In addition,

Table 4.1: Summary of Recent Techniques for Cooperative Communications.

| | Recent technique | References |
|--------------------------|---------------------------|-----------------------|
| Decoding techniques | Maximum ratio combining | [67], [75]–[77] |
| | Rank-based decoding | [68]–[71], [73], [74] |
| High spectral efficiency | Multiuser detection | [79] |
| | Interference cancellation | [80] |
| | Non-orthogonal channel | [78] |
| Cooperative strategies | Amplify-and-Forward | [65], [97] |
| | Decode-and-Forward | [65], [98] |
| | Compute-and-Forward | [96] |

the developed framework can handle a large cooperative network that has more than 100 nodes. To the best of our knowledge, this scale of wireless networks is unprecedented in DNC and GDNC performance evaluations. The proposed framework enables us to investigate its impact on the successful reconstruction of source messages based on varying outage probabilities, and on various key parameters such as the number of relays and the field sizes in DNC and GDNC schemes.

4.2 Other Recent Works and Relation to Our Work

In this section, and in Table 4.1, we provide an overview of the prevalent cooperative communications schemes believed to be closely related to the network coding schemes considered in this chapter.

Two cooperative wireless communications decoding approaches have been recently considered. The first is the Maximum Ratio Combining (MRC) decoding scheme [67], [75]–[77]. The main concept is to configure the network to coordinate the transmissions, and repeat a signal with a weak signal-to-noise ratio (SNR) multiple times over independent fading channels. In this manner, MRC allows the destination to maximize SNR. To implement an MRC scheme, all decoding information, as well as the success or failure of each source message at the base station, should be identified and forwarded to the relays. This is required to determine the source of the low SNR, for which retransmission was required. To enable its deployment in large-scale networks, the scheduling issue must be resolved.

Recently, two research groups have proposed advanced cooperative network schemes to achieve high spectral efficiency. In [78], Youssef and Amat have proposed the use of non-orthogonal channel allocation to improve spectral efficiency. For wireless networks where a multiuser detection receiver is utilized at the base station, cooperative transmission protocols with high spectral efficiency have been developed [79]. Furthermore, the work described in [80] has aimed to improve the spectral efficiency of cooperative systems using superposition coding and iterative detection methods.

We believe our analysis framework could be utilized in [78] with a necessary but simple modification. The first aspect to consider is that all wireless channels should not be modeled independently in the future. The outage probabilities are not independent from each other. This can be achieved by designing a joint probability distribution for the random matrix. The probability that the random transmission matrix is not full

rank can be obtained by considering such an event over the joint probability distribution.

Using NC on lattice codes, Nazer and Gastpar recently proposed the compute-and-forward (CF) relaying scheme [96]. In CF, a relay is configured with a linear combination of multiple codeword signals, which are simultaneously transmitted and superposed in the air. The key idea of using CF relaying in network coding is to utilize the lattice code property stating that the *integer combination* of lattice codewords remains a lattice codeword. Thus, the relay receives a codeword with additive noise. After a denoising step, the relay retransmits the decoded lattice codeword to the base station. Therefore, the benefit of using CF relaying in network coding is evident. Because transmissions from all sources to the relay are performed simultaneously, the spectral efficiency is significantly enhanced.

There are two widely recognized cooperative relaying strategies, referred to as amplify-and-forward (AF) [65], [97] and decode-and-forward (DF) [65], [98]. AF and DF cooperative relaying strategies perform effectively in either low or high SNR regimes, while CF approach offers advantages in moderate SNR regimes where both interference and noise are significant factors [96]. The DNC and GDNC schemes we consider in this chapter are categorized as DF-based network coding strategies.

Cooperative wireless communications with multiple sources and multiple relays closely related to our work have attracted significant attention because of their higher achievability rate [88], and better error performance [90], [91] as well as diversity-multiplexing tradeoffs [72], [89]. There are two types of error propagation models that should be con-

sidered here. The authors in [92]–[95] assume a network channel model where erroneous messages are permitted to propagate throughout the network. For the erasure channel model, [68]–[71], erroneous messages at the relays are discarded, to avoid unnecessary error propagation caused by encoding and forwarding operations.

The recent studies [68]–[74] closely related to this paper have focused on the performance analysis and the design of network code matrices for cooperative networks with erasure channel models. In particular, the problem of designing network code matrices subject to link failures was studied [68]–[71], to maximize diversity order in a multiple-access network. In [70] it is shown that the design of network code matrices is equivalent to the design of linear block codes for erasure correction coding. It was shown that maximum diversity order is guaranteed if an MDS code generator matrix is utilized as the network code matrix. In addition, Nguyen *et al.* [74] have defined upper and lower bounds on GDNC scheme recovery performance. For random linear network coding schemes, Trullols-Cruces *et al.* [73] have derived the exact decoding probability of obtaining network codes of full rank.

4.3 Cooperative Network

We consider an (N, M) cooperative scheme for wireless networks as shown in Figure 4.1, in which there are N sources, $\{U_1, U_2, \dots, U_N\}$, and M relays, $\{R_1, R_2, \dots, R_M\}$. There are two cooperating transmission phases: *broadcasting* and *relaying*. In the broadcasting phase, each source transmits its message to the base station (BS). Owing to the nature of wireless channels, the relays in this phase can, in general, receive and

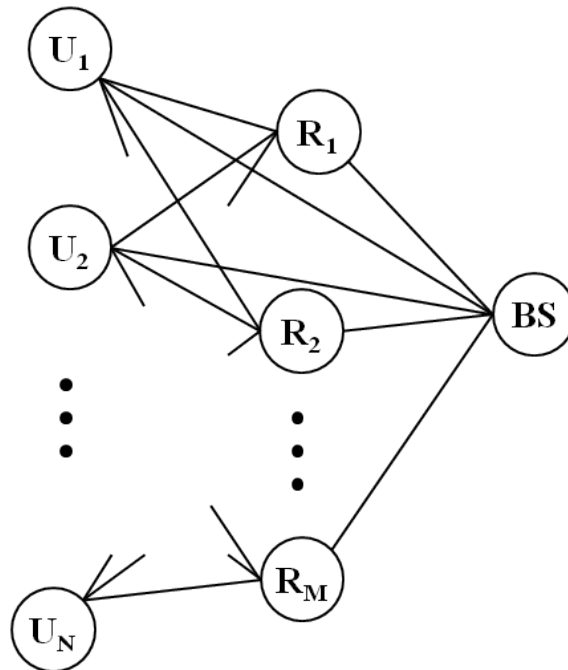


Figure 4.1: An (N, M) cooperative network with N sources and M relays.

successfully decode the messages from the sources. In the relay phase, each relay can generate a parity message constructed from a linear combination of these messages, and forward it to the BS. In this work, we assume that the received message for a single channel is considered either completely corrupted – an outage and therefore not available at the receiver – or error-free, i.e., no outage. For more complicated cooperative communications error models that have been studied in [92]–[95], we have a discussion included in Chapter 4.2.

For both transmission types, we assume that all transmitters send their signals through orthogonal channels using either time- or frequency-division multiple access, and that all channels are spatially independent, flat-faded, and perturbed by additive white Gaussian noise (AWGN). We further assume that the channel gains are indepen-

dent in both the broadcasting and relay phases. A discussion is included in Chapter 4.2 in which no orthogonal transmissions are utilized and inter-user channels are not independent.

In the broadcasting phase, the signal y_{u,d_1} received at node d_1 for $d_1 \in \{R_1, R_2, \dots, R_M, BS\}$ is given by $y_{u,d_1} = \sqrt{P_u}h_{u,d_1}x_{u,d_1} + n_{u,d_1}$, where u denotes the transmitter node, i.e., $u \in \{U_1, U_2, \dots, U_N\}$; P_u denotes the transmit power at node u ; h_{u,d_1} denotes the channel gain between the two nodes u and d_1 , which is a circular symmetric complex-valued Gaussian random variable with zero mean and variance $\sigma_{u,d_1}^2/2$ per dimension; x_{u,d_1} is the signal transmitted from node u ; and noise n_{u,d_1} denotes the complex-valued AWGN with zero mean and variance $N_0/2$ per dimension. In the relay phase, the signal y_{r,d_2} received at the BS is $y_{r,d_2} = \sqrt{P_r}h_{r,d_2}x_{r,d_2} + n_{r,d_2}$, where r denotes the relay node, i.e., $r \in \{R_1, R_2, \dots, R_M\}$; d_2 denotes the BS; P_r denotes the transmit power at relay node r ; h_{r,d_2} denotes the channel gain between the relay node r and the BS, which is a circular symmetric complex-valued Gaussian random variable with zero mean and variance $\sigma_{r,d_2}^2/2$ per dimension; x_{r,d_2} is the signal transmitted from relay node r ; and noise n_{r,d_2} denotes the same AWGN as in the broadcasting phase. For Rayleigh fading channels, the variances of channel gains are defined as $\sigma_{u,d_1}^2 := \rho_{u,d_1}^{-\eta}$ and $\sigma_{r,d_2}^2 := \rho_{r,d_2}^{-\eta}$, letting ρ_{u,d_1} and ρ_{r,d_2} be the distances for u -to- d_1 and r -to- d_2 , respectively, and η be the path-loss exponent, i.e., $2 \leq \eta \leq 6$ [99]. Throughout this chapter, we use $\eta = 3$. The instantaneous SNRs of the two channels are denoted as $\gamma_{u,d_1} := |h_{u,d_1}|^2 P_u / N_0$ and $\gamma_{r,d_2} := |h_{r,d_2}|^2 P_r / N_0$.

In the broadcasting phase, the outage probability δ_{u,d_1} for a given channel is repre-

sented as follows [100]

$$\begin{aligned}\delta_{u,d_1} &\stackrel{(a)}{:=} \Pr\{\log(1 + \gamma_{u,d_1}) < R_{th}\} \\ &\stackrel{(b)}{=} 1 - \exp\left\{-\frac{N_0(2^{R_{th}} - 1)}{P_u\sigma_{u,d_1}^2}\right\},\end{aligned}\tag{4.1}$$

where R_{th} is the predefined threshold of the spectral efficiency in bits/s/Hz. Throughout this chapter, we use $R_{th} = 1$ bits/s/Hz. The expression (a) in (4.1) originates from the definition of channel capacity, (b) reflects the assumption that $|h_{u,d_1}|^2$ follows the exponential distribution with parameter $P_u/N_0\rho_{u,d_1}^\eta$. Similarly, the outage probability δ_{r,d_2} of each channel in the relay phase is obtained as follows:

$$\begin{aligned}\delta_{r,d_2} &:= \Pr\{\log(1 + \gamma_{r,d_2}) < R_{th}\} \\ &= 1 - \exp\left\{-\frac{N_0(2^{R_{th}} - 1)}{P_r\sigma_{r,d_2}^2}\right\}.\end{aligned}\tag{4.2}$$

Each of both outage probabilities (4.1) and (4.2) is a function of the instantaneous SNR and the distance between two nodes. We can use these outage probabilities to model the elements of a transmission matrix.

4.4 Modeling of Transmission Matrices

4.4.1 Transmission Matrix

We utilize the outage probabilities defined in Chapter 4.3 the elements of the transmission matrix. A random transmission matrix can be used to represent a family of network coding matrices for an (N, M) cooperative scheme shown in Figure 4.1 in which two transmissions occur over a multiple access network with N sources and M relays. Let \mathbb{F}_q be a finite field of size q . Let $\mathbf{x} \in \mathbb{F}_q^{N \times 1}$ denote the $N \times 1$ vector of transmitted messages, $\mathbf{y} \in \mathbb{F}_q^{(N+M) \times 1}$ denote the $(N + M) \times 1$ vector of messages received at

the BS, and $\mathbf{A} \in \mathbb{F}_q^{(N+M) \times N}$ denote the $(N + M) \times N$ transmission matrix. The vector \mathbf{y} received at the BS is then given by

$$\mathbf{y} = \mathbf{A}\mathbf{x}, \quad (4.3)$$

where the transmission matrix \mathbf{A} consists of the $N \times N$ direct matrix \mathbf{D} and the $M \times N$ combination matrix \mathbf{P} ; i.e., $\mathbf{A} := \begin{bmatrix} \mathbf{D} \\ \mathbf{P} \end{bmatrix}$. Note that all of the arithmetic operations are performed over finite fields.

The direct matrix \mathbf{D} can be modeled as a diagonal matrix, i.e., one with zeroes for all off-diagonal elements. If there are no outage events for the channel links between the sources and the BS, the diagonal elements of this direct matrix are all set to one; otherwise, the corresponding elements are set to zero. Let α_{ii} denote the i th diagonal element of \mathbf{D} , i.e., $\alpha_{ii} \in \{0, 1\}$ for $i \in \{1, 2, \dots, N\}$, then the i th element $y_{i,1}$ of \mathbf{y} is represented as $y_{i,1} = \alpha_{ii}x_i$, where $x_i \in \mathbb{F}_q$ denotes the i th element of \mathbf{x} , and 1 in the subscript of $y_{i,1}$ indicates the broadcasting phase for $j \in \{1, 2, \dots, M\}$. Let $\beta_{ji} \in \mathbb{F}_q$ denote an element of \mathbf{P} , then the $(N + j)$ th element $y_{j,2}$ of \mathbf{y} is represented by $y_{j,2} = \sum_{i=1}^N \beta_{ji}x_i$, where 2 in the subscript of $y_{j,2}$ indicates the relay phase. As the BS receives $N + M$ messages from N sources and M relays, we can represent the

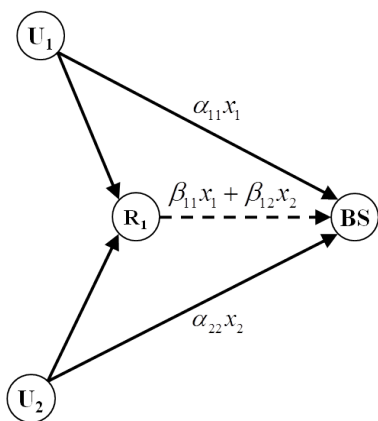


Figure 4.2: The (2,1) cooperative wireless network with $N = 2$ and $M = 1$. The solid lines indicate the broadcasting phase, and the dashed line indicates the relay phase.

transmission matrix as

$$\begin{bmatrix} y_{1,1} \\ \vdots \\ y_{N,1} \\ y_{1,2} \\ \vdots \\ y_{M,2} \end{bmatrix} = \begin{bmatrix} \alpha_{11} & \cdots & 0 \\ \vdots & \ddots & \vdots \\ 0 & \cdots & \alpha_{NN} \\ \beta_{11} & \cdots & \beta_{1N} \\ \vdots & \ddots & \vdots \\ \beta_{M1} & \cdots & \beta_{MN} \end{bmatrix} \begin{bmatrix} x_1 \\ x_2 \\ \vdots \\ x_N \end{bmatrix}. \quad (4.4)$$

Note that all elements of the transmission matrix \mathbf{A} are random variables except for the off-diagonal terms of \mathbf{D} . The following simple example illustrates the method for determining the elements of the transmission matrix.

Example 4.1: Consider two sources (U_1 and U_2) and one relay (R_1) in a (2,1) cooperative wireless network shown in Figure 4.2. Let the size of the finite field for the network coding be 2, $q = 2$. In the broadcasting phase, source U_1 transmits message

x_1 to the BS and relay R_1 , while U_2 transmits message x_2 to the BS and R_1 . The relay overhears, decodes, and then linearly combines the decoded messages to generate a parity message that is forwarded to the BS. Thus, the BS receives three messages: x_1 and x_2 from the respective sources and a parity message from the relay. This transmission mechanism is depicted in Figure 4.2.

The transmission matrix in this example is given by

$$\begin{bmatrix} y_{1,1} \\ y_{2,1} \\ y_{1,2} \end{bmatrix} = \begin{bmatrix} \alpha_{11} & 0 \\ 0 & \alpha_{22} \\ \beta_{11} & \beta_{12} \end{bmatrix} \begin{bmatrix} x_1 \\ x_2 \end{bmatrix}. \quad (4.5)$$

Here, the connectivities of the channel links (U_1 -BS and U_2 -BS) are represented by α_{11} and α_{22} in the transmission matrix. If a channel link (U_1 -BS) or (U_2 -BS) incurs an outage, then its associated connectivity, α_{11} or α_{22} , will be set to zero; otherwise, this element is set to one. Similarly, two elements β_{11} and β_{12} represent the joint factors of the qualities of the three channel links: (U_1 - R_1), (U_2 - R_1), and (R_1 -BS). If both links, (U_2 - R_1) and (R_1 -BS), do not simultaneously incur outages, β_{12} is set one; conversely, if either of the two links undergoes an outage, β_{11} will be set to zero. Thus, the transmission matrix will be determined by the condition of all five channel links in the wireless network, and if the transmission matrix at a given condition has full rank, the BS can successfully decode the two source messages x_1 and x_2 . Table 4.2 summarizes all outage events of the transmission matrix for the (2,1) cooperative wireless network in which there are two sources and one relay. ■

Table 4.2: Determination of the Transmission Matrix for all Cases of Failures for $q = 2$, where “O” indicates no outage, “×” indicates an outage, and “-” indicates Don’t care

| U_1 -BS | U_2 -BS | D | U_1 - R_1 | U_2 - R_1 | R_1 -BS | P |
|-----------|-----------|--|---------------|---------------|-----------|---------------------------------------|
| O | O | $\begin{bmatrix} 1 & 0 \\ 0 & 1 \end{bmatrix}$ | O | O | O | $\begin{bmatrix} 1 & 1 \end{bmatrix}$ |
| O | × | $\begin{bmatrix} 1 & 0 \\ 0 & 0 \end{bmatrix}$ | O | × | O | $\begin{bmatrix} 1 & 0 \end{bmatrix}$ |
| × | O | $\begin{bmatrix} 0 & 0 \\ 0 & 1 \end{bmatrix}$ | × | O | O | $\begin{bmatrix} 0 & 1 \end{bmatrix}$ |
| × | × | $\begin{bmatrix} 0 & 0 \\ 0 & 0 \end{bmatrix}$ | ×/- | ×/- | O /× | $\begin{bmatrix} 0 & 0 \end{bmatrix}$ |

4.4.2 Modeling of Random Elements

In this subsection, we provide techniques for defining the elements of the transmission matrix as random variables. We assume that all outage events are mutually independent from each other, which is reasonable for typical wireless networks. Then, the probability distribution of the elements can be determined based on the outage probabilities of the wireless channels as follows. First, the probability distribution for each diagonal element of \mathbf{D} is modeled using the outage probability of the source-to-BS channels. Second, by simultaneously considering the outage events in both channels (i.e., source-relay and relay-BS), we determine the probability distribution for each element of \mathbf{P} .

To model each diagonal element of \mathbf{D} , the probability of the i th diagonal element α_{ii} , $i \in \{1, 2, \dots, N\}$, can be defined from the set of possible outage events between the sources and the BS in the broadcasting phase as:

$$\Pr\{\alpha_{ii} = \theta\} = \begin{cases} \delta_{U_i,BS} & \text{if } \theta = 0, \\ 1 - \delta_{U_i,BS} & \text{if } \theta = 1, \end{cases} \quad (4.6)$$

where $\delta_{U_i,BS}$ the outage probability defined in (4.1) where an outage occurs in the single link between the i th source U_i and the BS.

Next, to model each element of the combination matrix \mathbf{P} , we consider two types of probability distributions. The first is to permit the nonzero values of each element in \mathbf{P} to be uniformly distributed. This distribution is reasonable, considering the recent result in [101] where it is acknowledged that a uniform distribution for linear network coding provides various benefits, including decentralized operation and robustness to

network changes or link failures in multisource, multicast networks. The second is to allow the nonzero value to be predetermined. This specific value can be set using MDS codes [102] in coding theory. It is well known that MDS codes achieve the Singleton bounds. This supports the consideration of MDS codes for optimum reconstruction performance. In the latest literature, Rebelatto *et al.* [70] have proved that a systematic MDS code generator matrix, operating over sufficiently large finite fields such as the transmission matrix, is sufficient for obtaining full diversity in cooperative networks. However, MDS codes use a large field size that may result in excessive complexity, especially in cases where the dimension of the code is large.

Uniform distribution

When modeling the elements of the combination matrix \mathbf{P} , we have to consider the outage events in both the source-to-relay and relay-to-BS links, as the occurrence of either or both of these events will prevent the relay from delivering the source message to the BS. Let $\bar{\mathcal{E}}_j$ and \mathcal{E}_j denote the nonoccurrence and occurrence of an outage from the j th relay R_j , $j \in \{1, 2, \dots, M\}$, to the BS, respectively. Thus, both probabilities are: $\Pr\{\bar{\mathcal{E}}_j\} = 1 - \delta_{R_j, BS}$ and $\Pr\{\mathcal{E}_j\} = \delta_{R_j, BS}$. Because the outage event from a source to a relay is independent of any other outage events, the conditional probability $\Pr\{\beta_{ji} = \theta \mid \bar{\mathcal{E}}_j\}$ of this element of the combination matrix \mathbf{P} can be modeled as

$$\Pr\{\beta_{ji} = \theta \mid \bar{\mathcal{E}}_j\} = \begin{cases} \delta_{U_i, R_j} & \text{if } \theta = 0, \\ (1 - \delta_{U_i, R_j}) / (q - 1) & \text{if } \theta \neq 0, \end{cases} \quad (4.7)$$

where δ_{U_i, R_j} denotes the probability that the outage occurs from the i th source U_i to the j th relay R_j . Each outage probability δ_{U_i, R_j} can be determined independently in

(4.1).

In (4.7), the elements of \mathbf{P} are nonzero when both outage events do not occur simultaneously; however, when an outage event from the j th relay to the BS occurs, i.e., when \mathcal{E}_j is true, the conditional probability is set as $\Pr\{\beta_{ji} = 0 | \mathcal{E}_j\} = 1$, regardless of the condition of the outage event (source–relay).

MDS distribution

Next, we consider modeling the elements of \mathbf{P} based on the systematic generator matrix of MDS codes. The difference from the aforementioned uniform distribution is that the nonzero value of each element should be taken from the pertinent value of a predefined MDS code. In this subsection, we refer to this as the MDS distribution. By considering the MDS distribution, we can compare its reconstruction performance to that of the uniform distribution given in (4.7). For the MDS distribution, the conditional probability $\Pr\{\beta_{ji} = \theta | \bar{\mathcal{E}}_j\}$ defined similarly to that in (4.7) is given by

$$\Pr\{\beta_{ji} = \theta | \bar{\mathcal{E}}_j\} = \begin{cases} \delta_{U_i, R_j} & \text{if } \theta = 0, \\ 1 - \delta_{U_i, R_j} & \text{if } \theta = \chi, \\ 0 & \text{otherwise,} \end{cases} \quad (4.8)$$

where χ denotes the coefficient that is predefined from the systematic generator matrix of MDS codes. To generate this code, we used the software application SAGE [103]. For $N = 8$ and $M = 4$, for example, the 4×8 submatrix of the systematic MDS code

is:

$$\begin{bmatrix} 9 & 13 & 14 & 7 & 2 & 15 & 13 & 12 \\ 15 & 3 & 9 & 12 & 12 & 10 & 12 & 2 \\ 14 & 9 & 12 & 7 & 8 & 1 & 3 & 7 \\ 4 & 5 & 5 & 10 & 9 & 3 & 4 & 1 \end{bmatrix}. \quad (4.9)$$

In example (4.9), the conditional probability $\Pr\{\beta_{11} = 9 \mid \bar{\mathcal{E}}_1\}$ is $1 - \delta_{U_1, R_1}$, and for any $\theta \in \mathbb{F}_{16} \setminus \{0, 9\}$, it is set to zero, i.e., $\Pr\{\beta_{11} = \theta \mid \bar{\mathcal{E}}_1\} = 0$. Based on this, we can investigate the improvement in reconstruction performance that is achieved when using MDS codes in a cooperative wireless network.

Remark 4.1. *In this work, we assume that all the inter-node channels are independent from each other. Thereby, probability distributions of random elements are defined independently. If channel correlations are considered, the distributions, i.e., (4.6), (4.7), and (4.8), should be modeled as a joint distribution corresponding to the channel correlation. Using joint distributions, we can evaluate the performance of correlated wireless network coding schemes. Example 4.3 shows that the proposed framework can be extended to correlation cases. A generalized version of the proposed framework for channel correlations will be another direction of future research.*

4.5 Upper Bound on Reconstruction of Messages

If a transmission matrix for a dynamic network topology randomly generated using the probability distributions given in (4.6), (4.7), and (4.8), has full rank, the BS can uniquely decode all messages from all sources. In this section, we aim to derive an upper bound on the decoding failure probability, and the dimension of the nullspace

of the random transmission matrix of an (N, M) cooperative wireless network. We then connect them to investigate the manner in which network coding performance varies based on wireless channel conditions, the number of relays, field sizes, and the positions of nodes deployed in a 2D space. Throughout this chapter, we use the random transmission matrix as a bold face, i.e., \mathbf{A} , while the realized transmission matrix in sans-serif style, i.e., A .

We define the dimension of the nullspace within the column space of a transmission matrix as follows. Let \mathbf{A} be an $(N + M) \times N$ matrix over the finite field with size q as \mathbb{F}_q . Based on linear algebra theory, the columns A_1, \dots, A_N of \mathbf{A} are linearly dependent if and only if a vector $\mathbf{c} = (c_1, \dots, c_N) \in \mathbb{F}_q^N$ exists, with at least one nonzero c_i , such that

$$\sum_{i=1}^N c_i A_i = 0. \quad (4.10)$$

Definition 4.1. (*Number of nonzero coefficient vectors*) Let $L(\mathbf{A})$ be the number of all such nonzero vectors \mathbf{c} belonging to the nullspace of the given matrix \mathbf{A} . Let the column rank of a realized transmission matrix be $\text{rank}(\mathbf{A})$. Thus, $L(\mathbf{A})$ can be represented as

$$L(A) = q^{N - \text{rank}(\mathbf{A})} - 1. \quad (4.11)$$

Definition 4.2. (*Nullity*) Let $\text{nullity}(\mathbf{A})$ be the dimension of the nullspace in the column space of \mathbf{A} .

Proposition 4.3. For a random matrix \mathbf{A} , the expectation of the nullity of \mathbf{A} is upper bounded by $\mathbb{E}[\text{nullity}(\mathbf{A})] \leq \log_q(\mathbb{E}[L(\mathbf{A})] + 1)$, where $\mathbb{E}[\cdot]$ denotes the expectation.

Proof: For any $(N + M) \times N$ matrix \mathbf{A} , we follow $\text{nullity}(\mathbf{A}) = N - \text{rank}(\mathbf{A})$, known as the rank-nullity theorem of linear algebra [104]. Considering the expectation for a random transmission matrix in both sides of (4.11), we obtain the following upper bound using Jensen's inequality:

$$\begin{aligned} \mathbb{E}[\text{nullity}(\mathbf{A})] &:= N - \mathbb{E}[\text{rank}(\mathbf{A})] \\ &= \mathbb{E}[\log_q(L(\mathbf{A}) + 1)] \\ &\leq \log_q(\mathbb{E}[L(\mathbf{A})] + 1), \end{aligned} \tag{4.12}$$

■

Theorem 4.4. Let P_{fail} be the decoding failure probability for the reconstruction of source messages. Then, $P_{fail} \leq \min \left\{ 1, \frac{1}{q-1} \mathbb{E}[L(\mathbf{A})] \right\}$.

Proof: The probability P_{fail} is defined and upper bounded by

$$\begin{aligned} P_{fail} &= \Pr \{ \text{rank}(\mathbf{A}) < N \} \\ &= \Pr \left\{ \exists \mathbf{c} : \sum_{i=1}^N c_i A_i = 0 \right\} \\ &\stackrel{(a)}{\leq} \sum_{\mathbf{c} \in \mathbb{F}_q^N \setminus \{0^T\}} \Pr \{ \mathbf{A}\mathbf{c} = 0^T \} \\ &= \mathbb{E}[L(\mathbf{A})]. \end{aligned} \tag{4.13}$$

where inequality (a) is due to the union bound; note that $\mathbb{E}[L(\mathbf{A})] = \sum_{\mathbf{c} \in \mathbb{F}_q^N \setminus \{0^T\}} \Pr \{ \mathbf{A}\mathbf{c} = 0^T \}$.

Then, the upper bound on the probability P_{fail} can be tightened as

$$P_{fail} \leq \min \left\{ 1, \frac{1}{q-1} \mathbb{E}[L(\mathbf{A})] \right\}, \tag{4.14}$$

where the $1/(q-1)$ factor is due to the following reason. Suppose a nonzero vector \mathbf{c} exists such that $\mathbf{A}\mathbf{c} = 0^T$. Then, other $q-2$ nonzero vectors $\theta\mathbf{c}$, $\theta^2\mathbf{c}$, ..., $\theta^{q-2}\mathbf{c}$

certainly exist for a primitive element $\theta \in \mathbb{F}_q \setminus \{0\}$, where each satisfies $\mathbf{A}\theta^i \mathbf{c} = 0^T$ for $i \in \{1, \dots, q-2\}$. Then, we note $\bigcup_{\mathbf{c}_1 \in \{\theta \mathbf{c}, \dots, \theta^{q-2} \mathbf{c}\}} \{\mathbf{A} : \mathbf{A}\mathbf{c}_1 = 0^T\} = \{\mathbf{A} : \mathbf{A}\mathbf{c} = 0^T\}$.

■

Remark 4.2. *Proposition 4.3 and Theorem 4.4 provide the groundwork to novel performance evaluation framework of cooperative wireless NC schemes. These results allow us to carry out the calculation of the decoding failure probability without going through the exhaustive search of all the possible cases individually. They belong to the new key steps in making our evaluation framework to be computationally efficient which are not available in the literature, such as [68]–[71].*

Next, we will derive $\mathbb{E}[L(\mathbf{A})]$ for three types of cooperative wireless networks.

4.5.1 Homogeneous and Heterogeneous Connectivity

In this subsection, we aim to find $\mathbb{E}[L(\mathbf{A})]$ for two cases: i) *homogeneous connectivity* in which all outage probabilities in the wireless network are identical, i.e., $\delta = \delta_{U_i, BS} = \delta_{U_i, R_j} = \delta_{R_j, BS}$ given in (4.1) and (4.2) for $i \in \{1, 2, \dots, N\}$ and $j \in \{1, 2, \dots, M\}$, assuming that all the channel qualities in networks are equal, and ii) *heterogeneous connectivity* in which two types of outage probabilities exist, i.e., $\delta_1 = \delta_{U_i, BS} = \delta_{U_i, R_j}$ and $\delta_2 = \delta_{R_j, BS}$, with each outage probability assumed to be merely a function of transmit power. Note that each element of a random matrix follows the probability distributions defined in (4.6) and (4.7).

Let S_k denote the probability, i.e., $S_k := \Pr \left\{ \sum_{i=1}^k \beta_{ji} = 0 \right\}$, for the sum of a linear combination of the first k random elements $k \in \{1, 2, \dots, N\}$ in the j th row of a

combination matrix \mathbf{P} . For the homogeneous case, Lemma 4.5 gives this probability S_k .

Lemma 4.5. For the homogeneous connectivity with the distributions (4.6) and (4.7), the probability S_k is given by

$$S_k = \delta + (1 - \delta) \left(q^{-1} + (1 - q^{-1}) \left(1 - \frac{1 - \delta}{1 - q^{-1}} \right)^k \right). \quad (4.15)$$

Proof: For the homogeneous connectivity, we use $\delta = \delta_{U_i, BS} = \delta_{U_i, R_j} = \delta_{R_j, BS}$. The conditional probability $\Pr \{ \beta_{ji} = \theta | \bar{\mathcal{E}}_j \}$ of each element β_{ji} is defined using (4.7), and the other conditional probability can be set to $\Pr \{ \beta_{ji} = 0 | \mathcal{E}_j \} = 1$. Using the total probability theorem, the probability $\Pr \left\{ \sum_{i=1}^k \beta_{ji} = 0 \right\}$ can be decomposed by the condition of the outage event \mathcal{E}_j , and then given as follows:

$$\begin{aligned} S_k &= \Pr \{ \mathcal{E}_j \} \Pr \left\{ \sum_{i=1}^k \beta_{ji} = 0 \middle| \mathcal{E}_j \right\} + \Pr \{ \bar{\mathcal{E}}_j \} \Pr \left\{ \sum_{i=1}^k \beta_{ji} = 0 \middle| \bar{\mathcal{E}}_j \right\} \\ &\stackrel{(a)}{=} \delta + (1 - \delta) \Pr \left\{ \sum_{i=1}^k \beta_{ji} = 0 \middle| \bar{\mathcal{E}}_j \right\}, \end{aligned} \quad (4.16)$$

where (a) follows from the fact that $\Pr \left\{ \sum_{i=1}^k \beta_{ji} = 0 | \mathcal{E}_j \right\} = 1$, as $\Pr \{ \beta_{ji} = 0 | \mathcal{E}_j \} = 1$ (note that the conditional probability $\Pr \{ \beta_{ji} = \theta | \bar{\mathcal{E}}_j \}$ is independent of this). Let f_k be the probability, i.e., $f_k := \Pr \left\{ \sum_{i=1}^k \beta_{ji} = 0 | \bar{\mathcal{E}}_j \right\}$. Given the conditional probability defined in (4.7) and $f_0 = 1$, the probability f_k can be rewritten by

$$\begin{aligned} f_k &:= \Pr \left\{ \sum_{i=1}^k \beta_{ji} = 0 \middle| \bar{\mathcal{E}}_j \right\} \\ &= \Pr \left\{ \sum_{i=1}^{k-1} \beta_{ji} = 0 \middle| \bar{\mathcal{E}}_j \right\} \Pr \{ \beta_{jk} = 0 | \bar{\mathcal{E}}_j \} \\ &\quad + \sum_{\theta \in \mathbb{F}_q \setminus \{0\}} \Pr \left\{ \sum_{i=1}^{k-1} \beta_{ji} = \theta \middle| \bar{\mathcal{E}}_j \right\} \Pr \{ \beta_{jk} = -\theta | \bar{\mathcal{E}}_j \} \\ &= f_{k-1} \delta + (1 - f_{k-1}) \frac{1 - \delta}{q - 1}. \end{aligned} \quad (4.17)$$

Let $g_k := f_k - q^{-1}$. By rewriting (4.17) as a function of g_k , we have a simple closed form:

$$g_k = g_{k-1} \left(1 - \frac{1 - \delta}{1 - q^{-1}} \right). \quad (4.18)$$

Applying a geometric series to (4.18), we obtain f_k as follows:

$$f_k = q^{-1} + (1 - q^{-1}) \left(1 - \frac{1 - \delta}{1 - q^{-1}} \right)^k. \quad (4.19)$$

Finally, the probability S_k can be obtained by substituting (4.19) into (4.16):

$$S_k = \delta + (1 - \delta) \left(q^{-1} + (1 - q^{-1}) \left(1 - \frac{1 - \delta}{1 - q^{-1}} \right)^k \right). \quad (4.20)$$

The proof of Lemma 4.5 is completed. ■

Before attempting to derive $\mathbb{E}[L(\mathbf{A})]$ of a random matrix \mathbf{A} from Lemma 4.5, recall that $L(A)$ is the number of all nonzero vectors \mathbf{c} satisfying the linear dependency, i.e., (4.10). The following Proposition 4.6 gives $\mathbb{E}[L(\mathbf{A})]$ for the homogeneous (N, M) wireless cooperative network.

Proposition 4.6. Given an (N, M) cooperative network with the homogeneous connectivity based on some outage probability δ , $\mathbb{E}[L(\mathbf{A})]$ of a $(N + M) \times N$ random transmission matrix \mathbf{A} over the finite field \mathbb{F}_q is

$$\mathbb{E}[L(\mathbf{A})] = \sum_{k=1}^N \binom{N}{k} (q-1)^k \delta^k \left[\delta + (1 - \delta) \left(q^{-1} + (1 - q^{-1}) \left(1 - \frac{1 - \delta}{1 - q^{-1}} \right)^k \right) \right]^M. \quad (4.21)$$

Proof: Let us consider a vector $\mathbf{c} = (c_1, \dots, c_N) \in \mathbb{F}_q^N$ in which the first k entries (and only the first k entries) are nonzero, i.e., $\mathbf{c} = (c_1, \dots, c_k, 0, \dots, 0)$. Let P_k be the probability that the sum of a linear combination of the first k column vectors is zero,

i.e., $P_k := \Pr \left\{ \sum_{i=1}^k c_i A_i = 0 \right\}$. As (4.22), $\mathbb{E}[L(\mathbf{A})]$ is given by

$$\begin{aligned} \mathbb{E}[L(\mathbf{A})] &= \sum_{\mathbf{c} \in \mathbb{F}_q^N \setminus \{0^T\}} \Pr \{ \mathbf{A}\mathbf{c} = 0^T \} \\ &= \sum_{k=1}^N \binom{N}{k} (q-1)^k P_k. \end{aligned} \quad (4.22)$$

Since all the links in the wireless network are assumed to be spatially and temporally independent in Chapter 4.2.2, the rows of the transmission matrix are also independent.

Thus, P_k is given by

$$\begin{aligned} P_k &= \Pr \left\{ \sum_{i=1}^k c_i A_i = 0 \right\} \\ &= \prod_{i=1}^k \Pr \{ c_i \alpha_{ii} = 0 \} \prod_{j=1}^M \Pr \left\{ \sum_{i=1}^k c_i \beta_{ji} = 0 \right\}. \end{aligned} \quad (4.23)$$

Let H_k be the probability as $H_k := \Pr \left\{ \sum_{i=1}^k c_i \beta_{ji} = 0 \right\}$. For $k = 1$, it is easy to show $\Pr \{ c_1 \beta_{j1} = 0 \} = \Pr \{ \beta_{j1} = 0 \}$ for $c_1 \in \mathbb{F}_q \setminus \{0\}$ because of multiplication property in finite fields. Next, we prove that $H_k = S_k$ for $k \geq 2$ where $c_1, c_2, \dots, c_k \in \mathbb{F}_q \setminus \{0\}$ denote the k nonzero elements. The probability H_k is represented by

$$\begin{aligned} H_k &= \sum_{\theta \in \mathbb{F}_q} \Pr \left\{ \sum_{i=1}^{k-1} c_i \beta_{ji} = \theta, c_k \beta_{jk} = -\theta \right\} \\ &= \Pr \left\{ \sum_{i=1}^{k-1} c_i \beta_{ji} = 0, c_k \beta_{jk} = 0 \right\} + \sum_{\theta \in \mathbb{F}_q \setminus \{0\}} \Pr \left\{ \sum_{i=1}^{k-1} c_i \beta_{ji} = \theta, c_k \beta_{jk} = -\theta \right\}. \end{aligned} \quad (4.24)$$

Decomposing the outage event \mathcal{E}_j , (4.24) can be rewritten by

$$\begin{aligned}
H_k &= \Pr \left\{ \sum_{i=1}^{k-1} c_i \beta_{ji} = 0, c_k \beta_{jk} = 0 \middle| \bar{\mathcal{E}}_j \right\} \Pr \{ \bar{\mathcal{E}}_j \} + \Pr \left\{ \sum_{i=1}^{k-1} c_i \beta_{ji} = 0, c_k \beta_{jk} = 0 \middle| \mathcal{E}_j \right\} \Pr \{ \mathcal{E}_j \} \\
&+ \sum_{\theta \in \mathbb{F}_q \setminus \{0\}} \left(\Pr \left\{ \sum_{i=1}^{k-1} c_i \beta_{ji} = \theta, c_k \beta_{jk} = -\theta \middle| \bar{\mathcal{E}}_j \right\} \Pr \{ \bar{\mathcal{E}}_j \} \right. \\
&\quad \left. + \Pr \left\{ \sum_{i=1}^{k-1} c_i \beta_{ji} = \theta, c_k \beta_{jk} = -\theta \middle| \mathcal{E}_j \right\} \Pr \{ \mathcal{E}_j \} \right).
\end{aligned} \tag{4.25}$$

Since $\Pr \{ \beta_{ji} = 0 | \mathcal{E}_j \} = 1$, (4.25) can be represented by

$$\begin{aligned}
H_k &= \Pr \left\{ \sum_{i=1}^{k-1} c_i \beta_{ji} = 0, c_k \beta_{jk} = 0 \middle| \bar{\mathcal{E}}_j \right\} \Pr \{ \bar{\mathcal{E}}_j \} + \Pr \{ \mathcal{E}_j \} \\
&+ \sum_{\theta \in \mathbb{F}_q \setminus \{0\}} \Pr \left\{ \sum_{i=1}^{k-1} c_i \beta_{ji} = \theta, c_k \beta_{jk} = -\theta \middle| \bar{\mathcal{E}}_j \right\} \Pr \{ \bar{\mathcal{E}}_j \}.
\end{aligned} \tag{4.26}$$

Noting that wireless channels are independent with each other under the condition of $\bar{\mathcal{E}}_j$, (4.26) can be decomposed by

$$\begin{aligned}
H_k &= \Pr \left\{ \sum_{i=1}^{k-1} c_i \beta_{ji} = 0 \middle| \bar{\mathcal{E}}_j \right\} \Pr \left\{ c_k \beta_{jk} = 0 \middle| \bar{\mathcal{E}}_j \right\} \Pr \{ \bar{\mathcal{E}}_j \} + \Pr \{ \mathcal{E}_j \} \\
&+ \sum_{\theta \in \mathbb{F}_q \setminus \{0\}} \Pr \left\{ \sum_{i=1}^{k-1} c_i \beta_{ji} = \theta \middle| \bar{\mathcal{E}}_j \right\} \Pr \left\{ c_k \beta_{jk} = -\theta \middle| \bar{\mathcal{E}}_j \right\} \Pr \{ \bar{\mathcal{E}}_j \}.
\end{aligned} \tag{4.27}$$

Using recursion, the probability H_k is given by

$$\begin{aligned}
H_k &= \Pr \left\{ \sum_{i=1}^{k-1} \beta_{ji} = 0 \middle| \bar{\mathcal{E}}_j \right\} \Pr \left\{ \beta_{jk} = 0 \middle| \bar{\mathcal{E}}_j \right\} \Pr \{ \bar{\mathcal{E}}_j \} + \Pr \{ \mathcal{E}_j \} \\
&+ \sum_{\theta \in \mathbb{F}_q \setminus \{0\}} \Pr \left\{ \sum_{i=1}^{k-1} \beta_{ji} = \theta \middle| \bar{\mathcal{E}}_j \right\} \Pr \left\{ \beta_{jk} = -\theta \middle| \bar{\mathcal{E}}_j \right\} \Pr \{ \bar{\mathcal{E}}_j \} \\
&= \sum_{\theta \in \mathbb{F}_q} \Pr \left\{ \sum_{i=1}^{k-1} \beta_{ji} = \theta, \beta_{jk} = -\theta \right\} \\
&= \Pr \left\{ \sum_{i=1}^k \beta_{ji} = 0 \right\}.
\end{aligned} \tag{4.28}$$

Thus, we simply rewrite P_k as follows

$$P_k = \delta^k S_k^M. \quad (4.29)$$

The proof of Proposition 4.6 is completed. ■

Now, let us consider $\mathbb{E}[L(\mathbf{A})]$ under the heterogeneous case; i.e., $\delta_1 = \delta_{U_i,BS} = \delta_{U_i,R_j}$ and $\delta_2 = \delta_{R_j,BS}$. In what follows, we aim to study how the outage probabilities δ_1 and δ_2 affect the recovery performance, assuming that these outage probabilities rely on the transmit power at the sources and relays.

Proposition 4.7. Given the heterogeneous (N, M) cooperative network defined by the two outage probabilities δ_1 and δ_2 , $\mathbb{E}[L(\mathbf{A})]$ of a $(N + M) \times N$ random transmission matrix \mathbf{A} over finite fields \mathbb{F}_q is given by

$$\mathbb{E}[L(\mathbf{A})] = \sum_{k=1}^N \binom{N}{k} (q-1)^k \delta_1^k \left[\delta_2 + (1-\delta_2) \left(q^{-1} + (1-q^{-1}) \left(1 - \frac{1-\delta_1}{1-q^{-1}} \right)^k \right) \right]^M. \quad (4.30)$$

The proof is omitted. But it can be obtained by following the formalism given in Proposition 4.6, using two outage probability, δ_1 and δ_2 , instead of single outage probability as done in Proposition 4.6.

4.5.2 General Connectivity

Thus far, we have found $\mathbb{E}[L(\mathbf{A})]$ of a random transmission matrix \mathbf{A} for the homogeneous and heterogeneous cases. In this subsection, we extend it to a more general case, where δ_{U_i,R_j} , $\delta_{R_j,BS}$, and $\delta_{U_i,BS}$ are used as defined in Chapter 4.2.2. Outage probabilities for the wireless links are obtained using (4.1) and (4.2), which are a function of

the transmit power and the variance of the channel gain. After finding the outage probability for each link, we determine the probability distributions for all the elements in \mathbf{A} . We call this the *general connectivity* case. Because it involves the exhaustive search of combinations of column vectors in a random matrix, the general connectivity requires a more complicated computation than that of the homogeneous and the heterogeneous connectivity in order to derive $\mathbb{E}[L(\mathbf{A})]$ where the proposed approach using the upper bound on the dimension of nullspace will be most powerful.

Proposition 4.8. Given an (N, M) cooperative network with the general connectivity based on the outage probabilities defined in (4.1) and (4.2), $\mathbb{E}[L(\mathbf{A})]$ of a $(N + M) \times N$ random transmission matrix \mathbf{A} over finite fields \mathbb{F}_q is

$$\mathbb{E}[L(\mathbf{A})] = \sum_{k=1}^N (q - 1)^k Q_k, \quad (4.31)$$

where $Q_k := \sum_{l=1}^{|\mathcal{L}_k|} Q_{k,l}$, $l \in \{1, 2, \dots, |\mathcal{L}_k|\}$, $|\mathcal{L}_k| := \binom{N}{k}$, and $\mathcal{L}_{k,l}$ is the l th entry of a set \mathcal{L}_k . Let \mathcal{L}_k denote the collection of the sets of k distinct indices among $[N] := \{1, 2, \dots, N\}$, i.e., $\mathcal{L}_k := \{\{\lambda_1, \lambda_2, \dots, \lambda_k\} : \lambda_i \in \{1, 2, \dots, N\}, \lambda_i \neq \lambda_j, i \neq j\}$. And the probability $Q_{k,l}$ is defined as: $Q_{k,l} := \Pr \left\{ \sum_{i \in \mathcal{L}_{k,l}} c_i A_i = 0 \right\}$.

Proof: For the general connectivity, the probability distribution of each element of \mathbf{A} is different with each other. This leads to different probabilities $Q_{k,l}$ for that any k column vectors of \mathbf{A} are linearly dependent. The total number of $Q_{k,l}$ is $|\mathcal{L}_k| := \binom{N}{k}$. We have to consider all different probabilities $Q_{k,l}$ with respect to all the sets $\mathcal{L}_{k,l}$. The total probability Q_k should be summed over different probabilities $Q_{k,l}$, i.e., $Q_k := \sum_{l=1}^{|\mathcal{L}_k|} Q_{k,l}$ for $l \in \{1, 2, \dots, |\mathcal{L}_k|\}$ and $k \in \{1, 2, \dots, N\}$. Thus, all $Q_{k,l}$ are enumerated

and collected to obtain the probability Q_k , which is derived as follows:

$$\begin{aligned}
Q_k &= \sum_{l=1}^{|\mathcal{L}_k|} Q_{k,l} \\
&= \sum_{l=1}^{|\mathcal{L}_k|} \Pr \left\{ \sum_{i \in \mathcal{L}_{k,l}} c_i A_i = 0 \right\} \\
&= \sum_{l=1}^{|\mathcal{L}_k|} \prod_{m=1}^k \Pr \{ \alpha_{l_m l_m} = 0 \} \prod_{j=1}^M \Pr \left\{ \sum_{m=1}^k \beta_{j l_m} = 0 \right\},
\end{aligned} \tag{4.32}$$

where l_m is the m th entry of the set $\mathcal{L}_{k,l}$, $m \in \{1, 2, \dots, k\}$. As similarly obtained in (4.16), (4.32) can be rewritten as

$$Q_k = \sum_{l=1}^{|\mathcal{L}_k|} \prod_{m=1}^k \Pr \{ \alpha_{l_m l_m} = 0 \} \prod_{j=1}^M \left(\delta_{R_j, BS} + (1 - \delta_{R_j, BS}) \Pr \left\{ \sum_{m=1}^k \beta_{j l_m} = 0 \middle| \bar{\mathcal{E}}_j \right\} \right). \tag{4.33}$$

In order to find $\mathbb{E}[L(\mathbf{A})]$, we count the number of vectors \mathbf{c} having the first k nonzero elements, i.e., $(q-1)^k$. Finally, we then take the summation over all k , and obtain $\mathbb{E}[L(\mathbf{A})]$ as follows,

$$\mathbb{E}[L(\mathbf{A})] = \sum_{k=1}^N (q-1)^k Q_k. \tag{4.34}$$

The proof of Proposition 4.8 is completed. ■

We use Proposition 4.8 to find $\mathbb{E}[L(\mathbf{A})]$ for $q = 2$ in a $(2, 1)$ cooperative wireless network as follows.

Example 4.2: Let us consider a $(2, 1)$ cooperative wireless network for $q = 2$, $N = 2$, and $M = 1$. There are three nonzero vectors \mathbf{c} in \mathbb{F}_2^2 : (10) , (01) , and (11) . For each nonzero vector, we find the probability $Q_{k,l}$ as follows. First, the probability $Q_{1,1}$

is

$$\begin{aligned}
Q_{1,1} &= \Pr \{c_1 A_1 = 0\} \\
&= \Pr \{\alpha_{11} = 0\} \Pr \{\beta_{11} = 0\} \\
&= \delta_{U_1,BS} (\delta_{R_1,BS} + (1 - \delta_{R_1,BS}) \delta_{U_1,R_1}).
\end{aligned} \tag{4.35}$$

The probability $Q_{1,2}$ is

$$\begin{aligned}
Q_{1,2} &= \Pr \{c_2 A_2 = 0\} \\
&= \Pr \{\alpha_{22} = 0\} \Pr \{\beta_{12} = 0\} \\
&= \delta_{U_2,BS} (\delta_{R_1,BS} + (1 - \delta_{R_1,BS}) \delta_{U_2,R_1}).
\end{aligned} \tag{4.36}$$

The probability $Q_{2,1}$ is

$$\begin{aligned}
Q_{2,1} &= \Pr \{c_1 A_1 + c_2 A_2 = 0\} \\
&= \Pr \{\alpha_{11} = 0\} \Pr \{\alpha_{22} = 0\} \Pr \{\beta_{11} + \beta_{12} = 0\} \\
&= \delta_{U_1,BS} \delta_{U_2,BS} \left(\delta_{R_1,BS} + (1 - \delta_{R_1,BS}) \Pr \{\beta_{11} + \beta_{12} = 0 \mid \bar{\mathcal{E}}_1 \} \right).
\end{aligned} \tag{4.37}$$

In this example, $\mathbb{E}[L(\mathbf{A})]$ is then given by

$$\mathbb{E}[L(\mathbf{A})] = Q_{1,1} + Q_{1,2} + Q_{2,1}. \tag{4.38}$$

■

In addition, it is interesting to see if the proposed evaluation framework developed thus far can be extended to the cases where the outages between different links are not independent but correlated. Such cases may arise when the channels between two nodes are not perfectly orthogonal. Then, it becomes an interesting problem to show how the proposed analysis framework can be utilized to compute the decoding failure probability in the correlated link outages cases. This is in general a difficult task which

requires space of a new entire manuscript to nicely show all the details. Leaving the details as a future work, in this section, we aim to show that the framework is extendible to correlated link outage cases.

For this purpose, we again use Proposition 4.8 to compute $\mathbb{E}[L(\mathbf{A})]$ and extend Example 4.2 for correlated cases. The outage probabilities are not independent with each other. This can be dealt with the consideration of a joint probability distribution for the random matrix. Using the joint probability distribution, we can again compute the last line of (4.32) in Appendix, instead of the product of probabilities. This is a main change for correlated cases to extend the proposed evaluation framework. In Example 4.3, given joint probability distributions, we compute $Q_{1,1}$, $Q_{1,2}$, and $Q_{2,1}$ as shown in Example 4.2.

Example 4.3: Let us consider a $(2, 1)$ cooperative wireless network for $q = 2$, $N = 2$, and $M = 1$. There are two sets of channel correlations we assume in this example. The first set of correlated channels is between U_1 - R_1 and U_2 - R_1 ; the second set of correlated channels is between U_1 -BS and U_2 -BS. We assume that all other combinations of channels are mutually independent. Note that the both sets of correlation occur in the broadcasting phase. A pair of two outage events, U_1 -BS and U_2 -BS, makes a joint probability as $\Pr\{\alpha_{11} = \theta_1, \alpha_{22} = \theta_2\} = \Theta_{\theta_1, \theta_2}$ for each $(\theta_1, \theta_2) \in \mathbb{F}_2^2$, where $\sum_{\theta_1, \theta_2} \Theta_{\theta_1, \theta_2} = 1$. For example, when the both channels are simultaneously successful in the broadcasting phase, we can set the particular probability as $\Pr\{\alpha_{11} = 1, \alpha_{22} = 1\} = \Theta_{1,1}$. Similarly, other probabilities can be defined by the conditions of the two outage events, U_1 -BS and U_2 -BS. Note that the conditional joint

Table 4.3: Determination of the Conditional Joint Probability for the Two Elements

β_{11} and β_{12} “O” indicates no outage and “ \times ” indicates an outage

| (U_1-R_1, U_2-R_1) | (β_{11}, β_{12}) | $\Pr \{ \beta_{11} = \gamma_1, \beta_{12} = \gamma_2 \mid \bar{\mathcal{E}}_1 \}$ |
|-------------------------|----------------------------|---|
| (O, O) | (1, 1) | $\Gamma_{1,1}$ |
| (O, \times) | (1, 0) | $\Gamma_{1,0}$ |
| (\times , O) | (0, 1) | $\Gamma_{0,1}$ |
| (\times , \times) | (0, 0) | $\Gamma_{0,0}$ |

probability is set as $\Pr \{ \beta_{11} = 0, \beta_{12} = 0 \mid \mathcal{E}_1 \} = 1$ since the two elements, β_{11} and β_{12} , are zero when the channel outage between R_1 and BS occurs. In addition, a set of the two outage events, U_1-R_1 and U_2-R_1 , can determine the values of the two random elements β_{11} and β_{12} once the channel outage between R_1 and BS does not occur, i.e., when $\bar{\mathcal{E}}_1$ is true. In this case, let the conditional joint probability distribution be known and given as $\Pr \{ \beta_{11} = \gamma_1, \beta_{12} = \gamma_2 \mid \bar{\mathcal{E}}_1 \} = \Gamma_{\gamma_1, \gamma_2}$ for each $(\gamma_1, \gamma_2) \in \mathbb{F}_2^2$, where $\sum_{\gamma_1, \gamma_2} \Gamma_{\gamma_1, \gamma_2} = 1$. For $q = 2$, Table 4.3 summarizes this conditional joint probability distribution according to the conditions of the two outage events U_1-R_1 and U_2-R_1 .

For three nonzero vectors \mathbf{c} in \mathbb{F}_2^2 , we can again compute $Q_{1,1}$, $Q_{1,2}$, and $Q_{2,1}$. The computation of $Q_{1,1}$ and $Q_{1,2}$ is easy because of our assumption that the two sets of channel correlations are independent. The both results are

$$Q_{1,1} = (\Theta_{0,0} + \Theta_{0,1}) (\delta_{R_1, BS} + (1 - \delta_{R_1, BS}) (\Gamma_{0,0} + \Gamma_{0,1})) \quad (4.39)$$

and

$$Q_{1,1} = (\Theta_{0,0} + \Theta_{1,0}) (\delta_{R_1, BS} + (1 - \delta_{R_1, BS}) (\Gamma_{0,0} + \Gamma_{1,0})) \quad (4.40)$$

The computation of $Q_{2,1}$ is given as follows:

$$\begin{aligned}
Q_{2,1} &= \Pr \{c_1 A_1 + c_2 A_2 = 0\} \\
&= \Pr \{\alpha_{11} = 0, \alpha_{22} = 0, \beta_{11} + \beta_{12} = 0\} \\
&= \Pr \{\alpha_{11} = 0, \alpha_{22} = 0, \beta_{11} + \beta_{12} = 0 | \mathcal{E}_1\} \Pr \{\mathcal{E}_1\} \\
&\quad + \Pr \{\alpha_{11} = 0, \alpha_{22} = 0, \beta_{11} + \beta_{12} = 0 | \bar{\mathcal{E}}_1\} \Pr \{\bar{\mathcal{E}}_1\} \\
&\stackrel{(a)}{=} \Pr \{\alpha_{11} = 0, \alpha_{22} = 0\} \\
&\quad \times \left(\Pr \{\beta_{11} + \beta_{12} = 0 | \mathcal{E}_1\} \Pr \{\mathcal{E}_1\} + \Pr \{\beta_{11} + \beta_{12} = 0 | \bar{\mathcal{E}}_1\} \Pr \{\bar{\mathcal{E}}_1\} \right) \\
&= \Theta_{0,0}(\delta_{R_1,BS} + (\Gamma_{0,0} + \Gamma_{1,1})(1 - \delta_{R_1,BS})),
\end{aligned} \tag{4.41}$$

where equality (a) is from the fact that the relation between the two sets, $(\alpha_{11}, \alpha_{22})$ and (β_{11}, β_{12}) , is independent. We finally obtain $\mathbb{E}[L(\mathbf{A})] = Q_{1,1} + Q_{1,2} + Q_{2,1}$ for correlated cases by using the proposed evaluation framework. ■

4.5.3 Asymptotic Nullity

In practice, the computation of (4.31) spends a lot of time due to collecting all combinations of column vectors as the number of sources and relays grows. In a larger size of networks, this work is complicated so that we need to alleviate the load of this computation. In this subsection, we aim to find an asymptotic form of (4.31) for utilization in large scale networks.

As previously mentioned, the scheme of the homogeneous connectivity is a specific case of the general connectivity schemes. We can show a simple form of $\mathbb{E}[L(\mathbf{A})]$ in terms of Q_k for the homogeneous topology of cooperative networks. From this approach, we can obtain an asymptotic result of (4.31) in general connectivity schemes. Let

us consider $\mathbb{E}[L(\mathbf{A})]$ for $q = 2$ in the homogeneous connectivity. Thus, $\mathbb{E}[L(\mathbf{A})] = \sum_{k=1}^N Q_k$ in (4.31). Using (4.32), Q_1 is given by

$$Q_1 = N\delta S_1. \quad (4.42)$$

For $k = 2$, we have $Q_2 = \binom{N}{2}\delta^2 S_2$. We further find $Q_3 = \binom{N}{3}\delta^3 S_3$ for $k = 2$. The general expression of Q_k is given by

$$Q_k = \binom{N}{k}\delta^k S_k. \quad (4.43)$$

In this case, $\mathbb{E}[L(\mathbf{A})]$ in (4.31) is

$$\mathbb{E}[L(\mathbf{A})] = \sum_{k=1}^N \binom{N}{k}\delta^k S_k. \quad (4.44)$$

In high SNR regions, assuming δ is small, an approximation form of (4.44) is obtained as follows

$$\begin{aligned} \mathbb{E}[L(\mathbf{A})] &= \sum_{k=1}^N Q_k \\ &\stackrel{(a)}{\approx} \binom{N}{1}\delta^1 S_1 + \binom{N}{2}\delta^2 S_2, \end{aligned} \quad (4.45)$$

where (a) is from the fact that the order of Q_k for $k \geq 3$ is greater than 2 with respect to δ . This approximation means that for computation of $\mathbb{E}[L(\mathbf{A})]$, two terms Q_1 and Q_2 are sufficient in high SNR regions. Therefore, in the high SNR regions, $\mathbb{E}[L(\mathbf{A})]$ converges to 2 order of the transmit SNR. For any finite fields and the general connectivity, this approximation holds.

Corollary 4.9. Given an (N, M) cooperative network with the general connectivity with the distributions (4.6) and (4.7), $\mathbb{E}[L(\mathbf{A})]$ is simplified in the high SNR regime

$$\mathbb{E}[L(\mathbf{A})] \approx (q-1)Q_1 + (q-1)^2 Q_2. \quad (4.46)$$

Remark 4.3. *Proposition 4.8 provides a closed form solution to the expectation of the number of nonzero vectors in the nullspace of the random transmission matrix. This enables us to evaluate the performance of a general network with randomly deployed nodes without going through each count of transmission matrices separately. Corollary 4.9 is an approximation of (4.31) which is useful for performance evaluation of large size networks.*

4.6 Numerical and Simulation Results

In this section, the reconstruction performance of source messages at the BS is investigated by means of the proposed evaluation framework, i.e., $\mathbb{E}[\text{nullity}(\mathbf{A})]$ and P_{fail} . For the homogeneous connectivity scheme, we use Proposition 4.6 to analytically evaluate the upper bound on $\mathbb{E}[\text{nullity}(\mathbf{A})]$ as a function of the outage probabilities of the channel links. We compare the upper bounds with numerically simulated results of $\mathbb{E}[\text{nullity}(\mathbf{A})]$ as well as P_{fail} . Subsequently, we use Proposition 4.8 to evaluate the upper bounds for a general cooperative network in which sources and relays are deployed in a 2D space. Further, we examine the results of upper bounds on $\mathbb{E}[\text{nullity}(\mathbf{A})]$ and P_{fail} for a given transmission matrix in order to investigate the impact of the number of relays and the field size of NC

Figure 4.3 shows analytically obtained upper bounds and numerically averaged results of $\mathbb{E}[\text{nullity}(\mathbf{A})]$ for a random transmission matrix in a $(10, M)$ cooperative wireless network given the homogeneous connectivity scheme, where $N = 10$ and $M = 3, 10, \text{ and } 20$ for $q = 2$ and 4 . We see that $\mathbb{E}[\text{nullity}(\mathbf{A})]$ increases as the outage

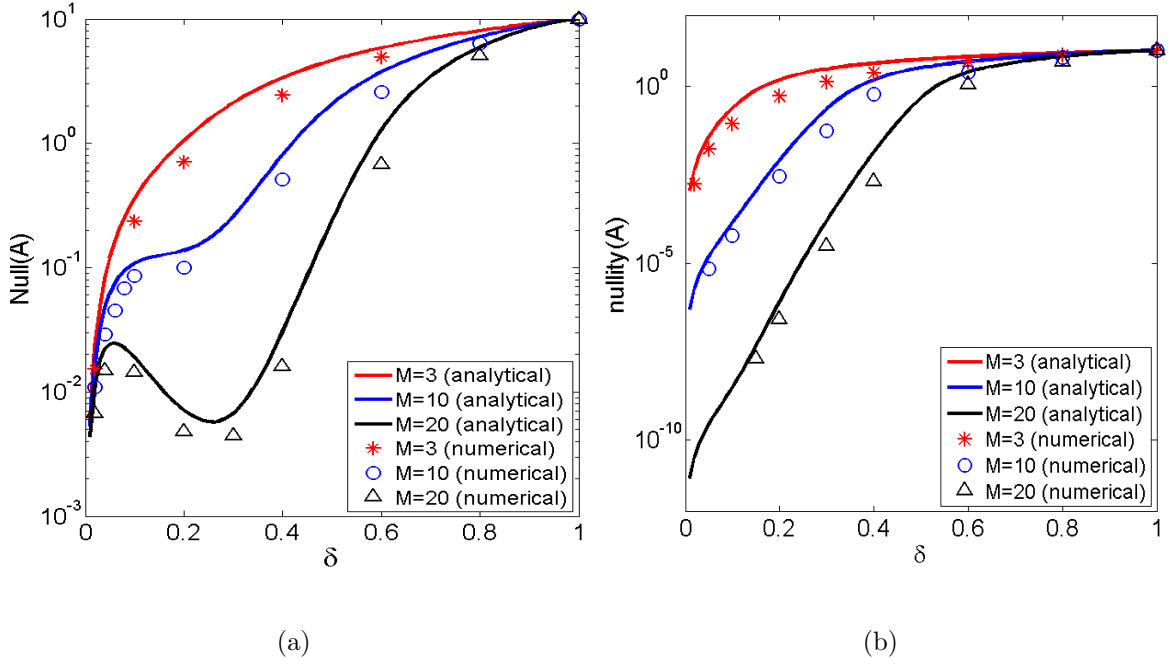


Figure 4.3: The nullity of random matrix \mathbf{A} for a homogeneous $(10, M)$ cooperative wireless network with $N = 10$ and $M = 3, 10,$ and 20 . Solid lines indicate the upper bounds on $\mathbb{E}[\text{nullity}(\mathbf{A})]$ using Proposition 4.6, and markers indicate numerically simulated results of $\mathbb{E}[\text{nullity}(\mathbf{A})]$, respectively: (a) $q = 2$ and (b) $q = 4$.

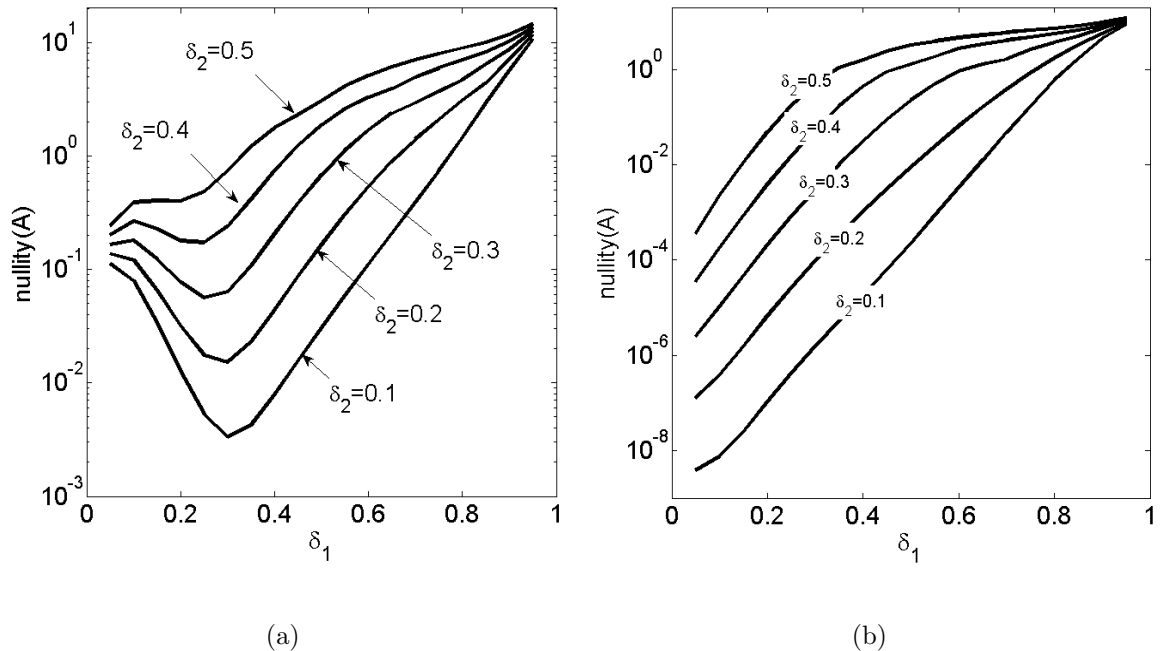


Figure 4.4: Upper bounds on $\mathbb{E}[\text{nullity}(\mathbf{A})]$ using Proposition 4.3 and 4.7 in a heterogeneous $(20, 20)$ cooperative wireless network with two outage probabilities δ_1 and δ_2 for (a) $q = 2$, and (b) $q = 4$.

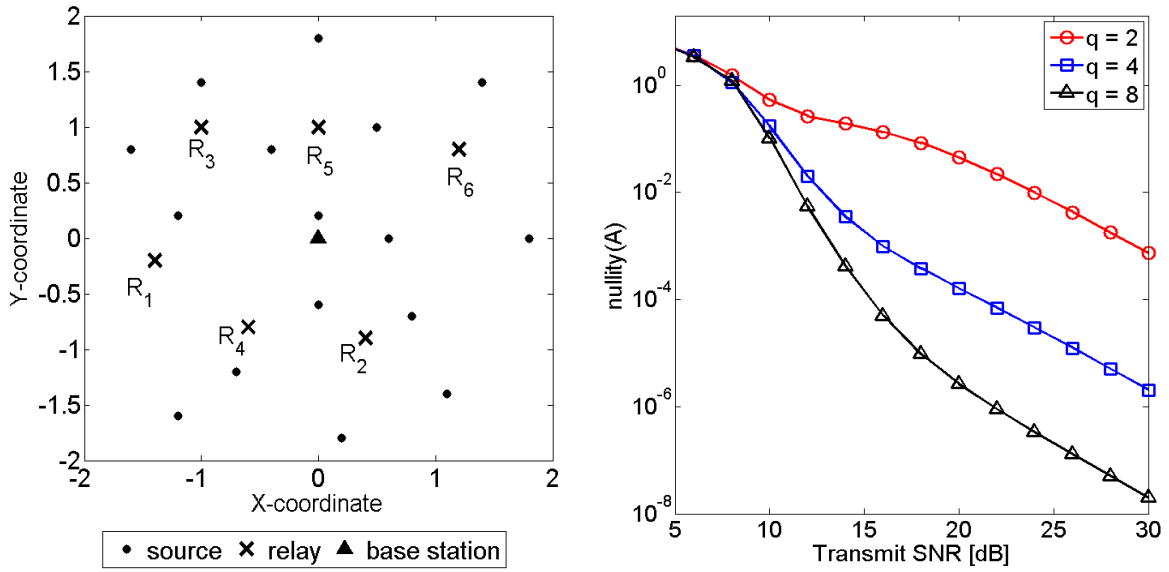
probability slightly increases. From Figure 4.3(b), it is clearly seen that a nonbinary NC scheme provides better reconstruction performance for source messages at the BS than binary coding, and that increasing the field size of NC also improves recovery performance. As the outage probability goes to zero, $\mathbb{E}[\text{nullity}(\mathbf{A})]$ approaches zero for all field sizes. The analytical results in Figure 4.3, which are indicated by solid lines, have a higher upper bound than the numerically simulated result indicated by a symbol, which has been evaluated by averaging random matrices in simulation.

Figure 4.4 shows the analytically derived upper bounds by using Proposition 4.7 for a heterogeneously connected $(20, 20)$ cooperative wireless network. Regardless of the

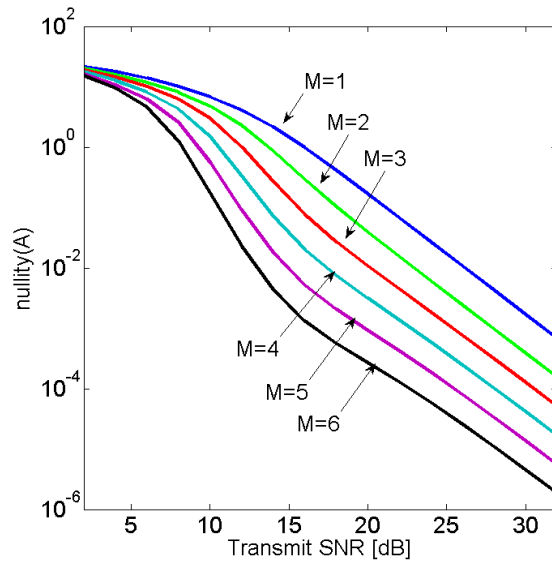
value of δ_2 , when the outage probability δ_1 goes to 1, $\mathbb{E}[\text{nullity}(\mathbf{A})]$ barely reaches 20 at both field sizes, i.e., $q = 2$ and 4. This means that all channel links undergo outage events, causing all elements of the transmission matrix to become zero. In Fig. 4.4(a), for $q = 2$, there is an oscillation around $\delta_1 = 0.3$ such that $\mathbb{E}[\text{nullity}(\mathbf{A})]$ decreases as δ_1 increases up to 0.3, and beyond this point $\mathbb{E}[\text{nullity}(\mathbf{A})]$ increases. This oscillation also appears in Fig. 4.3(a). This behavior is from the fact that the rows of \mathbf{P} tend to be identical as the outage probabilities δ_1 and δ_2 approach zero. For $q = 4$, however, this behavior vanishes due to the extension of the field size from binary to quaternary.

Now let us consider the (16, 6) cooperative wireless network shown in Figure 4.5(a), in which there are 16 sources and 6 relays: R_1 through R_6 . We randomly deploy these relays in a 2D space. We assume that all the transmit powers of sources and relays in both transmission phases are the same. Figure 4.5(b) shows the upper bound on $\mathbb{E}[\text{nullity}(\mathbf{A})]$ of the transmission matrix for $q = 2, 4$, and 8; the benefit of increasing the field size of NC appears in this scheme. Figure 4.5(c) shows the upper bound on $\mathbb{E}[\text{nullity}(\mathbf{A})]$ with respect to the number of relays. When $M = 1$, R_1 is used, while R_1 and R_2 are used as relays for $M = 2$, and relays R_1, R_2 , and R_3 are used for $M = 3$. For $M = 4, 5$, and 6, we deploy one relay in order. We investigate the impact of the number of relays, as shown in Figure 4.5(c), where as increasing the number of relays contributes to increasingly high likelihood of deriving random transmission matrices of full rank.

Other interesting results include that the value of $\mathbb{E}[\text{nullity}(\mathbf{A})]$ differs slightly for the uniform and MDS distributions of the combination matrix defined in Chapter 4.3.2, and



(a) (b)



(c)

Figure 4.5: (a) Location of 16 sources and 6 relays in 2D space for an (16, 6) cooperative wireless network. (b) Results of upper bounds on $\mathbb{E}[\text{nullity}(\mathbf{A})]$ with differing NC field sizes $q = 2, 4$, and 8 , (c) varying the number of relays at $q = 4$.

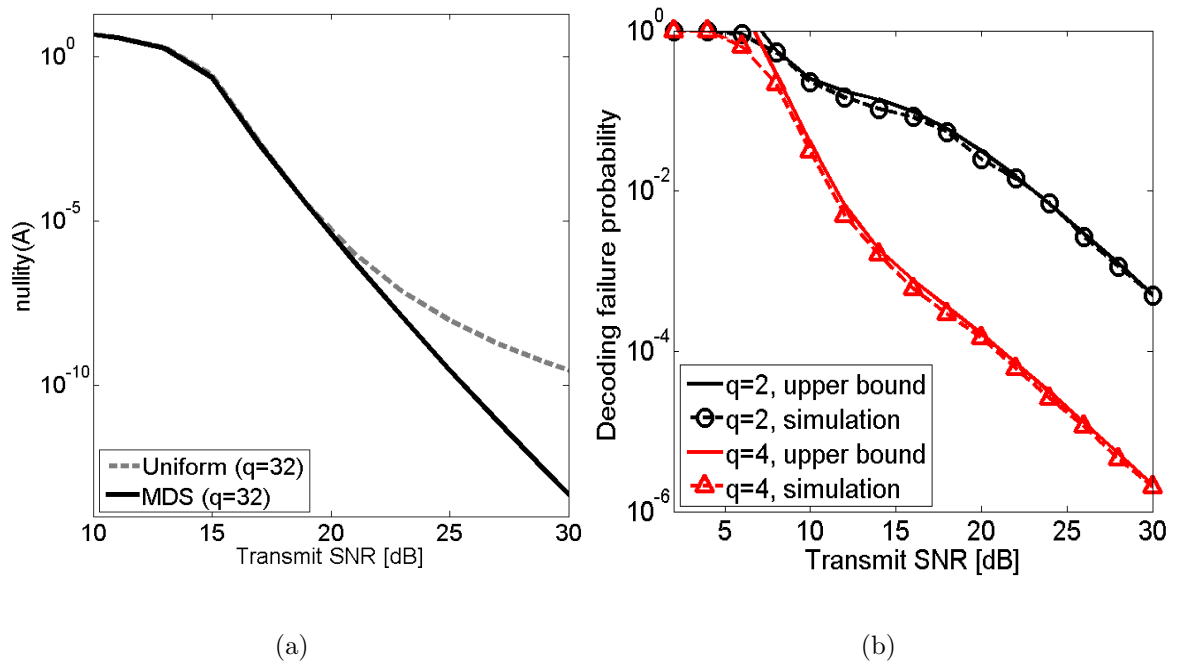
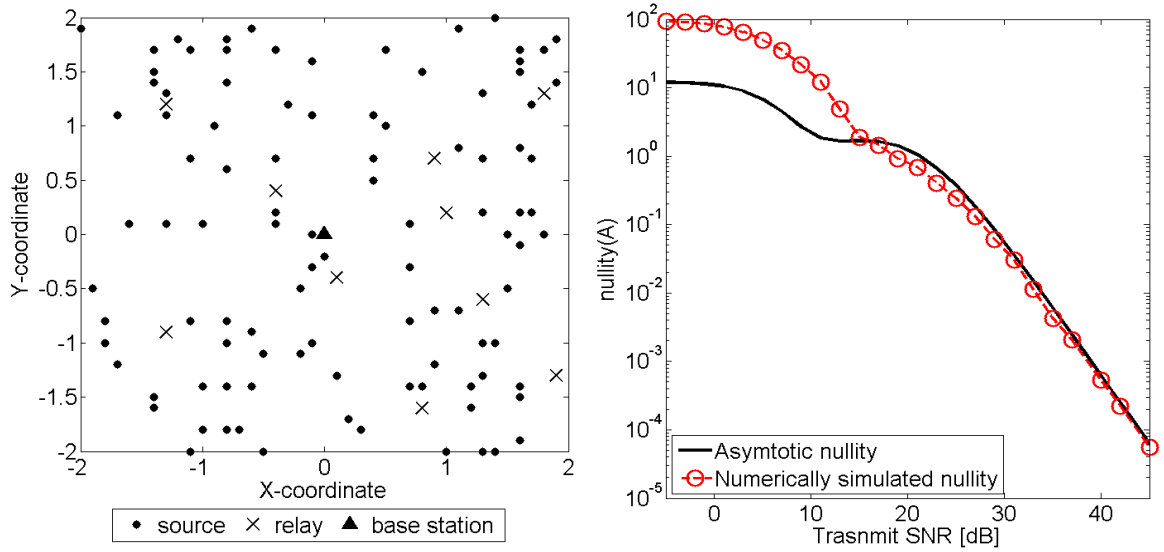
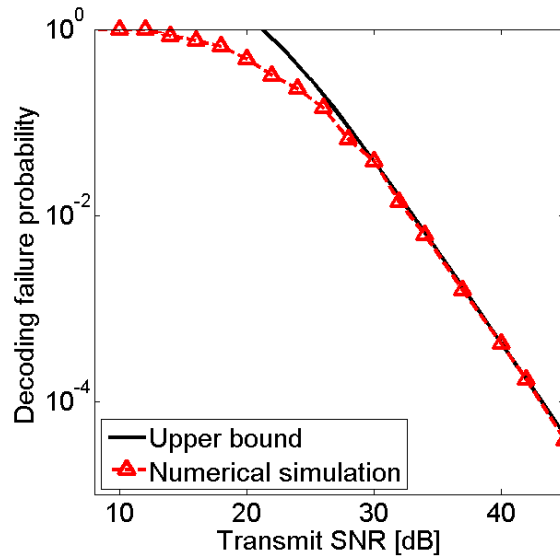


Figure 4.6: (a) Comparison of upper bounds on $\mathbb{E}[\text{nullity}(\mathbf{A})]$ for the uniform and MDS distributions. (b) Comparison of the decoding failure probabilities with the numerical simulation and the upper bound using Proposition 4.8 for $q = 2$ and 4.



(a)

(b)



(c)

Figure 4.7: (a) Location of 100 sources and 10 relays in 2D space for an (100, 10) cooperative wireless network, (b) Comparison of $\mathbb{E}[\text{nullity}(\mathbf{A})]$ with numerically simulated result and the asymptotic upper bound Corollary 4.9 with $q = 2$ and the uniform distribution. (c) Comparison of decoding failure probability with the numerical simulation and the upper bound using Corollary 4.9.

that the recovery performance obtained using the MDS distribution is better than that of the uniform distribution in high SNR regions. Comparative results of $\mathbb{E}[\text{nullity}(\mathbf{A})]$ for the two cooperative networks are shown in Figure 4.6(a). We see that there is nearly no difference between the uniform and MDS distributions for the recovery performance in the low SNR regions. In other words, the benefit of using the systematic generator of MDS codes appears only at high SNRs.

To validate usefulness of our asymptotic nullity, we consider a $(100, 10)$ cooperative wireless network as a large scale network in which 100 sources and 10 relays are deployed in the 2D space shown in Figure 4.7(a). For Corollary 4.9, we show that in the high SNR regions, the asymptotic nullity of (4.46) closes to the numerical results which was made from randomly generated transmission matrices. Comparison of those results is shown in Figure 4.7(b). Using the asymptotic nullity, the complexity of (4.31) can be not only dramatically reduced, but also the nullity of the random transmission matrix can be found efficiently. Our propose framework enables one to evaluate the reconstruction performance in large scale networks.

Figure 4.6(b) shows the comparison of numerically simulated decoding failure probabilities and upper bound on that Theorem 4.4 for a $(16, 6)$ cooperative wireless network with $q = 2$ and 4. The gap of both results appears in small SNR regions. But, the upper bound on decoding failure probability is tight in high SNR regions. This behavior is shown in Figure 4.7(c) in which the upper bound is obtained from the approximation form of $\mathbb{E}[\text{nullity}(\mathbf{A})]$ in (4.46). From those results, we show that predicting the reconstruction performance of source messages for a (N, M) cooperative wireless network is

easily possible in large scale networks.

4.7 Conclusions

In this chapter, we considered a cooperative wireless network where N sources are assisted with M relays in two phase transmissions. Our main goal was to propose a new performance analysis framework for evaluating the reconstruction performance of source messages at the BS. In order to cope with dynamic network topologies, we took the direction of modeling the elements of the transmission matrix as random variables. It allowed us to develop a systematic approach which can avoid the exhaustive evaluation used in DNC and GDNC schemes [68]–[71]. To complete the performance evaluation, we derived two tight upper bounds on the expected dimension of the nullspace of the random transmission matrix, as well as the decoding failure probability. What has been developed throughout this chapter is a more effective framework as it is compared to the rank-based method proposed in the earlier literature.

Three types of connectivity schemes are considered in this chapter as they make the framework to be general and scalable. They allowed us to show the reconstruction performance of our proposed framework using multiple sources and multiple relays randomly deployed in a 2D space, and to investigate the impact of the number of relays and the field size of NC on the system performance. In particular, being able to make precise prediction of the system performance for a network with a large number of sources and relays is a big empowerment. We can ask more challenging questions and have answers for them quickly without resorting to extensive computer simulations. For

example, we now can ask how much advantage there is exactly to use an MDS code rather than using a random code in designing the transmission matrices, as relays are added and field sizes are increased; how the position of relays and sources with respect to the base station locations affect the performance of cooperative communications. All these questions are important engineering inquiries when it comes to the design of wireless networks. They were not possible to be answered in the past but they can now be answered precisely using the proposed framework of this chapter. In addition, we show that the proposed framework can be extended to channel correlation cases, but it is needed to generalize for any family of cooperative wireless network coding schemes.

Chapter 5

Outage Probability for Cooperative Network Coding Schemes

5.1 Introduction

In wireless sensor networks (WSNs), sensor nodes operate on the limited energy source of onboard batteries, making power efficiency a key issue because replacement or recharging of batteries is difficult. The very high energy expenditure of WSNs makes long-range message transmission undesirable. Consequently, there are several ways to improve power efficiency, such as optimal transmit power allocation [105]-[109].

In this chapter, we consider a cooperative wireless network, where there are two source nodes and one base station (BS) as depicted in Figure 5.1. We investigate the effect of using NC and optimal transmit power allocation on power efficiency. Power efficiency is expressed as i) the outage probabilities from sources to destinations and ii) expansion of the network coverage area. We also derive a general and exact outage analysis framework using which we can investigate the impact of field size in NC, transmit powers, transmission rates, and network topologies on the outage performance of the network. Specifically, we show that using nonbinary NC (NBNC) yields full diversity order as well as expansion of the network coverage area. We show that a mere increase in the size of the finite field in NC, i.e., without incurring additional cost such

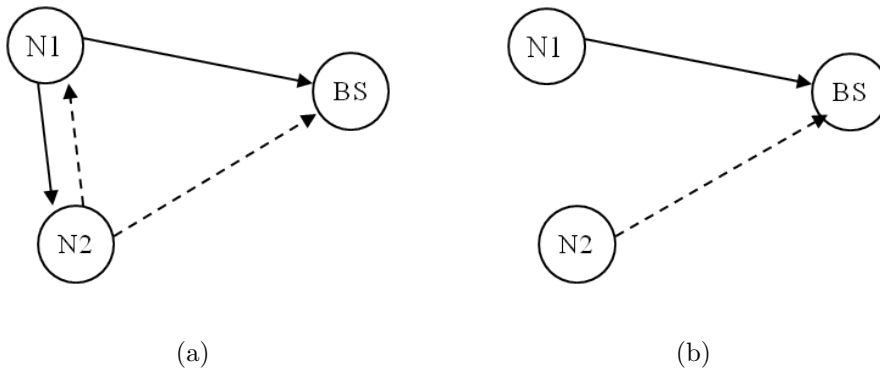


Figure 5.1: Two transmissions for cooperative schemes: (a) broadcasting, (b) relaying. Solid lines indicate the transmission of N1, and dashed lines for N2.

as boosting the transmit power level, can lead to a substantial gain in the network coverage area. To the best of our knowledge, there have been no reports that associate an increased field size in NC to expansion of network coverage area. In addition, an analysis of the optimal power allocation (OPA) for both cooperative schemes is useful for determining the power efficiency of various network environments, i.e., according to the positions of source nodes. Another interesting result obtained in this study is that the OPA depends on the size of finite fields.

5.2 System Description

5.2.1 Cooperative Schemes

Cooperative transmission schemes can be divided into two categories based on the method employed to process messages at intermediate nodes: the amplify-and-forward (AF) scheme and the decode-and-forward (DF) scheme are widely used relay protocols [65]. In the AF scheme, an intermediate node receives a noisy signal of the source's

message, amplifies it in non-regenerative mode, and forwards it to a destination. In the DF scheme, a relay node decodes the source's message, re-encodes it, and forwards it to the destination. We focus on the second of these cooperative transmission protocols, i.e., the DF scheme.

We consider a cooperative scheme for wireless networks as shown in Figure 5.1. There are two source nodes, nodes 1 (N1) and 2 (N2), and two phases: *broadcasting* and *relaying*, in the cooperative scheme. In the broadcasting phase, source nodes N1 and N2 transmit messages, S_1 and S_2 , respectively. In the relay phase, when both nodes successfully decode the transmitted messages, the messages are re-encoded and then forwarded to the BS. When a node is unable to successfully perform decoding, it repeats its message in the relay phase. When receiving repeated messages, the BS as a destination performs maximum ratio combining (MRC) of these messages, and recovers the transmitted messages. In this chapter, we assume that the transmission rate is selected to be sufficiently lower than the capacity of each channel so that near perfect decoding of messages can be accomplished with the use of a channel code. Thus, for all wireless channels, the received messages are either completely corrupted, and therefore not available at the receiving end, or considered error-free.

At the BS, the set of all possible received messages is $\{S_1, S_2, Z_1, Z_2\}$, where the subscript denotes the index of the source node. The first two messages are received in the first phase, and the latter two are linearly combined and sent from the sources in the relay phase. The alphabet of the combined message, Z_1 and Z_2 , is selected to be a finite field. The two finite fields considered in this study are GF(2) and GF(4).

Suppose that the relay nodes use a binary field for the NC operation, a method we refer to as binary NC (BNC) in this chapter. Then, the received messages at the BS in the two phases are represented as

$$\begin{aligned} \begin{bmatrix} S_1 \\ S_2 \\ Z_1 \\ Z_2 \end{bmatrix} &= \begin{bmatrix} 1 & 0 \\ 0 & 1 \\ 1 & 1 \\ 1 & 1 \end{bmatrix} \begin{bmatrix} S_1 \\ S_2 \end{bmatrix} \\ &= \mathbf{H}_2 \mathbf{S}, \end{aligned} \tag{5.1}$$

where \mathbf{H}_2 is the NC matrix with its elements drawn from GF(2) and \mathbf{S} is the source message vector. The arithmetic should follow that of GF(2). Most existing NC schemes are based on BNC.

For the case of NBNC with GF(4), referred to as NBNC-4 in this chapter, the messages received at the BS are rewritten as

$$\begin{aligned} \begin{bmatrix} S_1 \\ S_2 \\ Z_1 \\ Z_2 \end{bmatrix} &= \begin{bmatrix} 1 & 0 \\ 0 & 1 \\ 1 & 1 \\ 1 & 2 \end{bmatrix} \begin{bmatrix} S_1 \\ S_2 \end{bmatrix} \\ &= \mathbf{H}_4 \mathbf{S}, \end{aligned} \tag{5.2}$$

where \mathbf{H}_4 is the NC matrix composed of elements from GF(4) and the arithmetic operations are those of GF(4).

The core idea of cooperative communication systems is to alleviate the negative effects of communication channels, such as fading and noise, and to increase the proba-

bility of successful message reception via cooperation. With a closer look at the rows of \mathbf{H}_4 , we note that any two rows of \mathbf{H}_4 are linearly independent, while those of \mathbf{H}_2 may not be. This means that as long as any two messages out of the four, $\{S_1, S_2, Z_1, Z_2\}$, are received correctly, NBNC-4 can correctly decode the correct transmit messages S_1 and S_2 . This is not possible with the BNC scheme. For example, the last two rows of \mathbf{H}_2 are dependent on each other. Thus, with the reception of only Z_1 and Z_2 , the BNC scheme cannot decode the messages S_1 and S_2 accurately. For a network of two-user cooperation, this desirable behavior can be attained by increasing the field size to 4. This behavior was first observed in [68]. In this chapter, our focus again is to show how this favorable behavior can lead to power efficiency in terms of coverage expansion, and to study how the transmit power should be allocated differently between the two sensors given a fixed power budget.

5.2.2 Channel Model

Our system consists of a multiple access channel network in which there are two source nodes and one BS. In the broadcasting and relay phases, all source nodes transmit signals through orthogonal channels using time division multiple access or frequency division multiple access. The channels used in this study are assumed to be spatially independent, flat faded, and perturbed by additive white Gaussian noise (AWGN). We further assume that the channel gains in both the broadcasting and relay phases are mutually independent. The received signal at the j th node is thus

$$y_{i,j,k} = \sqrt{P_i} h_{i,j,k} x_{i,j,k} + n_{i,j,k}, \quad (5.3)$$

where $k \in \{1, 2\}$ denotes the transmission phase (broadcasting or relaying), and $i \in \{1, 2\}$ denotes the transmitted node (N1 or N2). Let j denote the received node for $j \in \{1, 2, d\}$, where d denotes the BS. The transmitted and received signals are given as $x_{i,j,k}$ and $y_{i,j,k}$ with $i \neq j$. P_i denotes the transmit power at the i th node. The channel gain is represented by $h_{i,j,k}$, with consist of the fading term $p_{i,j,k}$ and the path-loss coefficient $q_{i,j,k}$, i.e., $h_{i,j,k} = p_{i,j,k}q_{i,j,k}$.

Here, we assume that the fading term $p_{i,j,k}$ is random and the path-loss coefficient $q_{i,j,k}$ depends on the distance between nodes i and j . Noise is AWGN with a normal distribution $\mathcal{N}(0, N_0)$ having a zero mean and power spectral density N_0 . The path-loss coefficient is modeled as $q_{i,j,k} = (d_0/d_{i,j})^{\eta/2}$, where $2 \leq \eta \leq 6$ is the path-loss exponent, $d_{i,j}$ is the distance between i and j , and d_0 is the reference distance. In this chapter, we use $d_0 = 1$ and $\eta = 3$, and $|h_{i,j,k}|$ is assumed to be Rayleigh distributed such that the channel energy of power $|h_{i,j,k}|^2$ is exponentially distributed. We assume that the fading term $p_{i,j,k}$ is a complex-valued, i.i.d. Gaussian in each dimension with a zero mean and $1/2$ variance. The average power of $h_{i,j,k}$ is then represented by the average power of $q_{i,j,k}$, which depends on the distance between the transmitter and the receiver. All channel gains are assumed to be reciprocal, i.e., $h_{i,j,k} = h_{j,i,k}$. The instantaneous signal-to-noise (SNR) of each channel is denoted as $\gamma_{i,j,k} := |h_{i,j,k}|^2 P_i/N_0$, where P_i/N_0 is the transmit SNR at the source node i .

5.2.3 Outage Probability

The channel capacity as a function of the received SNR at the node j is given by

$$C_{i,j,k} = \log_2(1 + \gamma_{i,j,k}), \quad (5.4)$$

where $C_{i,j,k}$ denotes the channel capacity from nodes i to j at the k th transmission phase. In this chapter, we use the single channel capacity $C_{i,j,k} = \frac{1}{2} \log_2(1 + \gamma_{i,j,k})$ for each transmission phase because a factor of 2 represents the bandwidth expansion for each node in the cooperative scheme. Channel outage occurs if the capacity is less than the transmission rate R , where R is the desired spectral efficiency in bits/sec/Hz. For the Rayleigh fading channel, the outage probability is given and approximated at a high SNR in the following manner:

$$\begin{aligned} P_{out}(\gamma_{i,j,k}, R) &= \Pr \{ \gamma_{i,j,k} < (2^R - 1) \} \\ &= 1 - \exp \left\{ 1 - \frac{2^R - 1}{\Gamma_{i,j}} \right\} \\ &\approx \frac{2^R - 1}{\Gamma_{i,j}}, \end{aligned} \quad (5.5)$$

where $\Gamma_{i,j} = \sigma_{i,j}^2 P_i / N_0$, is the average SNR at the receiver j , $\sigma_{i,j}^2$ is the variance of the channel gain $h_{i,j,k}$ which depends only on the distance such that $\sigma_{i,j}^2 = \sigma_{i,j,1}^2 = \sigma_{i,j,2}^2$. The outage probability $P_{out}(\gamma_{i,j,k}, R)$ is a function of the average SNR and the transmission rate.

We assume that MRC is used at the BS for combining identical transmissions. For the case of MRC, the probability of an outage event is a function of two exponentially distributed random variables, which denote the instantaneous SNR for each channel. Thus, the outage probability for MRC at the BS is represented as

$\Pr \{ \gamma_{s,d,k} + \gamma_{r,d,k} < (2^{2R} - 1) \}$, for $s, r \in \{1, 2\}$. The outage probability with two random variables is obtained from the following cumulative distribution function. Let $w := u + v$, where u and v are independent exponential random variables with parameters λ_u and λ_v . The cumulative distribution function of the random variable w is given by

$$P_w(w) = \begin{cases} 1 - \left(\left(\frac{\lambda_v}{\lambda_v - \lambda_u} \right) e^{-\lambda_u w} + \left(\frac{\lambda_u}{\lambda_u - \lambda_v} \right) e^{-\lambda_v w} \right) & \lambda_u \neq \lambda_v, \\ 1 - (1 + \lambda w) e^{-\lambda w} & \lambda_u = \lambda_v. \end{cases} \quad (5.6)$$

5.3 Outage Probability for Cooperative Coding Schemes

In this section, we aim to derive the outage probability that allows us to investigate the effects of different outage events, transmit power allocation, channel gain, and field size (GF(2) *vs.* GF(4)) in NC, on power efficiency. This analysis is somewhat different from that given in a recent paper [68] that studied outage probabilities under a number of approximations: i) they did not consider all possible outage scenarios (for a full consideration see [116]), ii) all channel outages are treated with the same transmit powers, the same average channel gains, and thus the same average channel SNRs. Our analysis is exact and generalized, with consideration of different transmit powers, rates, and average channel gains. This generalized analysis framework enables us to conduct not only a diversity order analysis but also a complete outage probability analysis as a function of the transmit SNR. These results help us investigate the coverage area expansion and the OPA problems. Our outage probability analysis shows that the diversity order achievable with NBNC-4 is three, instead of two, as obtained in [66]. It should be noted that full diversity order is obtainable in the considered network

channel.

5.3.1 Outage Events in Cooperative Networks

In the broadcasting phase, both source nodes transmit their messages to the BS in an orthogonally multiplexed manner, and they overhear each other's message. In the relay phase, the two source nodes act independently with no knowledge of whether their own broadcasted message was successfully decoded by their neighbor node. No feedback channel is assumed between the two nodes. As such, there are four possible cooperation scenarios depending on whether the decoding of messages was successful in the broadcasting phase. These four outage events are depicted in Figure 5.2, and the four cooperative scenarios for each of the four outage events are denoted as Case 1, 2, 3, and 4.

In Case 1, both nodes successfully decode the partner's message. In the relay phase, each node linearly combines the neighbor's message with a NC, and forwards the encoded message to the BS, resulting in a fully cooperative scenario. In Case 2, N1 successfully decodes the message from N2, but N2 does not successfully decode the message from N1. Hence, N1 combines N2's message and forwards the re-encoded message to the BS in the relay phase in the same manner as in Case 1. However, N2 repeats its message in the relay phase. At the BS, the repeated messages are decoded using the MRC strategy. Case 3 is similar to Case 2 except that the role of N1 is switched with that of N2. In Case 4, every node fails to decode its neighbor's message in the broadcasting phase, and hence each node uses the available channel in the relay phase

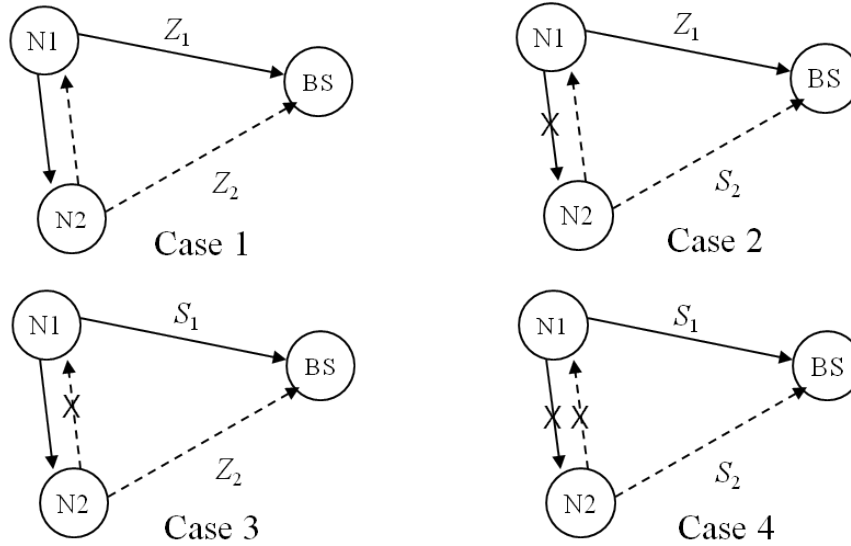


Figure 5.2: Four cooperative scenarios for relay phase transmission based on the decoding results in the broadcasting phase.

only to repeat its own message created in the broadcast phase. Thus, in this case, the system automatically reverts to a non-cooperative mode. In our cooperative schemes, we assume that the BS knows which case out of the four cases has occurred. The transmitted messages of each node for the four scenarios are summarized in Table 5.1. Next, we derive and evaluate the outage probability for BNC and NBNC-4 schemes.

5.3.2 Derivation on Outage Probability

In the following, we focus on the derivation of outage probability for the NBNC-4 and BNC schemes. First, NC in the relay phase is performed. Message transmission consists of two phases as described in the previous subsection. We analyze the outage event based on MRC. In this chapter, we assume that the instantaneous SNRs for the

Table 5.1: Transmitting messages for two nodes according to the four cases.

| Case | Broadcasting(N1) | Relay(N1) | Broadcasting(N2) | Relay(N2) |
|------|------------------|-----------|------------------|-----------|
| 1 | S_1 | Z_1 | S_2 | Z_2 |
| 2 | S_1 | Z_1 | S_2 | S_2 |
| 3 | S_1 | S_1 | S_2 | Z_2 |
| 4 | S_1 | S_1 | S_2 | S_2 |

broadcasting and relay phases are mutually independent.

Case 1: In this case, both nodes correctly decode each other's messages. Correct decoding events are defined as follows:

$$\{C_{1,2,1} > R_1\} \cap \{C_{2,1,1} > R_2\} \quad (5.7)$$

We define the transmission rate for each node as R_1 and R_2 , respectively. We consider the outage probability for N1, which is identical to that for N2 as a result of symmetry. NBNC-4 in the relay phase follows the NC method specified in (5.2).

Next, we consider the outage events for Case 1. Suppose that transmitted messages in the broadcasting phase from N1 and N2 are not decoded successfully at the BS. This amounts to an outage event except when both of the combined messages with rates R_1 and R_2 , respectively, are successfully decoded in the relay phase. In this case, the outage probability can be written as

$$\begin{aligned} & \Pr\left\{\left(C_{1,d,1} < R_1\right) \cap \left(C_{2,d,1} < R_2\right) \cap \left(\left(C_{1,d,2} < R_1\right) \cup \left(C_{2,d,2} < R_2\right)\right)\right\} \\ &= \Pr\left\{\gamma_{1,d,1} < r_1\right\} \Pr\left\{\gamma_{2,d,1} < r_2\right\} \left(1 - \Pr\left\{\gamma_{1,d,2} > r_1\right\} \Pr\left\{\gamma_{2,d,2} > r_2\right\}\right) \end{aligned} \quad (5.8)$$

where $r_1 = 2^{2R_1} - 1$ and $r_2 = 2^{2R_2} - 1$. In addition, consider the case in which the transmitted message in the broadcasting phase from N1 is not decoded successfully, but the transmitted message in the broadcasting phase from N2 is decoded successfully. An outage occurs only when decoding of both messages in the relay phase fails. This outage probability can be written as

$$\begin{aligned} & \Pr\left\{\left(C_{1,d,1} < R_1\right) \cap \left(C_{2,d,1} > R_2\right) \cap \left(C_{1,d,2} < R_1\right) \cap \left(C_{2,d,2} < R_2\right)\right\} \\ &= \Pr\left\{\gamma_{1,d,1} < r_1\right\} \Pr\left\{\gamma_{2,d,1} > r_2\right\} \Pr\left\{\gamma_{1,d,2} > r_1\right\} \Pr\left\{\gamma_{2,d,2} < r_2\right\} \end{aligned} \quad (5.9)$$

As a result, the outage probability of N1 for Case 1 can be obtained as

$$\begin{aligned} P_{out,4-ary}^1 &= \Pr\left\{\gamma_{1,2,1} > r_1\right\} \Pr\left\{\gamma_{2,1,1} > r_2\right\} \\ &\times \left(\Pr\left\{\gamma_{1,d,1} > r_1\right\} \Pr\left\{\gamma_{2,d,1} < r_2\right\} \left(1 - \Pr\left\{\gamma_{1,d,2} > r_2\right\} \Pr\left\{\gamma_{2,d,2} > r_2\right\}\right) \right. \\ &\quad \left. + \Pr\left\{\gamma_{1,d,1} < r_1\right\} \Pr\left\{\gamma_{2,d,1} > r_2\right\} \Pr\left\{\gamma_{1,d,2} < r_1\right\} \Pr\left\{\gamma_{2,d,1} < r_2\right\}\right) \end{aligned} \quad (5.10)$$

Case 2: In this case, N1 correctly decodes the message S_2 from N2, but N2 does not correctly decode the message S_1 from N1. This corresponds to the following events:

$$\{C_{1,2,1} < R_1\} \cap \{C_{2,1,1} > R_2\} \quad (5.11)$$

According to the transmission protocol, the BS receives N2's message S_2 twice, and decoding is performed using MRC. Hence, the outage probability of N2 for MRC is obtained as

$$\begin{aligned} \Pr\{MRC_2\} &= \Pr\left\{\gamma_{2,d,1} + \gamma_{2,d,2} < 2^{2R_2} - 1\right\} \\ &= 1 - \left(1 + \frac{r_2}{\Gamma_{2,d}}\right) \exp\left(-\frac{r_2}{2\Gamma_{2,d}}\right). \end{aligned} \quad (5.12)$$

The outage probability in the conditional case is

$$\begin{aligned} & \Pr\left\{\left((C_{1,d,1} < R_1) \cap (C_{1,d,2} < R_2)\right) \cup \left((C_{1,d,1} < R_1) \cap (C_{1,d,2} > R_1) \cap (MRC_2)\right)\right\} \\ &= \Pr\{\gamma_{1,d,1} > r_1\} \Pr\{\gamma_{1,d,2} < r_2\} + \Pr\{\gamma_{1,d,1} < r_1\} \Pr\{\gamma_{1,d,2} > r_1\} \Pr\{MRC_2\} \end{aligned} \quad (5.13)$$

where the first term of the R.H.S. of (5.13) is the outage probability for N1, and the second term is for N2 that uses MRC. The overall outage probability for Case 2 is

$$\begin{aligned} P_{out,4-ary}^2 &= \Pr\{\gamma_{1,2,1} < r_1\} \Pr\{\gamma_{2,1,1} > r_2\} \\ &\times \left(\Pr\{\gamma_{1,d,1} < r_1\} \Pr\{\gamma_{1,d,2} < r_2\} + \Pr\{\gamma_{1,d,2} > r_1\} \Pr\{MRC_2\} \right) \end{aligned} \quad (5.14)$$

Case 3: In this case, N2 correctly decodes N1's message S_1 , but N1 cannot decode the message S_2 . The corresponding event is

$$\{C_{1,2,1} > R_1\} \cap \{C_{2,1,1} < R_2\} \quad (5.15)$$

Using the same approach as for Case 2, we obtain the overall outage probability as follows

$$\begin{aligned} P_{out,4-ary}^3 &= \Pr\{\gamma_{1,2,1} > r_1\} \Pr\{\gamma_{2,1,1} < r_2\} \\ &\times \Pr\{MRC_1\} \left(\Pr\{\gamma_{2,d,1} < r_2\} + \Pr\{\gamma_{2,d,1} > r_2\} \Pr\{\gamma_{2,d,2} < r_2\} \right) \end{aligned} \quad (5.16)$$

The outage probability for N1 that uses MRC is

$$\begin{aligned} \Pr\{MRC_1\} &= \Pr\{\gamma_{1,d,1} + \gamma_{1,d,2} < 2^{2R_1} - 1\} \\ &= 1 - \left(1 + \frac{r_1}{\Gamma_{1,d}}\right) \exp\left(-\frac{r_1}{2\Gamma_{1,d}}\right). \end{aligned} \quad (5.17)$$

Case 4: Neither node decodes the message in the broadcasting phase successfully.

The overall outage probability for Case 4 is

$$P_{out,4-ary}^4 = \Pr\{\gamma_{1,2,1} < r_1\} \Pr\{\gamma_{2,1,1} < r_2\} \Pr\{MRC_1\} \quad (5.18)$$

Next, the exact outage probability with NBNC-4 for N1 is obtained by adding the results so far, i.e., (5.10), (5.14), (5.16) and (5.18), as follows:

$$P_{out,4-ary} = P_{out,4-ary}^1 + P_{out,4-ary}^2 + P_{out,4-ary}^3 + P_{out,4-ary}^4. \quad (5.19)$$

Using the high SNR approximation given in the last line of (5.5), we can approximate the outage probability as follows:

$$P_{out,4-ary} \approx \frac{A_1}{P_1^2 P_2} + \frac{A_2}{P_1 P_2^2} + \frac{A_3}{P_1^3}, \quad (5.20)$$

where

$$\begin{aligned} A_1 &:= \frac{2r_1^2 r_2 N_0^3}{\sigma_{1,d}^4 \sigma_{2,d}^2} + \frac{r_1^2 r_2 N_0^3}{2\sigma_{1,2}^2 \sigma_{1,d}^2 \sigma_{2,d}^2} + \frac{r_1^2 r_2 N_0^3}{2\sigma_{1,2}^2 \sigma_{2,1}^2 \sigma_{1,d}^2} \\ A_2 &:= \frac{r_1 r_2^2 N_0^3}{\sigma_{1,d}^2 \sigma_{2,d}^4} + \frac{r_1 r_2^2 N_0^3}{\sigma_{2,1}^2 \sigma_{1,d}^2 \sigma_{2,d}^2} \\ A_3 &:= \frac{r_1^2 r_2 N_0^3}{\sigma_{1,2}^2 \sigma_{1,d}^4}. \end{aligned}$$

The outage probability analysis for BNC is performed similarly to the analysis performed for the NBNC-4 scheme, with the result that the outage probabilities for BNC are identical to those for NBNC-4, except for Case 1, i.e., $P_{out,binary}^2 = P_{out,4-ary}^2$, $P_{out,binary}^3 = P_{out,4-ary}^3$, $P_{out,binary}^4 = P_{out,4-ary}^4$. The reason for this is that the outage events, in each of Case 2, 3, and 4, for the BNC scheme are identical to those of NBNC-4. The only difference comes from Case 1.

The outage probability of BNC for Case 1 is given by

$$\begin{aligned} P_{out,binary}^1 &= \Pr\{\gamma_{1,2,1} > r_1\} \Pr\{\gamma_{2,1,1} > r_2\} \\ &\quad \times \Pr\{\gamma_{1,d,1} < r_1\} \left(\Pr\{\gamma_{2,d,1} < r_2\} + \Pr\{MRC_1\} \Pr\{\gamma_{2,d,1} > r_2\} \right) \end{aligned} \quad (5.21)$$

The exact outage probability for BNC using (5.1) is again obtained by summing the results

$$P_{out,binary} = P_{out,binary}^1 + P_{out,binary}^2 + P_{out,binary}^3 + P_{out,binary}^4. \quad (5.22)$$

The high SNR approximation is then given by

$$P_{out,binary} \approx \frac{B_1}{P_1 P_2} + \frac{B_2}{P_1^2 P_2} + \frac{B_3}{P_1 P_2^2} + \frac{B_4}{P_1^3}, \quad (5.23)$$

where

$$\begin{aligned} B_1 &:= \frac{r_1 r_2 N_0^2}{\sigma_{1,d}^2 \sigma_{2,d}^2} \\ B_2 &:= \frac{r_1^2 r_2^2 N_0^3}{2\sigma_{1,2}^2 \sigma_{1,d}^2 \sigma_{2,d}^2} + \frac{r_1^2 r_2 N_0^3}{2\sigma_{1,2}^2 \sigma_{2,1}^2 \sigma_{1,d}^2} \\ B_3 &:= \frac{r_1 r_2^2 N_0^3}{\sigma_{2,1}^2 \sigma_{1,d}^2 \sigma_{2,d}^2} \\ B_4 &:= \frac{r_1^2 r_2 N_0^3}{\sigma_{1,2}^2 \sigma_{1,d}^4}. \end{aligned}$$

Due to the dominant term of (5.20) and (5.23) in the high SNR regime, we conclude that the diversity orders of BNC and NBNC-4 are two and three, respectively. This result well matches with the result of [68]. Our outage probabilities, however, are exact and general in terms of variances of channel gains and transmit powers compared to the Xiao's work. Next we investigate the performance of cooperative wireless networks with respect to transmit powers and location of nodes.

5.3.3 Performance Evaluation for Various Channel Environments

In this subsection, we evaluate the outage probability of N1 for both BNC and NBNC-4 in terms of the average SNRs and the transmission rates and . We show that using NBNC-4 provides improved outage probabilities compared to BNC for different channel environments. In Figure 5.3, we show evaluation results for which the benefits of NC can be obtained at mid to high SNR regions. We compare the outage probabilities for different network schemes, i.e., a non-cooperative scheme, a cooperative communication scheme with the binary network code, and a cooperative communica-

tion scheme with the 4-ary network code. These are labeled as Non Coop, Binary Coop, and 4-ary Coop, respectively.

In order to investigate the influence of different channel gains, we assume that the transmit powers of the two nodes are equal, i.e., $P_1 = P_2$, and we use the same transmission rates $R_1 = R_2 = 1$ b/s/Hz. As shown in Figure 5.3, we evaluate the effect of variances of the channel gains. We can observe that the NBNC-4 scheme achieves a diversity order of three, in contrast to a diversity order of two for both the BNC and the non-cooperative schemes. In Figure 5.3(a), we set all variances of the channel gains as $\sigma_{1,d}^2 = 1$, $\sigma_{2,d}^2 = 125$, $\sigma_{1,2}^2 = 2$. This means that the link quality between N2 and BS is better than the other. Since the variance of the channel gain depends on the distance, the case of Figure 5.3(a) reflects the channel environment where N2 is close to the BS. In Figure 5.3(b), $\sigma_{1,d}^2 = 1$ and $\sigma_{2,d}^2 = \sigma_{1,2}^2 = 8$, which means the link quality from N2 to the BS is higher than that from N1 to the BS, with equal power allocation (EPA). This setting has a geometrical meaning such that N2 is located in the middle of N1 and the BS. In Figure 5.3(c), we consider the case where N2 is located closer to N1, by setting $\sigma_{1,d}^2 = 1$, $\sigma_{2,d}^2 = 2$, and $\sigma_{1,2}^2 = 125$ with EPA. Note that the diversity orders for the three different schemes still hold. The diversity order for the non-cooperative scheme is still two, owing to the time diversity obtained by using MRC at the BS.

5.4 Power Efficiency Schemes

In this section, we consider two approaches for enhancing power efficiency. One is to increase the field size in NC and assess its effect on power efficiency. The other is to

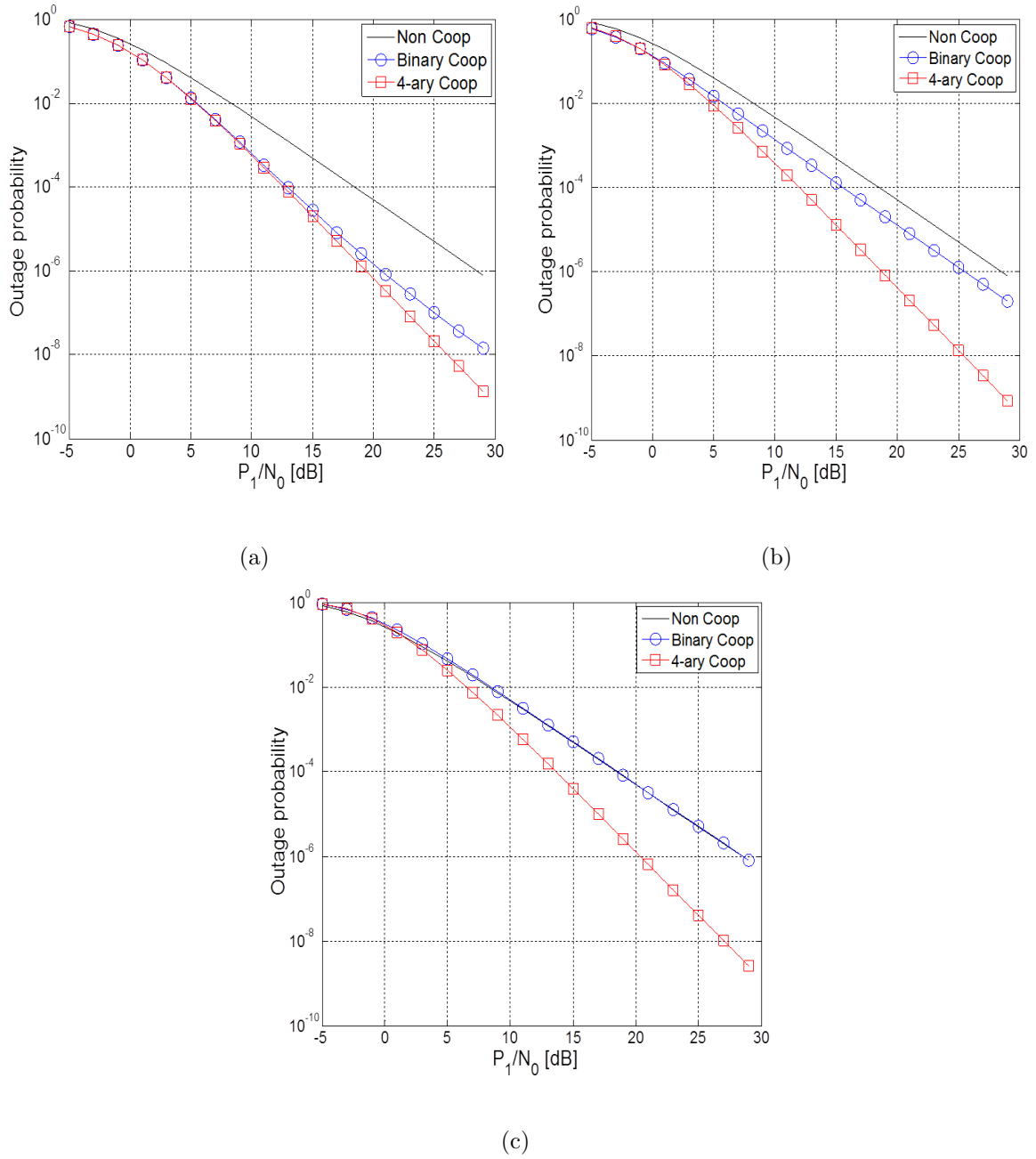


Figure 5.3: Exact outage probability with BNC and NBNC-4 for N1: $P_1 = P_2$, (a) $\sigma_{1,d}^2 = 1, \sigma_{2,d}^2 = 125, \sigma_{1,2}^2 = 2$, (b) $\sigma_{1,d}^2 = 1, \sigma_{2,d}^2 = \sigma_{1,2}^2 = 8$, (c) $\sigma_{1,d}^2 = 1, \sigma_{2,d}^2 = 2, \sigma_{1,2}^2 = 125$.

allocate a given level of transmit power to the two source nodes. In this section, power efficiency is expressed in terms of both outage probability and coverage expansion.

5.4.1 Coverage Expansion

Location Source Nodes

In cooperative networks, the location of source nodes should be taken into consideration so that with increasing distance between the transmitter and the receiver, the transmit power should be utilized for reliable transmissions. The advantage of using NC is investigated, without loss of generality, in a particular scenario in which a source node N1 is moved around in a two-dimensional (2D) network area, while the BS and the relay node N2 are fixed at given locations. Specifically, the BS is located at the origin and N2 at (1, 0) in the 2D space. The variance of the channel gain between N2 and the BS is set as $\sigma_{2,d}^2 = 1$. Consider the location of the source N1 in the 2D space. As mentioned in the channel model of Chapter 5.2.2, we make the variance of each channel gain depend on the distance between the two nodes. We use equal power allocation, $P_1 = P_2$, for both N1 and N2. The location (x, y) of N1 is varied inside the plane. Variances of the channel gains are obtained by

$$\begin{aligned}\sigma_{1,2}^2 &= \left(\sqrt{(x-1)^2 + y^2} \right)^{-\eta}, \\ \sigma_{1,d}^2 &= \left(\sqrt{x^2 + y^2} \right)^{-\eta}.\end{aligned}\tag{5.24}$$

Based on this 2D setting, the outage probability from the source N1 to the BS can be readily analyzed by substituting the variances in the relevant outage expressions given in Chapter 5.3.2.

Evaluation of Coverage Area Expansion

The contour of outage probabilities evaluated at 10^{-4} for the source N1 is plotted in Figure 5.4, where the blue and red lines indicate the results of using the BNC and NBNC-4 schemes, respectively. Figure 5.4 shows that the position of N1 is expanded by NBNC-4. We assumed that the transmit power of both nodes is $P_1/N_0 = P_2/N_0 = 20$ dB and $R_1 = R_2 = 1$ b/s/Hz. Suppose that the source N1 is located at $(2, 0)$. Then, NBNC-4 achieves an outage probability of 10^{-4} or less, whereas BNC does not. The contour of the outage probability at 10^{-4} for N1 has been extended with the use of NBNC-4, as compared to the use of BNC

In this work, we define the coverage area of N1 as the geographic area within which the outage probability of N1 is less than a particular level. We evaluate the coverage area of N1 having a guaranteed outage probability of 10^{-4} for the two different NC schemes. The results with respect to total transmit power constraints are shown in Figure 5.4. We assume EPA for both nodes, because OPA results in little improvement, as discussed in the following section. In this case, the coverage area for NBNC-4 is greater than that of BNC. However, in the high SNR region, say $P_t/N_0 > 25$ dB where $P_t = P_1 + P_2$, the effect of the field size interestingly is small. At a high SNR, the relay is less important since direct transmission from N1 to the BS shows good error performance. In the mid SNR region, the effect of field size is the greatest. For example, at 18 dB SNR the coverage area for NBNC-4 is about twofold greater than that for BNC. The low SNR region, in which there is no NC benefit, is of no further interest.

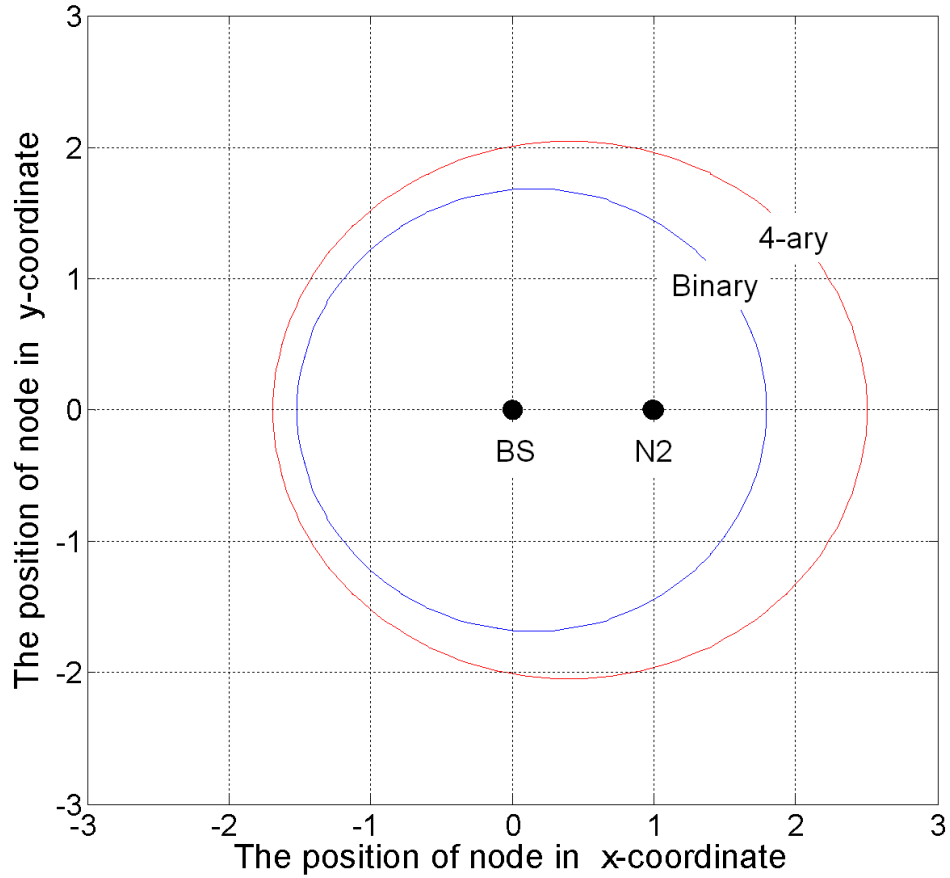


Figure 5.4: Contour plot of the locations of the source node (N1) whose outage probability is less than or equal to 10^{-4} , with the fixed BS and N2 locations as shown in the plot: the blue and red lines indicate for BNC and NBNC-4 schemes, respectively.

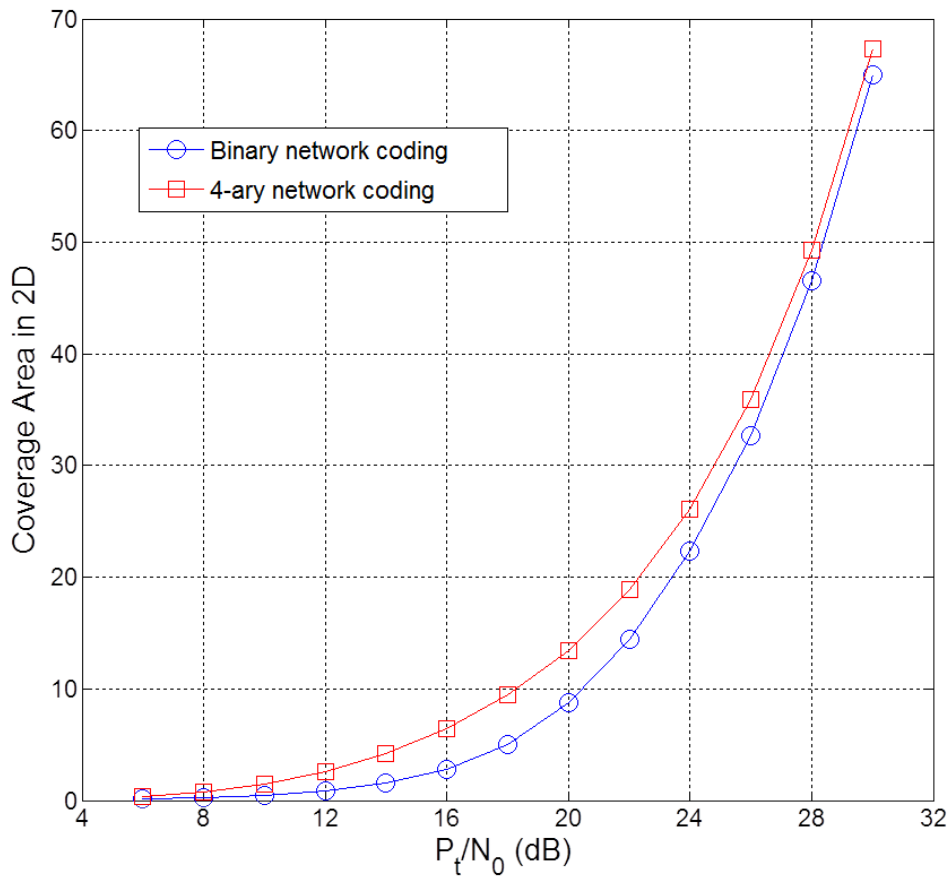


Figure 5.5: Coverage area of the source node (N1) for the outage probability of 10^{-4} with the fixed BS and N2 in a 2D space: the blue and red lines indicate for BNC and NBNC-4 schemes.

5.4.2 Optimal Power Allocation

The other power efficiency technique investigated in this study is a transmit power allocation. We investigate this problem for the two network codes, using the outage analysis framework developed in Chapter 5.3.2.

Formulation of Optimal Power Allocation

In [106], the authors attempted to minimize outage probability under a total transmit power constraint. Based on a symbol-error-rate analysis with M-PSK and M-QAM modulations, power allocation schemes for decode-and-forward protocols are presented in [108] and [117], where the authors considered MRC receivers. A power allocation problem for Nakagami fading channels is considered in [118]. We assume that each node knows all the channel state information by using an appropriate channel feedback scheme. We investigate the outage performance of optimal transmit power allocation subject to a total power constraint. In other words, the OPA solution is obtained based on minimization of the outage probability given under a total power constraint

We use the outage probabilities, P_{out} , in (5.20) and (5.23), for the BNC and NBNC-4 schemes, to deal with the optimization problem. Note that these are functions of transmit powers, variances of channel gains, and transmission rates. Given variances of channel gains and a transmission rate, the optimization problem can be written as follows

$$P_{out}(P_1^*, P_2^*, \sigma_{1,2}, \sigma_{1,d}, \sigma_{2,d}, R_1, R_2) = \arg \min_{P_1, P_2} P_{out}(P_1, P_2, \sigma_{1,2}, \sigma_{1,d}, \sigma_{2,d}, R_1, R_2), \quad (5.25)$$

subject to $P_1 + P_2 \leq P_t$, $P_1 \geq 0$, and $P_2 \geq 0$, where P_t is the total transmit power, and P_1^* and P_2^* denote the optimal transmit powers for the two nodes. For the outage probability for the NBNC-4 scheme, the Lagrangian with λ as the Lagrange multiplier can be written as

$$L(P_1, P_2, \lambda) = \frac{A_1}{P_1^2 P_2} + \frac{A_2}{P_1 P_2^2} + \frac{A_3}{P_1^3} + \lambda(P_1 + P_2 - P_t). \quad (5.26)$$

Similarly, the Lagrangian for the BNC scheme is

$$L(P_1, P_2, \lambda) = \frac{B_1}{P_1 P_2} + \frac{B_2}{P_1^2 P_2} + \frac{B_3}{P_1 P_2^2} + \frac{B_4}{P_1^3} + \lambda(P_1 + P_2 - P_t). \quad (5.27)$$

for either the binary or the 4-ary network code. Using a first-order derivative condition, the optimal power must satisfy

$$\frac{\partial L(P_1, P_2, \lambda)}{\partial P_1} = \frac{\partial L(P_1, P_2, \lambda)}{\partial P_2} = 0. \quad (5.28)$$

To find the optimal transmit power P_1 at the source for both cooperative schemes, we use the following equations:

$$\Lambda_{N,1} P_1^3 + \Lambda_{N,2} P_1^2 + \Lambda_{N,3} P_1 + \Lambda_{N,4} = 0, \quad (5.29)$$

where

$$\Lambda_{N,1} := 3A_1 - 3A_2 - 3A_3,$$

$$\Lambda_{N,2} := 9A_3 P_t - 5A_1 P_t + A_2 P_t,$$

$$\Lambda_{N,3} := 2A_1 P_t^2 - 9A_3 P_t^2,$$

$$\Lambda_{N,4} := 3A_3 P_t^3.$$

For BNC,

$$\Lambda_{B,1} P_1^4 + \Lambda_{B,2} P_1^3 + \Lambda_{B,3} P_1^2 + \Lambda_{B,4} P_1 + \Lambda_{B,5} = 0, \quad (5.30)$$

where

$$\begin{aligned}\Lambda_{B,1} &:= 2B_1, \\ \Lambda_{B,2} &:= 3B_2 - 3B_3 - 3B_4 - 3B_1P_t, \\ \Lambda_{B,3} &:= B_1P_t^2 + 9B_4P_t - 5B_2P_t + B_3P_t, \\ \Lambda_{B,4} &:= 2B_2P_t^2 - 9B_4P_t^2, \\ \Lambda_{N,4} &:= 3B_4P_t^3.\end{aligned}$$

For both cases, (5.29) and (5.30) correspond to the NBNC-4 and BNC schemes under the total power constraint. We define the ratio of the power allocation as

$$\rho = \frac{P_1}{P_t}. \quad (5.31)$$

We investigate the effect of variances of channel gains on the optimum ratio of power allocation, while the outage probability is minimized.

Discussion for Various Link Qualities

In this subsection, we discuss optimal transmit power allocation for various channel environments. We consider the position of nodes as follows: source node (N1) is located at coordinate (1, 0), the BS is at (0, 0), the relay node (N2) is free to move around in the 2D space. We investigate the effect of the position of the relay node N2 on optimal transmit power allocation. In addition, we aim to investigate the effect of the size of finite fields, used in the underlying NC scheme, on the results of optimum power allocation.

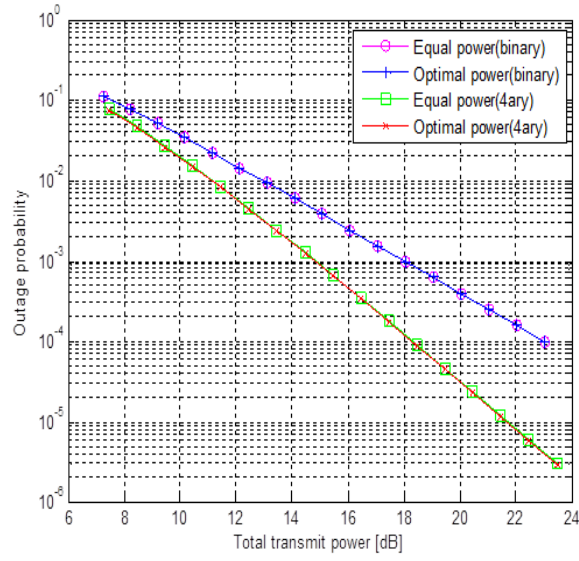
Let us consider three cases, based on the position of N2: i) N2 is at $(0.5, \sqrt{3}/2)$, ii) N2 at $(0.5, 0)$, and iii) N2 is at $(-2, 0)$. From the relation given at the channel model (Chapter

5.2.2), the variances of the channel gains can be found as i) $\sigma_{1,2}^2 = \sigma_{1,d}^2 = \sigma_{2,d}^2 = 1$, ii) $\sigma_{1,d}^2 = 1, \sigma_{1,2}^2 = \sigma_{2,d}^2 = 8$, and iii) $\sigma_{1,d}^2 = 1, \sigma_{1,2}^2 = 0.037, \sigma_{2,d}^2 = 0.125$, respectively. From these, one can find the exact outage probabilities by substituting them into (5.19) and (5.22). We fix the total transmit power, i.e., $P_t \geq P_1 + P_2$ at a particular level and show the outage probability as a function of total transmit power. The corresponding results are shown in Figure 5.6. Note that in both cases the link qualities of the two wireless channels, i.e., N1-to-N2 and N2-to-BS, are the same and they are good in terms of SNRs. In such cases, as indicated by Figure 5.6(a) and (b), EPA is as good as OPA. In the third case, OPA is obviously better than EPA in general, but this behavior is substantial only in the low-SNR region. From Figure 5.6(c), we note that as the total transmit power increases, the EPA results approach the results of OPA.

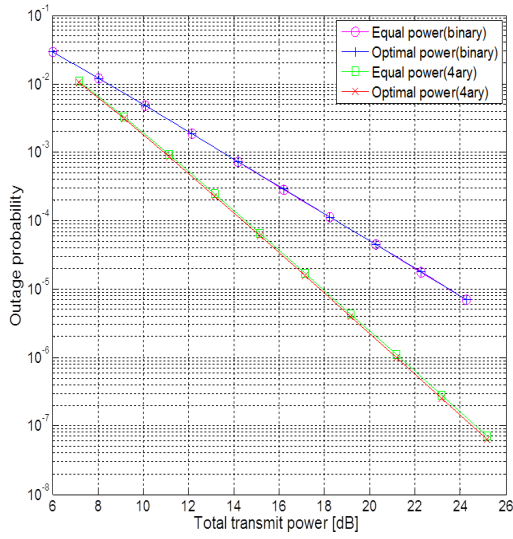
Since it is difficult to see from Figure 5.6 the amount of difference between EPA and OPA, we now aim to investigate how the outage probability changes as the ratio ρ of the transmit power allocation is swept from 0 to 1, while fixing the total transmit power to noise ratio at 20 dB. The result is given in Figure 5.7. We observe that at around EPA, i.e., $\rho = 0.5$, the outage probability is relatively flat, which is reasonable.

Next, we aim to find the optimum ratio ρ when N2, taking the role of relay for N1, is moved directly on a straight line from the BS to N1 and to investigate how much transmit power should be allocated at N1 to obtain the minimum outage probability. Figure 5.8 shows the results, where the x-axis indicates the x-coordinate of N2, and the y-axis is the optimum ρ .

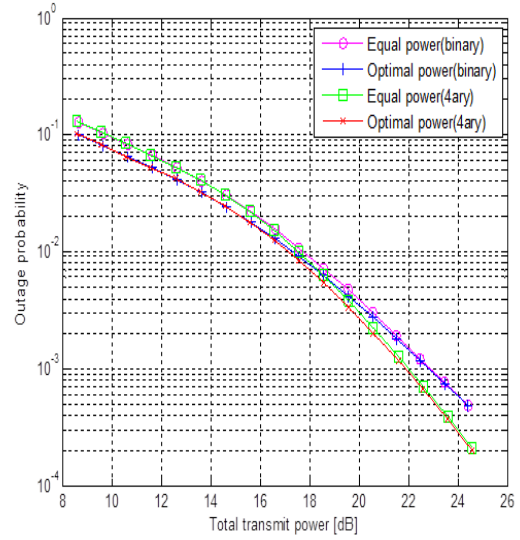
A noteworthy observation in Figure 5.8 is that there are two different approaches



(a)



(b)



(c)

Figure 5.6: Outage probability as a function of total transmit power: (a) $P_1 = P_2$, (a) $\sigma_{1,d}^2 = \sigma_{2,d}^2 = \sigma_{1,2}^2 = 1$, (b) $\sigma_{1,d}^2 = 1, \sigma_{2,d}^2 = \sigma_{1,2}^2 = 8$, (c) $\sigma_{1,d}^2 = 1, \sigma_{2,d}^2 = 0.125, \sigma_{1,2}^2 = 0.037$.

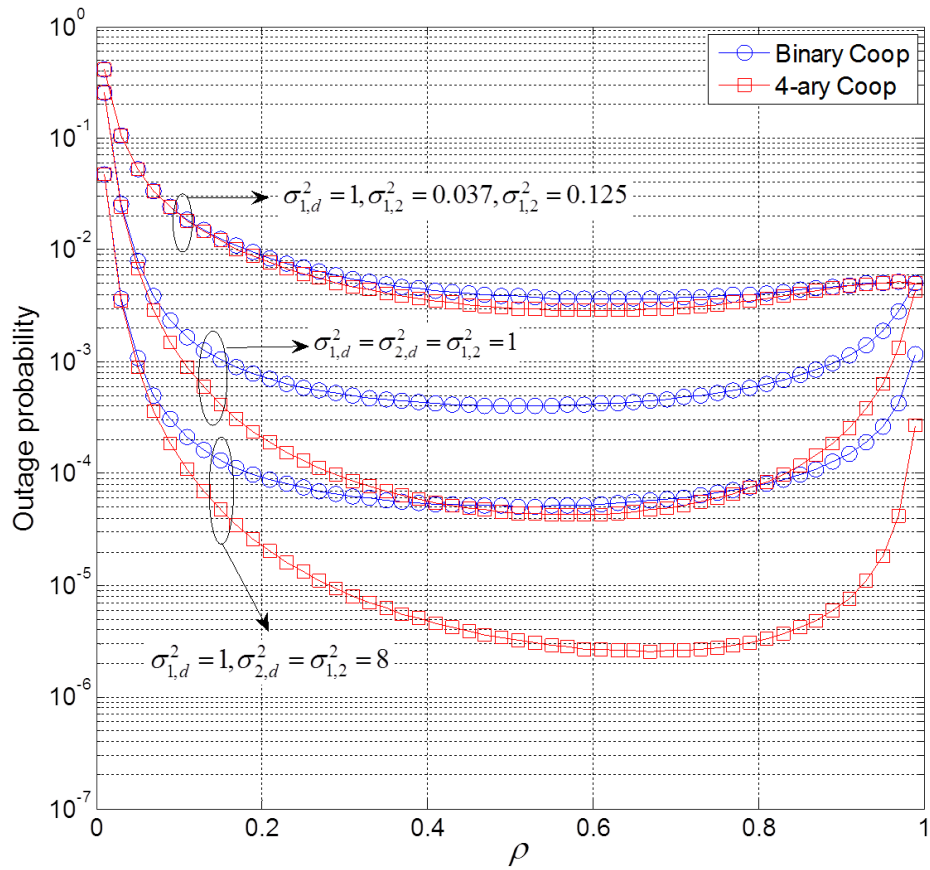


Figure 5.7: Outage probability as a function of the power allocation ratio ρ at $P_t/N_0 = 20$ dB.

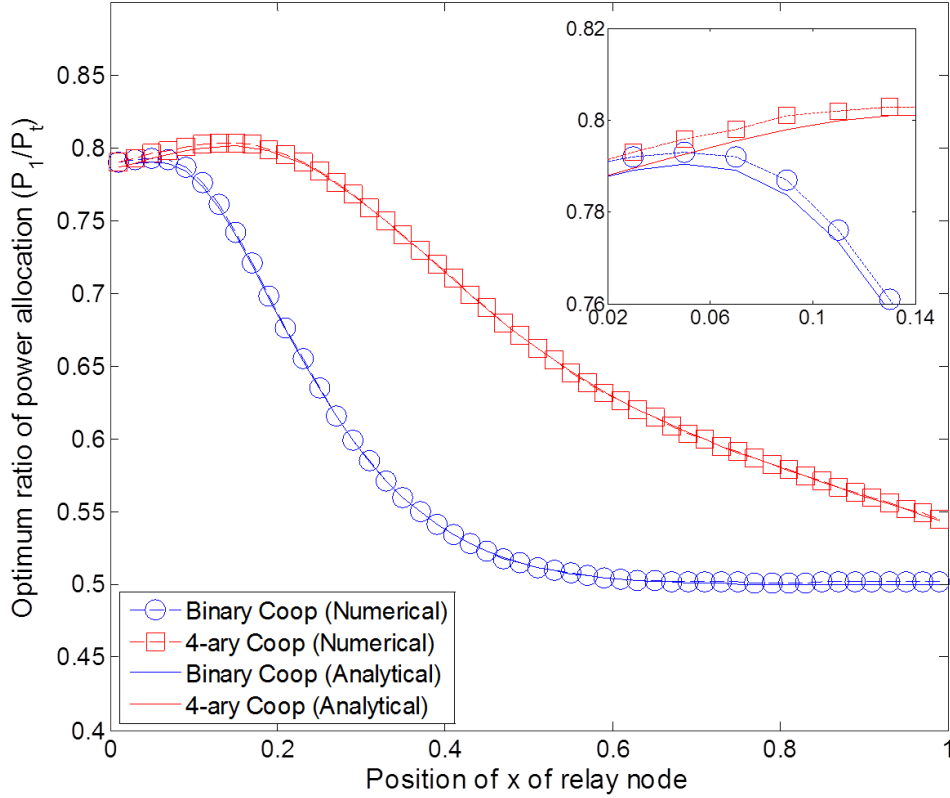


Figure 5.8: Optimum ratio of power allocation for the position of the relay node (N2) from 0 to 1 at $P_t/N_0 = 20$ dB.

for obtaining the optimum ratio. One is the analytical approach of solving the optimization problems (5.29) and (5.30), which are based on the approximated outage probabilities (5.20) and (5.23). Another observation is the results obtained from exhaustive numerical evaluations of the exact outage probabilities (5.19) and (5.22) as a function of ρ for both the BNC and NBNC-4 schemes. Note that the results from the two approaches are almost identical. This validates the optimization problem set up in (5.25).

Now returning to our discussion of the optimum ratio ρ , Figure 5.8 shows that,

the optimum ratio ρ is, approximately, less than 0.8 and larger than or equal to 0.5 for the two NC schemes. In more exact terms, when the relay N2 moves closer to the BS, i.e., $x \rightarrow 0$, the transmit power P_1 rises to $0.78P_t$ ($\rho = 0.78$), while the transmit power P_2 for the relay N2 goes to $0.22P_t$. 78 percentage of the total transmit power should be allocated at the source N1 for optimum results. The technical reason for this result is found from close investigation of (5.20) and (5.23) approximated, such that the channel variance $\sigma_{2,d}^2$ becomes much larger than the other fixed parameters, and the approximated outage probabilities are dominated mainly by the two terms $A_1/P_1^2P_2$ and A_3/P_1^3 . Note that P_1 is taken to the second and third powers in these terms, while P_2 is at its first power. Therefore, it is easy to see that more power should be allocated to P_1 than to P_2 in order to obtain a smaller outage probability. The result that more transmit power should be allocated to the source N1 rather than to the relay N2 as $x \rightarrow 0$ is reasonable, since the role of the relay becomes decreasingly critical as it moves away from the source and becomes closer to the BS.

On the other hand, we consider the other case in which relay N2 is moved closer to source N1. In the BNC case, we note that, the optimal ratio approaches 1/2, i.e., the transmit powers P_1 and P_2 approach $P_t/2$. In the NBNC-4 case, however, a very interesting behavior is observed. More transmit power P_1 should be used at the source rather than at the relay to achieve the minimum outage probability. This phenomenon is more interesting with NBNC-4 in the case where relay N2 is closer to source N1.

The optimum ratio increases as the size of the finite field used in NC is increased from 2 to 4. We can observe from Figure 5.8 that the optimum ratio of power allocation

for the NBNC-4 scheme is generally much greater than that of the BNC at any position of x . In other words, more transmit power should be used at source N1 to obtain smaller outage probability. This is because the combined messages Z_1 and Z_2 are maximally used in NBNC-4. Recall the two different NC matrices, \mathbf{H}_2 for BNC and \mathbf{H}_4 for NBNC-4, defined in (5.1) and (5.2) respectively. The rank of any 2×2 submatrix, i.e., any two rows of \mathbf{H}_4 , is always 2, while that of \mathbf{H}_2 is not always 2 (some may be 1). The crucial difference between the two NC schemes can be seen in Case 1 in Chapter 5.3.2. This is the outage event considered in (5.8). With the NBNC-4 scheme, it is possible for only the BS to recover the original messages S_1 and S_2 with the availability of only Z_1 and Z_2 . This is not possible with the BNC scheme. Figure 5.7 and Figure 5.8 show this in detail. In other words, they show how the crucial difference in Case 1 affects the result of OPA, as well as the corresponding outage probability results.

5.5 Conclusions

In wireless sensor networks, sensor nodes operate from finite capacity energy sources, i.e., onboard batteries; thus, designing a system with high power efficiency is a key issue. In this study, the power efficiency is investigated as the size of finite fields for the linear NC is increased from 2 to 4, and as the allocation of transmit power, i.e., the power used at the source node vs. the power at the relay node, is varied. To evaluate the benefits of these techniques, we derived the outage probability expressions for the considered NC schemes. We then analyzed the diversity order for the NC schemes, one with GF(2) and the other with GF(4). Our results indicate that the diversity order

using GF(4) is three, but that the diversity order using the binary network code is only two. We studied the effects of increased field size on the expansion of the network coverage area. Coverage area expansion by only changing the field size in NC, without increasing the transmit powers, is a creditable and interesting research result of this study. Our result indicates that the power efficiency benefit of GF(4) as compared to that of GF(2) is substantial and, it manifests not only in increased diversity order but also in noteworthy coverage area expansion.

Chapter 6

Conclusions and Future Research

6.1 Summary and Conclusions

This dissertation investigates multiple instances of inverse problems under the perspective of modern challenges in CS and cooperative networks. We have first studied the recovery problems of sparse signals in the field of CS. We have derived upper and lower bounds on the recovery performance of CS frameworks in finite fields. Next, we have proposed a newly analytical framework for performance evaluation in cooperative networks. In particular, we have derived upper bounds on the decoding failure probability and nullity of random matrices. We have then studied the outage probability of a simple cooperative network, and investigated the impact of the field size of NC and transmit power on system performance.

We first addressed the inverse problem of a CS framework over finite fields. We derived the sufficient and necessary conditions for recovery of sparse signals. We showed that the both conditions are tight. Both bounds coincide when the sparse factor of the sensing matrix is sufficiently large. We found that for recovery of ultra-sparse signals, the sensing matrix is required to be dense. One interesting result is that when the sensing matrix is sufficiently large and dense, and the field size is large, the number of measurements needed for perfect recovery is only $M > K$.

Next, we considered the recovery problem of sparse signals for CS frameworks over finite fields. In this framework, low-density matrices, e.g., Gallager’s regular LDPC codes, were used as the sensing matrices. We proposed a PD algorithm based on the message passing algorithm which was shown to be very good performance closely achieving the information-theoretical bounds. This work enables us to evaluate the transition diagram in a finite field based on CS.

We considered a cooperative wireless network where N sources are assisted with M relays in two phase transmissions: broadcasting phase and relaying phase. We proposed a newly analytical framework for evaluating the reconstruction performance of source messages at the BS. The evaluation framework was based on the expectation of the dimension of the nullspace in a random transmission matrix. Due to a dynamic network topology, we modeled the elements of the transmission matrix as random variables. We utilized outage probabilities of wireless links between nodes. Using these probabilities, the probability distributions of the elements of a random transmission matrix were made. And then, for performance evaluation, we derived the upper bound on the expected dimension of the nullspace and decoding failure probability of the random transmission matrix. This is a more effective and useful framework compared to the rank based method developed in the earlier literature. We showed the upper bounds for three types of connectivity schemes as varying outage probabilities and the field size of NC. Furthermore, we demonstrated the reconstruction performance of our proposed framework using multiple sources and relays deployed in a 2D space, and showed the impact of system performance on the number of relays and the field size of NC.

We compared the upper bounds for two types of modeling of a combination matrix, generated from the uniform and MDS distributions, and showed that the advantage of using the systematic generator of MDS codes appeared in high SNR regions. For a large scale network, we showed that the asymptotic nullity closes to the numerically simulated results in high SNR regions.

We investigated the outage probability for a simple cooperative network in which that two source nodes and one base station are deployed. To do this, we derived the outage probability expressions for the considered NC schemes. We then analyzed the diversity order for the NC schemes, one with GF(2) and the other with GF(4). Our results indicate that the diversity order using GF(4) is three, but that the diversity order using the binary network code is only two. We studied the effects of increased field size on the expansion of the network coverage area. Coverage area expansion by only changing the field size in NC, without increasing the transmit powers, is a creditable and interesting research result of this study. Our result indicates that the power efficiency benefit of GF(4) as compared to that of GF(2) is substantial and, it manifests not only in increased diversity order but also in noteworthy coverage area expansion.

6.2 Directions for Future Research

6.2.1 Construction of Sensing Matrix over Finite Fields

The good construction of the sensing matrices in CS theory is a main work such that RIP property is satisfied. So far, most of the approaches to construct the sensing

matrices have intensively been from random techniques, e.g., Gaussian and Bernoulli sensing matrices. The benefit is that this construction allows us to provide incoherence with a basis and universal property for any signal. Even though random sensing matrices ensure high probability in reconstruction, they also have many drawbacks such excessive complexity in reconstruction, significant space requirement for storage, and no efficient algorithm to verify whether a sensing matrix satisfies RIP property. Therefore, exploiting specific structures of deterministic sensing matrices is required to overcome these drawbacks of the random sensing matrices. Recently, several studies have proposed the construction of deterministic sensing matrices by using algebraic curves over finite fields [119], second order Reed-Muller codes [120], and unbalanced expander graphs [121]. In addition, for data gathering using CS in wireless sensor networks the constrained construction of the sensing matrix should be considered due to a predefined routing topology [122]. Over finite fields, we shall consider good construction of the sensing matrix for the future research.

6.2.2 Sparse Representation over Finite Fields

Sparsity in CS theory is important notion. Using sparsity of signals, Candes, Tao, and Donoho have proved that unknown signals are reconstructed with fewer samples than the Nyquist-Shannon theorem requires. Since then, many researchers have investigated which basis in a certain domain is better to represent a signal with the smallest sparsity, e.g., Fourier, Wavelet, Curvelet, Wave atom transform, etc. Indeed the most works of sparse representation are performed in real and complex valued numbers. To

the best of our knowledge, however, no study for sparse representation over finite fields has been performed. To reduce decoding complexity in coding theory, sparse encoding vectors [123] are exploited so that a fast algorithm by Wiedemann [124] for solving a system of linear equations can be used. Future research about sparse representation over finite fields is one of possible directions. In addition, it is need to consider relation between RIP condition and Hamming weight in coding theory.

Bibliography

1. Heinz W. Engl, Martin Hanke, and Andreas Neubauer, *Regularization of inverse problems*, Kluwer Academic Publishers, 2000.
2. Charles L. Epstein, *Introduction to the mathematics of medical imaging*, SIAM, 2008.
3. F. Natterer, *The mathematics of computerized tomography*, B. G. Teubner, Stuttgart, 1986.
4. S. Riad, “The Deconvolution Problem: An Overview,” *Proc. IEEE*, vol. 74, no. 1, pp. 82–85, Jan. 1986.
5. Y. Bar-Shalom, X. R. Li and T. Kirubarajan, *Estimation with Applications to Tracking and Navigation*, John Wiley-Sons, NY, USA, 2001.
6. B. Chalmond, *Modeling and Inverse Problems in Image Analysis*, Springer-Verlag, NY, USA, 2003.
7. M. Sambridge and K. Mosegaard, “Monte Carlo Methods in Geophysical Inverse Problems,” *Rev. of Geophysics*, vol. 40, no. 3, Sep. 2002.
8. R. Snieder and J. Trampert, *Inverse problems in geophysics*, Samizdat Press, 1999.
9. P. Buhlmann and T. Hothorn, “Boosting Algorithms: Regularization, Prediction and Model Fitting,” *Statistical Science*, vol. 22, no. 2, pp. 477–505, 2007.

10. C. Thurber and D. Eberhart-Phillips, “Local earthquake tomography with flexible gridding,” *Computers and Geosciences*, vol. 25, pp. 809–818, 1999.
11. G. K. Skinner and T. J. Ponman, “Inverse problems in X-ray and gamma-ray astronomical imaging,” *Inverse Problems*, vol. 11, no. 4, pp. 655–676, 1995.
12. N. Bissantz, T. Hohage, A. Munk, F. Ruymgaart, “Convergence rates of general regularization methods for statistical inverse problems and applications,” *SIAM Journal on Numerical Analysis*, vol. 45, no. 6, pp. 2610–2636, 2007.
13. E. J. Candes and T. Tao, “Near-optimal signal recovery from random projection: Universal encoding strategies?,” *IEEE Trans. Info. Theory*, vol. 52, no. 12, pp. 5406–5425, Dec. 2006.
14. D. L. Donoho, “Compressed sensing,” *IEEE Trans. Info. Theory*, vol. 52, no. 4, pp. 1289–1306, Apr. 2006.
15. R. G. Baraniuk, “Compressive sensing,” *Lecture Notes in IEEE Signal Processing Magazine*, vol. 24, no. 4, pp. 118–120, Jul. 2007.
16. E. J. Candes, J. Romberg, and T. Tao, “Robust uncertainty principles: Exact signal reconstruction for highly incomplete frequency information,” *IEEE Trans. Info. Theory*, vol. 52, no. 2, pp. 489–509, Feb. 2006.
17. R. Ahlswede, N. Cai, S.-Y. R. Li, R. W. Yeung, “Network information flow,” *IEEE Trans. Info. Theory*, vol. 46, no. 4, pp. 1204–1216, 2000.

18. C. Fragouli and E. Soljanin, “Network coding fundamentals,” *Foundations and Trends in Networking*, vol. 2, no. 1, pp. 1–133, 2007.
19. R. W. Yeung, S.-Y. R. Li, N. Cai, and Z. Zhang, “Network coding theory,” *Foundations and Trends in Communications and Information Theory*, vol. 2, no. 4, pp. 241–381, 2005.
20. P. A. Chou and Y. Wu, “Network coding for the internet and wireless networks,” *IEEE Signal Processing Mag.*, vol. 24, no. 5, pp. 77–85, Sep. 2007.
21. N. Cai and R. Yeung, “Secure network coding,” in *Proc. IEEE ISIT*, Lausanne, Switzerland, Jun. 2002, pp. 323.
22. A. G. Dimakis, P. B. Godfrey, M. Wainwright, and K. Ramchandran, “Network coding for distributed storage,” *IEEE INFOCOM*, Anchorage, AK, Mar. 2007, pp. 2000–2008.
23. A. G. Dimakis, P. B. Godfrey, Y. Wu, M. J. Wainwright, and K. Ramchandran, “Network coding for distributed storage systems,” *IEEE Trans. Info. Theory*, vol. 56, no. 9, pp. 4539–4551, Sep. 2010.
24. C. Gkantsidis and P. R. Rodriguez, “Network coding for large scale content distribution,” *IEEE INFOCOM*, vol. 4, Miami, FL, Mar. 2005, pp. 2235–2245.
25. R. Costa, D. Munaretto, J. Widmer, and J. Barros, “Informed network coding for minimum decoding delay,” *International Conference on Mobile Ad hoc and Sensor Networks*, Atlanta, GA, Sep. 2008, pp. 80–91.

26. J.-S. Park, M. Gerla, D. S. Lun, Y. Yi, and M. Médard, “Codecast: a network-codingbased ad hoc multicast protocol,” *IEEE Trans. Wirel. Commu.*, vol. 13, no. 5, pp. 76–81, Oct. 2006.
27. H. Seferoglu and A. Markopoulou, “Opportunistic network coding for video streaming over wireless,” in *Proc. of the Packet Video Conference*, Lausanne, Switzerland, Nov. 2007, pp. 191–200.
28. C. Fragouli and A. Markopoulou, “A network coding approach to network monitoring,” in *Proc. of the 43rd Annual Allerton Conference on Communication, Control, and Computing*, Monticello, IL, Sep. 2005.
29. C. Fragouli, A. Markopoulou, and S. Diggavi, “Topology inference using network coding techniques,” in *Proc. of the 44th Annual Allerton Conference on Communication, Control, and Computing*, Monticello, IL, Sep. 2006.
30. N. Cai and R. W. Yeung, “Secure network coding on a wiretap network,” *IEEE Trans. Info. Theory*, vol. 57, no. 1, pp. 424–435, Jan. 2011.
31. S. Jaggi, M. Langberg, S. Katti, T. Ho, D. Katabi, M. Médard, and M. Effros, “Resilient network coding in the presence of byzantine adversaries,” *IEEE Trans. Info. Theory*, vol. 54, no. 6, pp. 2596–2603, June 2008.
32. D. Wang, Q. Zhang, and J. Liu, “Partial network coding: Concept, performance, and application for continuous data collection in sensor networks,” *ACM Trans. Sensor Networks*, vol. 4, no. 3, pp. 1–22, May 2008.

33. C. Fragouli and E. Soljanin, “Network coding applications,” *Foundations and Trends in Networking*, vol. 2, no. 2, pp. 135–269, 2007.
34. P. A. Chou, Y. Wu, and K. Jain, “Practical network coding,” in *Proc. of the 41st Annual Allerton Conference on Communication, Control, and Computing*, Monticello, IL, Oct. 2003, pp. 40–49.
35. C. Fragouli, D. Katabi, A. Markopoulou, M. Médard, and H. Rahul, “Wireless network coding: Opportunities and challenges,” in *Proc. of the IEEE Military Communication Conference*, Orlando, FL, Oct. 2007, pp. 1–8.
36. S. Katti, H. Rahul, W. Hu, D. Katabi, M. Médard, and J. Crowcroft, “XORs in the air: Practical wireless network coding,” *IEEE/ACM Transactions on Networking*, vol. 16, no. 3, pp. 497–510, June 2008.
37. S. Katti, D. Katabi, H. Balakrishnan, and M. Médard, “Symbol-level network coding for wireless mesh networks,” in *Proc. of the ACM SIGCOMM*, vol. 38, no. 4, Seattle, WA, Oct. 2008, pp. 401–412.
38. Jin-Taek Seong and Heung-No Lee, “Necessary and Sufficient Conditions for Recovery of Sparse Signals over Finite Fields,” *IEEE Communications Letters*, vol. 17, no. 10, pp. 1976–1979, Oct. 2013.
39. Jin-Taek Seong and Heung-No Lee, “Method for reconstructing sparse signal in finite field, apparatus for reconstructing sparse signal in finite field, and recording medium for recording reconstruction method,” *US patent*, Pending, PCT/KR2013/004875.

40. Jin-Taek Seong and Heung-No Lee, "Concatenation of LDPC codes with Golden Space-Time Block Codes over the Block Fading MIMO Channels: System Design and Performance Analysis," *45th Annual Conference on Information Science and Systems (CISS)*, MD, USA, Mar. 2011.
41. Jin-Taek Seong and Heung-No Lee, "Predicting the Performance of Cooperative Wireless Networking Schemes with Random Network Coding," Early Access, *IEEE Transactions on Communications*
42. Jin-Taek Seong and Heung-No Lee, "4-ary Network Coding for Two Nodes in Cooperative Wireless Networks: Exact Outage Probability and Coverage Expansion," *EURASIP Journal on Wireless Communications and Networking*, 2012:366, Dec. 2012.
43. Jin-Taek Seong and Heung-No Lee, "Evaluation Framework for Reconstruction of Messages in Cooperative Coding Schemes of Multiple-Sources and Multiple-Relays," *IEEE International Conference on Computing, Networking and Communications (ICNC)*, Honolulu, USA, Feb. 2014.
44. Jin-Taek Seong and Heung-No Lee, "Exact Outage Probability of Two Nodes for Cooperative Networking using GF(4)," *IEEE IEEE International Workshop Signal Processing Advances in Wireless Communications (SPAWC)*, Darmstadt, Germany, Jun. 2013.
45. Jin-Taek Seong and Heung-No Lee, "Exact Outage Probability and Power Allocation of Two Nodes in Cooperative Networks," *IEEE International Wireless*

- Communications and Networking Conference (WCNC)*, Shanghai, China, Apr. 2013.
46. F. Bassi, C. Liu, L. Iwaza, M. Kieffer, “Compressive linear network coding for efficient data collection in wireless sensor networks,” *20th European Signal Processing Conf. (EUSIPCO)*, Bucharest, Romania, 2012, pp. 714–718
 47. E. Bourtsoulatze, N. Thomos, P. Frossard, “Correlation-aware reconstruction of network coded sources,” *International Symposium on Network Coding (NetCod)*, MA, USA, 2012, pp. 91–96.
 48. K. Rajawat, C. Alfonso, and G. Giannakis, “Network-compressive coding for wireless sensors with correlated data,” *IEEE Trans. Communications*, vol. 11, no. 12, pp. 4264–4274, 2012.
 49. W. Li, F. Bassi, and M. Kieffer, “Robust Bayesian compressed sensing over finite fields: asymptotic performance analysis,” Arxiv web, <http://arxiv.org/pdf/1401.4313v1.pdf>
 50. S. C. Draper and S. Malekpour, “Compressed sensing over finite fields,” in *Proc. IEEE Intl. Symp. on Info. Theory (ISIT)*, Seoul, Korea, 2009, pp.669–673.
 51. V. Y. F. Tan, L. Balzano, S. C. Draper, “Rank Minimization over Finite Fields: Fundamental Limits and Coding-Theoretic Interpretations,” *IEEE Trans. Info. Theory*, vol. 58, no. 4, pp. 2018–2039, Apr. 2012.

52. M. Cheraghchi, A. Hormati, A. Karbasi, M. Vetterli, “Group Testing With Probabilistic Tests: Theory, Design and Application,” *IEEE Trans. Info. Theory*, vol. 57, no. 10, pp. 7057–7067, Oct. 2011.
53. T. Tasic, N. Thomos, and P. Frossard, “Distributed sensor failure detection in sensor networks,” *Signal Processing*, vol. 93, no. 2, pp. 388–410. Feb. 2013.
54. C. Huimin, “Distributed file sharing: Network coding meets compressed sensing,” *First Intl. Conf. on Communications and Networking in China*, Beijing, China, 2006.
55. M. Firooz, S. Roy, et al., “Link failure monitoring via network coding,” in *Proc. IEEE 35th Conf. Local Computer Networks*, Denver, USA, 2010. Pp. 1068–1075.
56. C. Turner, “Recursive discrete-time sinusoidal oscillators,” *IEEE Signal Processing Mag.*, vol. 20, no. 3, pp. 103–111, May 2003.
57. T. M. Cover and J. A. Thomas, *Elements of Information Theory*, Wiley-Interscience, 2nd ed., 2006.
58. R. G. Gallager, *Low-Density Parity-Check Codes*, Cambridge, MA, MIT. Press, 1963.
59. Heung-No Lee, *Introduction to Compressed Sensing*, Lecture Note, Spring 2011.
60. F. Zhang and H.D. Pfister, “Compressed sensing and linear codes over real numbers,” in *Proc. 3rd Annual Workshop in Inform. and its Appl.*, San Diego, CA, Feb. 2008.

61. A. G. Dimakis and P. O. Vontobel, “LP decoding meets LP decoding: A connection between channel coding and compressed sensing,” in *Proc. 47th Allerton Conf. on Commun. Cont. and Comp.*, IL, USA, 2009.
62. S. Sarvotham, D. Baron, and R.G. Baraniuk, “Compressed sensing reconstruction via belief propagation,” *Tech. Report ECE-06-01 in Rice Univ.*, July 2006.
63. D. L. Donoho, A. Maleki, and A. Montanari, “Message-passing algorithms for compressed sensing,” *Proc. Natl. Acad. Sci.*, USA, vol. 106, no. 45, pp. 18914–18919, 2009.
64. M.C. Davey and D. Mackey, “Low-density parity-check codes over $GF(q)$,” *IEEE Commun. Lett.*, vol. 2, no. 6, pp. 165-167, Jan. 1998.
65. J. L. Laneman, David N. C. Tse, G. W. Wornell, “Cooperative diversity in wireless networks: efficient protocols and outage behavior,” *IEEE Trans. Info. Theory*, vol. 50, no. 12, pp. 3062–3080, 2004.
66. Y. Chen, S. Kishore, J. Li, “Wireless diversity through network coding,” *IEEE Wirel. Comm. Net. Conf. (WCNC)*, Las Vegas, USA, Apr. 2006, pp. 1681–1686.
67. D. H. Woldegebreal, H. Karl, “Network-coding based adaptive decode and forward cooperative transmission in a wireless network: outage analysis,” *13th European Wireless Conference*, Paris, France, Apr. 2007, pp. 1–6.

68. M. Xiao, M. Skoglund, “Multiple-User Cooperative Communications Based on Linear Network Coding,” *IEEE Trans. Commu.*, vol. 58, no. 12, pp. 3345–3351, 2010.
69. M. Xiao and M. Skoglund, “Design of network codes for multiple-user multiple-relay wireless networks,” in *Proc. IEEE ISIT*, Seoul, Korea, Jun. 2009, pp. 2562–2566.
70. J. L. Rebelatto, B. F. U.-Filho, Y. Li, B. Vucetic, “Multiuser Cooperative Diversity through Network Coding Based on Classical Coding Theory,” *IEEE Trans. Sig. Proc.*, vol. 60, no. 2, pp. 916–926, 2012.
71. J. L. Rebelatto, B. F. U.-Filho, Y. Li, B. Vucetic, “Adaptive Distributed Network-Channel Coding,” *IEEE Trans. Wirel. Commu.*, vol. 10, no. 9, pp. 2818–2822, 2011.
72. H. Topakkaya, Z. Wang, “Wireless network code design and performance analysis using diversity-multiplexing tradeoff,” *IEEE Trans. Commu.*, vol. 59, no. 2, pp. 488–496, 2011.
73. T.-Cruces, J. M. B.-Ordinas, M. Fiore, “Exact Decoding Probability Under Random Linear Network Coding,” *IEEE Commu. Lett.*, vol. 15, no. 1, pp. 67–69, 2011.
74. H. V. Nguyen, S. X. Ng, L. Hanzo, “Performance Bounds of Network Coding Aided Cooperative Multiuser Systems,” *IEEE Sig. Proc. Lett.*, vol. 18, no. 7, pp. 435–438, 2011.

75. T. Wang, G. B. Giannakis, “Complex Field Network Coding for Multiuser Cooperative Communications,” *IEEE Jour. Selected Areas in Commu.*, vol. 26, no. 3, pp. 561–571, Apr. 2008.
76. T. Islam, A. Nasri, R. Schober, R. K. Mallik, and V. K. Bhargava, “Network Coded Multi-Source Cooperative Communication in BICM-OFDM Networks,” *IEEE Trans. Wirel. Commu.*, vol. 11, no. 9, pp. 3180–193, Sep. 2012.
77. X.-T. Vu, M. D. Renzo and P. Duhamel, “BER Analysis of Joint Network/Channel decoding in Block Rayleigh fading channels,” *IEEE International Symposium on Personal, Indoor and Mobile Radio Communications (PIMRC)*, London, UK, Sep. 2013.
78. R. Youssef and A. Graell i Amat, “Network Coded Multi-Source Cooperative Communication in BICM-OFDM Networks,” *IEEE Trans. Wirel. Commu.*, vol. 10, no. 1, pp. 253–263, Jan. 2011.
79. Z. Han, X. Zhang, and H. V. Poor, “High performance cooperative transmission protocols based on multiuser detection and network coding,” *IEEE Trans. Wirel. Commu.*, vol. 8, no. 5, pp. 2352–2361, May 2009.
80. T.-W. Yune, D. Kim, and G.-H. Im, “Iterative detection for spectral efficient user cooperative transmissions over multipath fading channels,” *IEEE Trans. Commu.*, vol. 58, no. 4, pp. 1121–1128, Apr. 2010.
81. S. Katti, H. Rahul, W. Hu, D. Katabi, M. Medard, J. Crowcroft, “XORs in the

- air: practical wireless network coding,” *IEEE/ACM Trans. Networking*, vol. 16, no. 3, pp. 497–510, Jun. 2008.
82. A. Argyriou, “Wireless network coding with improved opportunistic listening,” *IEEE Trans. Wirel. Commu.*, vol. 8, no. 4, pp. 2014–2023, Apr. 2009.
83. J. Zhang, Y. P. Chen, I. Marsic, “MAC-layer proactive mixing for network coding in multi-hop wireless networks,” *Computer Networks*, vol. 54, no. 2, pp. 196–207. Feb. 2010.
84. A. Antonopoulos, C. Verikoukis, C. Skianis, and O. B. Akan, “Energy Efficient Network Coding-based MAC for Cooperative ARQ Wireless Networks,” *Ad Hoc Networks*, vol. 11, no. 1, pp. 190–200, 2013.
85. X. Wang, J. Li, and F. Tang, “Network Coding Aware Cooperative MAC Protocol for Wireless Ad Hoc Networks,” *IEEE Trans. Paral. Dist. Systems*, vol. 25, no. 1, pp. 167–179, Jan. 2014.
86. M. H. Firooz, Z. Chen, S. Roy, and H. Liu, “Wireless Network Coding via Modified 802.11 MAC/PHY: Design and Implementation on SDR,” *IEEE Jour. Sel. Areas in Commu.*, vol. 31, no. 8, pp. 1618–1628, Aug. 2013.
87. S. Wang, Q. Song, X. Wang, and A. Jamalipour, “Distributed MAC Protocol Supporting Physical-Layer Network Coding,” *IEEE Trans. Mobile Computing*, vol. 12, no. 5, pp. 1023–1036, May 2013.
88. J. Li, J. Yuan, R. Malaney, M. Azmi, and M. Xiao, “Network Coding Based LDPC

- Code Design for a Multi-source Relaying System,” *IEEE Trans. Wirel. Comm.*, vol. 10, pp. 1538–1551, May 2011.
89. C. Wang, M. Xiao, and M. Skoglund, “Diversity-multiplexing tradeoff analysis of coded multi-user relay networks,” *IEEE Trans. Commu.*, vol. 59, no. 7, pp. 1995–2005, Jul. 2011.
 90. M. Xiao and T. Aulin, “On the Bit Error Probability of Noisy Channel Networks with Intermediate Node Encoding,” *IEEE Trans. Info. Theory*, vol. 54, no. 11, pp. 5188–5198, Nov. 2008.
 91. M. Xiao and T. Aulin, “Optimal Decoding and Performance Analysis of a Noisy Channel Network with Network Coding,” *IEEE Trans. Commun.*, vol. 57, no. 5, pp. 1402–1412, May 2009.
 92. H.-T. Lin, Y.-Y. Lin, and H.-J. Kang, “Adaptive Network Coding for Broadband Wireless Access Networks,” *IEEE Trans. Parallel and Distributed Systems*, vol. 24, no. 1, pp. 4–18, 2013.
 93. M. D. Renzo, M. Iezzi, and F. Graziosi, “Error Performance and Diversity Analysis of Multi-Source Multi-Relay Wireless Networks with Binary Network Coding and Cooperative MRC,” *IEEE Trans. Wirel. Commu.*, vol. 12, no. 6, pp. 2883–29.3, 2013.
 94. M. D. Renzo, M. Iezzi, and F. Graziosi, “On Diversity Order and Coding Gain of Multisource Multirelay Cooperative Wireless Networks With Binary Network Coding,” *IEEE Trans. Vehicular Tech.*, vol. 62, no. 3, pp. 1138–1157, 2013.

95. J. Li, J. Yuan, R. Malaney, M. Xiao, and W. Chen, "Full-Diversity Binary Frame-Wise Network Coding for Multiple-Source Multiple-Relay Networks Over Slow-Fading Channels," *IEEE Trans. Vehicular Tech.*, vol. 61, no. 3, pp. 1346–1360, 2012.
96. B. Nazer and M. Gastp, "Compute-and-Forward: Harnessing Interference Through Structured Codes," *IEEE Trans. Info. Theory*, vol. 57, no. 10, pp. 6463–6486, Oct. 2011.
97. S. Borade, L. Zheng, and R. Gallager, "Amplify-and-forward in wireless relay networks: Rate, diversity, and network size," *IEEE Trans. Info. Theory*, vol. 53, pp. 3302–3318, Oct. 2007.
98. G. Kramer, M. Gastpar, and P. Gupta, "Cooperative strategies and capacity theorems for relay networks," *IEEE Trans. Info. Theory*, vol. 51, pp. 3037–3063, Sep. 2005.
99. T. S. Rappaport, *Wireless Communications: Principles and Practice*, Upper Saddle River, NJ: Prentice-Hall, 1996.
100. J. N. Laneman and G. W. Wornell, "Distributed space-time-coded protocols for exploiting cooperative diversity in wireless networks," *IEEE Trans. Inf. Theory*, vol. 49, no. 10, pp. 2415–2425, 2003.
101. T. Ho, M. Medar, R. Koetter, D. R. Karger, M. Effros, J. Shi, and B. Leng, "A random linear network coding approach to multicast," *IEEE Trans. Inf. Theory*, vol. 52, no. 10, pp. 4413–4430, 2006.

102. F. J. Macwilliams and N. J. Sloane, *The Theory of Error-Correcting Codes*, NY, Notrh-Holland, 1977.
103. SAGE, Open Source Mathematics Software, Available on www.sagemath.org.
104. C. D. Meyer, *Matrix Analysis and Applied Linear Algebra*, SIAM, Philadelphia, PA, 2000.
105. J. Luo, R. S. Blum, L. J. Cimini, L. J. Greestein, A. M. Haimovich, “Decode-and-forward cooperative diversity with power allocation in wireless networks,” in *Proc. IEEE Globecomn Conf.*, St. Louis, USA, Dec. 2005, pp. 3048–3052.
106. M. O. Hasna, M. S. Alouini, “Optimal power allocation for relayed transmission over Rayleigh-Fading channels,” *IEEE Trans. Wirel. Commun.*, vol. 3, no. 6, pp. 1999–2004.
107. R. Annavajjala, P. C. Cosman, L. B. Milstein, “Statistical channel knowledge-based optimal power allocation for relaying protocols in the high SNR regime,” *IEEE J. Sel. Areas Commun.*, vol. 25, no. 2, pp. 292–305, 2007.
108. W. Su., A. K. Sadek, K. J. R. Liu, “SER performance analysis and optimum power allocation for decode-and-forward cooperation protocol in wireless networks,” in *Proc. IEEE Wire. Comm. Net. Conf. (WCNC)*, New Orleans, USA, Mar. 2005, pp. 984–989.
109. N. Ahmed, M. Khojastepour, B. Aazhang, “Outage minimization and optimal

- power control for the fading relay channel,” in *Proc. IEEE Inform. Theory Workshop*, San Antonio, USA, Oct. 2004, pp. 458–462.
110. M. Yu, J. Li, R. S. Blum, “User cooperation through network coding,” in *Proc. IEEE Intl. Conf. Commun.*, Glasgow, Scotland, Jun. 2007, pp. 4064–4069.
111. C. Peng, A. Zhang, M. Zhao, Y. Yao, W. Jia, “On the performance analysis of network-coded cooperation in wireless networks,” *IEEE Trans. Wireless Commun.*, vol. 7, no. 8, pp. 3090–3097, 2008.
112. X. Bao, J. Li, “Adaptive Network Coded Cooperative (ANCC) for Wireless Relay Networks: Matching Code-on-Graph with Network-on-Graph,” *IEEE Trans. Wireless Comm.*, vol. 7, no. 2, pp. 574–583, 2008.
113. B. Du, J. Zhang, “Parity-Check Network Coding for Multiple Access Relay Channel in Wireless Sensor Cooperative Communications,” *EURASIP Jour. Wireless Comm. Networking*, pp. 1–15, 2010.
114. D. Duyck, D. Cahirone, J. J. Boutros, M. Moeneclaey, “Analysis and Construction of Full-Diversity Joint Network-LDPC Codes for Cooperative Communications,” *EURASIP Jour. Wireless Comm. Networking*, pp. 1–16, 2010.
115. L. Xiao, T. E. Fuja, J. Kliewer, D. J. Costello, “A Network Coding Approach to Cooperative Diversity,” *IEEE Trans. Info. Theory*, vol. 53, no. 10, pp. 3714–3722, 2007.

116. T. E. Hunter, Shahab Sanayei, Aria Nosratinia, “Outage Analysis of Coded Cooperation,” *IEEE Trans. Info. Theory*, vol. 52, no. 2, pp. 375–391, 2006.
117. W. Su, A. K. Sadek, K. J. Ray Liu, “Cooperative communications in wireless networks: performance analysis and optimum power allocation,” *Wireless Personal Communications*, vol. 59, pp. 181–217, 2008.
118. Y. Lee, M.-H. Tsai, S.-I. Sou, “Performance of Decode-and-Forward Cooperative Communications with Multiple Dual-Hop Relays over Nakagami-m Fading Channels,” *IEEE Trans. Wirel. Commun.*, vol. 8, no. 6, pp. 2853–2859, 2009.
119. S. Li, F. Gao, G. Ge, and S. Zhang, “Deterministic Construction of Compressed Sensing Matrices via Algebraic Curves,” *IEEE Trans. Info. Theory*, vol. 58, no. 8, pp. 5035–5041, 2012.
120. S. D. Howard, A. R. Calderbank, and S. J. Searle, “A fast reconstruction algorithm for deterministic compressive sensing using second order reed-muller codes,” in *Proc. the 42nd Annual Conf. Info. Science and Systems (CISS)*, Princeton, NJ, USA, March, 2008.
121. P. Indyk, “Explicit Constructions for Compressed Sensing of Sparse Signals,” in *Proc. the 19th Annual ACM-SIAM Symp. Discrete Algo.*, San Francisco, USA, Jan. 2008.
122. M. Cheraghchi, A. Karbasi, S. Mohajer, and V. Saligrama, “Graph-Constrained Group Testing,” *IEEE Trans. Info. Theory*, vol. 58, no. 1, pp. 248–262, Jan. 2012.

123. H. Y. Kwan, K. W. Shum, and C. W. Sung, “Linear Network Code for Erasure Broadcast Channel with Feedback: Complexity and Algorithm,” *Submitted to IEEE Trans. Info. Theory*, arXiv:1205.5324v1
124. D. H. Wiedemann, “Solving sparse linear equations over finite fields,” *IEEE Trans. Info. Theory*, vol. 32, no. 1, pp. 54–62, Jan. 1986.